

PARAMETRIC MODELLING FOR THE MITIGATION OF URBAN HEAT
ISLAND EFFECT: A MODEL PROPOSAL

A THESIS SUBMITTED TO
THE GRADUATE SCHOOL OF NATURAL AND APPLIED SCIENCES
OF
MIDDLE EAST TECHNICAL UNIVERSITY

BY

BEGÜM SAKAR

IN PARTIAL FULFILLMENT OF THE REQUIREMENTS
FOR
THE DEGREE OF MASTER OF SCIENCE
IN
URBAN DESIGN
IN
CITY AND REGIONAL PLANNING

AUGUST 2018

Approval of the thesis:

**PARAMETRIC MODELLING FOR THE MITIGATION OF URBAN HEAT
ISLAND EFFECT: A MODEL PROPOSAL**

submitted by **Begüm Sakar** in partial fulfillment of the requirements for the degree of **Master of Science in Urban Design in City and Regional Planning, Middle East Technical University** by,

Prof. Dr. Halil Kalıpçılar
Dean, Graduate School of **Natural and Applied Sciences**

Prof. Dr. Çağatay Keskinok
Head of Department, **City and Regional Planning**

Assoc. Prof. Dr. Olgu Çalışkan
Supervisor, **City and Regional Planning Dept., METU**

Examining Committee Members:

Prof. Dr. Adnan Barlas
Department of City and Regional Planning, METU

Assoc. Prof. Dr. Olgu Çalışkan
Department of City and Regional Planning, METU

Assist. Prof. Dr. Meltem Şenol Balaban
Department of City and Regional Planning, METU

Assist. Prof. Dr. Yücel Can Severcan
Department of City and Regional Planning, METU

Assist. Prof. Dr. Aktan Acar
Department of Architecture, TOBB UET

Date: 13.08.2018

I hereby declare that all information in this document has been obtained and presented in accordance with academic rules and ethical conduct. I also declare that, as required by these rules and conduct, I have fully cited and referenced all material and results that are not original to this work.

Name, Last Name: Begüm Sakar

Signature :

ABSTRACT

PARAMETRIC MODELLING FOR THE MITIGATION OF URBAN HEAT ISLAND EFFECT: A MODEL PROPOSAL

Sakar, Begüm

M.S., Urban Design, Department of City and Regional

Supervisor: Assoc. Prof. Dr. Olgu Çalışkan

August 2018, 132 pages

Morphological characteristics of urban settlements as the outcome of the long-term planning decisions influence microclimatic conditions of our cities and more specifically induces the “Urban Heat Island” (UHI) effect, which generates many undesirable conditions in the living environment. In the very context of global warming that generate intensive UHI in the cities, any change in the thermal balance of the urban environment is associated with the main parameters of urban geometry. This is actually the issue that necessitates more research for the mitigation of heat island intensity by design. In this regard, this study investigates the potentials of computational modelling for analyzing the key morphological components of urban areas, and generating alternative typologies of urban fabric to mitigate UHI intensity. From this standpoint, the current research proposes a parametric model to provide urban design and planning practice with a computational and generative basis in the way of a robust morphological perspective to the mitigation of UHI effect.

Since the development of UHI has a strong correlation with the “Sky View Factor” (SVF) value, the methodological framework of this research is formed on the basis of

the SVF measurement to estimate UHI intensity via parametric modelling. The alternative form compositions and configurations are generated to simulate different conditions of heat island intensity in accordance with the different values of the basic parametric indicators (i.e. building height, coverage ratio, setback distance), which are utilized as the basic building codes in the spatial planning system in Turkey. The integration of computation and form generation within an algorithmic model, essentially, suggests an effective integration of morphology (analysis) and design to be applied on actual urban context.

In this framework, Mustafa Kemal Neighborhood, one of the recent urban transformation site in Ankara is selected as the case study area for the application of the proposed model. Rather than searching for an ideal urban form, the model application focuses on the generation of the best performing form alternatives with regards to the focused issue of UHI effect. From the generative perspective of urban design, the methodological framework with the proposed model is believed to provide a kind of “Decision Support System” (DSS) in planning on the way of the development of an evidence-based urban design approach in practice.

Keywords: Parametric Modelling, Generative Urban Design, Urban Heat Island

ÖZ

KENTSEL ISI ADASI ETKİSİ AZALTIMINDA PARAMETRİK MODELLEME: BİR MODEL ÖNERİSİ

Sakar, Begüm

Yüksek Lisans, Kentsel Tasarım, Şehir ve Bölge Planlama Bölümü

Tez Yöneticisi: Doç. Dr. Olgu Çalışkan

Ağustos 2018, 132 sayfa

Yoğun kentsel dönüşüm süreçleri doğrultusunda biçimlenen kent formunun değişen morfolojik karakteri, kentlerin iklimsel koşullarını etkileyerek birçok olumsuz sonuca yol açabilmektedir. Küresel ısınma bağlamında bu olumsuz etkilerin başında “Kentsel Isı Adası” (KIA) gelmektedir. Kentlerde ısı adası oluşumunu koşullayan kentsel geometrinin değişkenleri kentin termal dengesinde de değişime neden olabilmektedir. Bu değişim, ısı adası yoğunluğunun tasarım yoluyla azaltılmasına yönelik daha fazla araştırma yapılmasına yönelik gereği açığa çıkarmıştır. Bu bağlamda, söz konusu çalışma, kentsel alanların morfolojik bileşenlerini analiz ederek ısı adası etkisini azaltmaya yönelik alternatif kentsel doku tipolojileri üretmek üzere hesaplamalı (computational) modelleme yöntemlerinin potansiyellerini araştırmaktadır. Bu açıdan mevcut araştırma, kentsel tasarım ve planlama uygulamalarında KIA etkisinin azaltılmasına yönelik, çözümsel (analitik) ve üretken (generative) nitelikte morfolojik bir yöntemsel bakış açısını sağlamak için parametrik bir model önerisinde bulunmaktadır.

Kentsel Isı Adası (KIA) oluşumu ile “Gökyüzü Görüş Açısı” (GGA) arasında güçlü

bir ilişki olduğundan, bu araştırmanın metodolojik çerçevesi, parametrik modelleme aracılığıyla kentsel alanlarda GGA ölçümü yaparak KIA yoğunluğunu hesaplamak üzerine kurgulanmıştır. Isı adası oluşumundaki farklılıkları test etmek üzere, Türkiye'deki mekânsal planlama pratiğinde yer alan yapılaşma kodları (bina yüksekliği, taban alanı, çekme mesafesi, vb.) temel form değişkenleri olarak modele girdi kullanılmış ve alternatif kentsel doku tipolojileri üretilmiştir. Algoritmik model tabanında entegre edilen hesaplama ve form üretim modeli aynı zamanda, kentsel bağlamda uygulanabilecek analiz ve tasarım aşamalarını bütünleştirme potansiyeline sahiptir.

Bu kapsamda, önerilen modelin uygulanması için Ankara'daki kentsel dönüşüm alanlarından biri olan Mustafa Kemal Mahallesi örnek çalışma alanı olarak seçilmiştir. Yapılan çalışma, 'ideal' bir kentsel formun ortaya konması yerine, KIA sorununa yönelik olarak en iyi performansı gösteren form alternatiflerinin üretilmesini hedeflemektedir. Hesaplamalı ve üretken model altlığı doğrultusunda önerilen metodolojik çerçevesinin, planlamada bir tür "Karar Destek Sistemi" (KDS) oluşturarak kanıta dayalı kentsel tasarım yaklaşımının geliştirilmesine de katkı sağlayacağı savlanmaktadır.

Keywords: Parametrik Modelleme, Üretken Kentsel Tasarım, Kentsel Isı Adası

To who encourage me...

ACKNOWLEDGEMENTS

This thesis has been completed with the guidance, support and help of several people who have contributed throughout the process.

I would like to express my deepest gratitude to my advisor, Assoc. Prof. Dr. Olgu Çalışkan for all his incredible guidance, encouragement and patient throughout this research. I would not complete this thesis without his contribution and assistance. I would also like to thank the examining committee, Prof. Dr. Adnan Barlas, Assist. Prof. Dr. Meltem Şenol Balaban, Assist. Prof. Dr. Yücel Can Severcan and Assist. Prof. Dr. Aktan Acar for their valuable comments and suggestions.

In particular, I owe special thanks to Ayşem Şebnem Ötkür for her help and guidance throughout this year. I would not improve my writing skill without her incredible personality and teaching method. I would also like to offer my special thanks to Y. Baver Barut for his help whenever I need it.

I would like to express my gratitude to the members of METU MUD and Research Collective team. I would also like to offer my special thanks to my beloved friends Derya Yılmaz and Busen Özgür for their presence and support. I am also thankful to H. Eren Efeoğlu, Neşe Aydın and Damla Karagöz for their contribution.

Lastly, I would like to express my sincere gratitude to my beloved mother, Yasemin Sakar for her unlimited love and support in every stage of my life. I owe her everything I have. I am also heartily thankful to Yalçın Akyel for being so caring and supportive. Thanks to him, I was able to overcome all problems even if I didn't believe I could. I appreciate him for his endless patience and moral support.

TABLE OF CONTENTS

ABSTRACT	v
ÖZ	vii
ACKNOWLEDGEMENTS	x
TABLE OF CONTENTS	xi
LIST OF TABLES	xiii
LIST OF FIGURES	xiv
1. INTRODUCTION	1
1.1. Definition of the Research Problem.....	1
1.2. Aims and Objectives of the Research	3
1.3. Method of the Research	4
1.4. Structure of the Research	5
2. URBAN HEAT ISLAND PHENOMENON.....	7
2.1. Definition of Urban Heat Island	7
2.1.1. Formation of UHI.....	11
2.1.1.1. Physical Principles of Energy Balance.....	12
2.1.1.2. Energy Balance Differences between Urban and Rural Areas.....	15
2.1.2. Causes of UHI	18
2.1.2.1. Urban Population.....	19
2.1.2.2. Urban Geometry	20
2.1.2.3. Thermal Properties of Urban Surfaces	24
2.1.2.4. Lack of Vegetation Areas	27
2.1.2.5. Anthropogenic Heat Release	31
2.1.3. Negative Impacts of UHI and Need For Mitigation	32
2.2. The Relation between UHI and Urban Geometry	35
2.2.1. Characterizing Indicators of Urban Geometry	35
2.2.1.1. Aspect Ratio (H/W).....	35

2.2.1.2. Sky View Factor (SVF)	39
2.2.1.3. Orientation	45
2.2.2. Calculation of UHI Intensity based on Urban Geometry	49
2.3. Evaluation of UHI Related Studies in the Literature	52
2.3.1. Previous Studies on UHI	52
2.3.1.1. Measurement Related Studies	53
2.3.1.2. Simulation Related Studies	54
2.3.2. The Overall Critics on Existing Methods of UHI	57
3. PARAMETRIC MODELLING FOR THE ANALYSIS AND SIMULATION OF UHI: A MODEL PROPOSAL	59
3.1. Methodical Approach.....	59
3.2. Parametric Modelling: Tools and Techniques	61
3.3. Definition of Computational Framework for the Mitigation of UHI.....	66
3.3.1. Algorithmic Definitions of the Morphological Indicators of UHI	66
3.3.2. Algorithmic Setting of Analysis.....	71
3.3.3. Algorithmic Setting of Simulation	77
4. APPLICATION OF THE MODEL IN ACTUAL URBAN CONTEXT: PERFORMANCE ASSESSMENT OF AN URBAN TRANSFORMATION	87
4.1. Case Study Area: Mustafa Kemal Neighborhood.....	88
4.2. Case Study Analysis: SVF Calculation.....	93
4.3. Simulation Application for the Mitigation of UHI Effect	98
4.3.1. Generation of Form Variations	99
4.3.2. Overview of the Findings	111
5. CONCLUSION	113
5.1. The Main Problematic Issues to Revisit	113
5.2. Main Findings and Contributions of the Research	116
5.3. Main Limitations of the Research.....	118
5.4. Recommendations for Future Studies	120
REFERENCES.....	123

LIST OF TABLES

TABLES

Table 2.1: World's population by size of settlement, 2016 and 2030.....	7
Table 2.2: Albedo values of surface materials	26
Table 2.3: Examination of measurement-based studies	53
Table 2.4: Examination of simulation-based studies	56
Table 3.1: The comparison of SVF extraction models	76
Table 4.1: Simulation results of the first scenario.....	100
Table 4.2: Simulation results of the second scenario	105
Table 4.3: Simulation results of the third scenario	107
Table 4.4: Simulation results of the fourth scenario	109

LIST OF FIGURES

FIGURES

Figure 2.1: Spatial distribution of surface and air temperatures	11
Figure 2.2: Energy conversion system in the environment	12
Figure 2.3: Schematic depiction of energy balance components	14
Figure 2.4: Energy balance of rural and suburban areas	17
Figure 2.5: Daily heating/cooling rates and air temperature changes in urban and rural areas	18
Figure 2.6: The relation between UHI intensity ($\Delta T_{u-r(max)}$) and population (log P) for North American (a) and European (b) cities	20
Figure 2.7: Schematic depiction of an urban canyon	22
Figure 2.8: The reflection of incoming radiation from different surfaces	23
Figure 2.9: Daily surface temperatures of different colored panels	27
Figure 2.10: Daily energy fluxes for two configurations of canyon depth and evaporation area	28
Figure 2.11: Temperature reductions in Sacramento and Phoenix with additional tree cover in summer period.....	29
Figure 2.12: The rise in air temperature in proportion to the distance from green area during day-time and night-time.....	30
Figure 2.13: The calculation of H/W ratio for a symmetrical canyon	36
Figure 2.14: The calculation of H/W ratio for non-uniform buildings	36
Figure 2.15: The calculation of H/W ratio for an asymmetrical canyon.....	37
Figure 2.16: The relation between H/W ratio and UHI intensity.....	38
Figure 2.17: The hourly variations of the air temperature in different canyon profiles (Source: Bakarman and Chang, 2015)	39
Figure 2.18: The relation between SVF values and emitted long-wave radiation	40
Figure 2.19: Schematic depiction of the SVF calculation.....	41

Figure 2.20: Image-based SVF calculation process.....	43
Figure 2.21: Energy balances of canyon surfaces based on hourly measurements ...	46
Figure 2.22: Advection of the canyon air volume due to the wind direction: N-north, S-south, V-variable	47
Figure 2.23: Schematic depiction of flow patterns	48
Figure 2.24: UHI intensity distribution according to the model of Oke (1981) and to the new statistical model	50
Figure 2.25: Comparison of estimated heat island intensities by different models ...	51
Figure 2.26: Generated form samples based on the best density distribution.....	55
Figure 3.1: Schematic depiction of the workflow	61
Figure 3.2: Rhinoceros and Grasshopper softwares with basic explanations	63
Figure 3.3: Fitness process of the Galapagos tool.....	65
Figure 3.4: Schematic depiction of the effect of morphological parameters on the visibility of sky.....	67
Figure 3.5: Definition of basic elements of morphological components	68
Figure 3.6: Schematic depiction of algorithmic attributions.....	69
Figure 3.7: Algorithmic definition of Building Coverage Ratio (BCR) and Floor Area Ratio (FAR).....	70
Figure 3.8: The detection process of the measurement point and areas (Phase 1).....	72
Figure 3.9: The projection process of the buildings on the hemisphere (Phase 2)	73
Figure 3.10: The SVF extraction from the fisheye image model (Phase 3).....	74
Figure 3.11: The SVF extraction from the hemispherical projection model (Phase 3)	75
Figure 3.12: The comparison of SVF measurement results of the different number of buildings.....	77
Figure 3.13: Workflow of the algorithmic setting of the simulation	78
Figure 3.14: The SVF simulation based on the building height	79
Figure 3.15: The SVF simulation based on the distance parameter.....	80
Figure 3.16: Different form configurations for the same ‘distance simulation’ result	81
Figure 3.17: The SVF simulation based on the building size	82
Figure 3.18: The SVF simulation based on the Floor Area Ratio (for all buildings)	83

Figure 3.19: The SVF simulation based on the Floor Area Ratio (for each building)	84
Figure 3.20: Different form configurations for the same ‘FAR simulation’ result....	85
Figure 4.1: Land use situation of Mustafa Kemal Neighborhood in 1970.....	89
Figure 4.2: Land use situation of Mustafa Kemal Neighborhood in 1997.....	90
Figure 4.3: Land use situation of Mustafa Kemal Neighborhood in 2005.....	90
Figure 4.4: Satellite image of Mustafa Kemal Neighborhood in 2018	90
Figure 4.5: 2023 Master Plan decisions for central-west area of Ankara	91
Figure 4.6: Case study area selection from Mustafa Kemal neighborhood	91
Figure 4.7: Satellite images of the case study area for 2005 (a) and 2018 (b) years .	92
Figure 4.8: Comparison of the figure-ground map of the informal housing area (a) and the transformed housing area (b)	92
Figure 4.9: Comparison of the street network of the informal housing area (a) and the transformed housing area (b).....	93
Figure 4.10: Algorithmic setting of the building selection for each measurement point.....	94
Figure 4.11: Application of the algorithmic set of analysis on the area.....	95
Figure 4.12: Algorithmic setting of the analysis phase of the proposed model	96
Figure 4.13: Detail sections from the SVF calculations.....	96
Figure 4.14: Comparison of measurement results (SVF and UHI intensity) of informal and actual urban transformation areas	97
Figure 4.15: Comparison of simulation results for the first scenario.....	101
Figure 4.16: Design variations for the first scenario (from 1st to 6th generation)...	103
Figure 4.17: Design variations for the first scenario (from 7th to 15th generation)	104
Figure 4.18: Comparison of simulation results for the second scenario	106
Figure 4.19: Comparison of simulation results for the third scenario.....	108
Figure 4.20: Comparison of simulation results for the fourth scenario	110
Figure 4.21: Comparison of the actual morphology of the area before and after transformation (top row) with the alternative form variations generated by the simulation (bottom row).....	111

CHAPTER 1

INTRODUCTION

1.1. Definition of the Research Problem

Urban climate affects urban livability which is influenced by the complexity of physical and morphological characteristics of cities such as urban form and geometry, urban density, thermal properties of urban surfaces and the availability of vegetation coverage. The intrinsic physical nature of the cities as the cumulative outcome of all of these factors, result in subtle differentiations in the particular conditions of urban microclimate. Urban Heat Island (UHI) is one of the prominent issue discussed by spatial researchers on performativity differentiation based on urban morphology. Defined as differentiation in the air temperature between urban areas and its surroundings, the phenomenon of Urban Heat Island (UHI) is considered one of the major issues regarding the perceived spatial quality urban environments. The development of larger heat island intensity causes climate modifications from local to global scale. At least 1°C rise in air temperature of cities has a knock-on effect on the global warming. In fact, this warming trend has negative impacts on the environment both ecological and economical, and on the human health (Erell et al., 2011; Santamouris et al., 2001). Emerging problems from increased UHI effect in urban areas, essentially, call for specification of the influential factors on the change in the thermal balance of the environment as an outcome of the urbanization.

Urban geometry, one of the most influential factors in the development of heat island intensity, has been evaluated, and its critical effects have been proved by several studies, so far. Accordingly, the variation on the main parameters of urban geometry,

which are defined as form, location, orientation, height of the buildings and spaces between them influence air temperature, wind speed and direction, and the amount of radiation absorbed and emitted. Over the years, researchers have established numerous correlations between geometrical features of urban areas and the ambient air temperature to overcome the issue of characterizing the calculation of UHI in regard to the urban geometry. In order to represent that relation, the aspect ratio (H/W), which is based on the height-to-width ratio of urban canyons, and sky view factor (SVF), which is based on the ratio of visibility of sky from the ground level, are the prominent morphological indicators used in order to simulate urban canyons, and to estimate the UHI intensity in the areas of investigation.

In order to specify the real effect of urban geometry indicators on UHI, and to determine the increase in the air temperature due to any change in the geometrical features, many studies have been conducted by using measurement tools on the actual urban areas. Since those models have become a focus of measurement-based studies, the lack of predictive tools for the simulation of UHI intensity has emerged in the research field. Then, simulation-based studies have come into the agenda to experiment the influence of urban geometry on the air temperature through different scenarios, and to test various form configurations to mitigate the UHI effect. In addition to benefits of improved simulation tools to estimate heat island intensity for different urban areas by using three-dimensional urban geometry data, they have also weakness in generating from configurations and searching better solutions in terms of mitigation of UHI intensity. Limitations on the number of tested scenarios, estimations based on specific simulated areas, non-flexible tools, and restrictions on the form generations by computational design tools necessitate the development of new tools and techniques to enable designers and planner in building a robust perspective on climate responsive urban design.

Since the development of parametric modelling tools, designers have enormous ability to generate numerous form configurations and design alternatives, and to create set of algorithms for analyzing design problems to guide finding better solutions. Since parametric modelling provides infinite possibilities, such as searching, generating,

analyzing and operating design settings, it has gained a wide acceptance in the field of architectural and urban design. Nevertheless, despite its increasing use in design practice, its use in spatial analysis and research has fallen limited and insufficient.

Considering its wide range of opportunities, the current research argues that parametric modeling can be explored in order to come up with an efficient integration between analysis and design on the basis of a possible generative approach to the issue of urban heat island. Since urban geometry-based UHI studies are generally specialized either on measurement or on simulation techniques, the current analytical tools are not integrated with each other. Therefore, in specific urban areas, design proposals for heat island mitigation cannot be generated according to the exact result of morphological analysis that leads to the inability of the applications to achieve better solutions. In other words, the studies fall short to test the various development alternatives based on certain for indicators in certain contexts. Thus, to tackle these shortcomings, a model proposal that combines analysis and design processes to mitigate UHI intensity is suggested as response to the essential problem statement of the research.

1.2. Aims and Objectives of the Research

The aim of this research is to investigate the potentials of parametric modelling for analyzing morphological components of urban areas, and testing the design solutions to mitigate the Urban Heat Island (UHI) effect. By developing a parametric approach, following the calculation of UHI intensity in urban areas, one could proceed the design process to generate form compositions and configurations according to the analysis results.

The proposed integrative parametric model of analysis and design aims to provide designers an effective calculation of UHI intensity through various form generations, simultaneously, via the computational algorithms. Thus, this research will bring an analytical and generative perspective to urban design and planning while opening up a methodological discussion on the problematic issue of urban heat island (UHI). Within this context, for the demonstration of the applicability of the proposed

parametric model, and for the integration of parametric modelling with urban design and urban planning practices, this model will be applied and experienced in an actual urban context.

In the urban context selection, Ankara, which has a tendency to develop and transform rapidly on the southwestern corridor, is taken into consideration due to the land use of that corridor and its surroundings has been remarkably changed by upper scale plans, and implementation plan decisions. One of the developed part of this corridor where public institutions, business centers and residential-office mixed projects area mainly took place in recent years, Mustafa Kemal neighborhood, is exposed to many alterations from 1970s to 2010s. Recently, the declaration of this area as an urban transformation and regeneration project allows to make a comparison between demolished informal fabric, renewed formal fabric and design alternatives to be generated by the model in regard to their contribution to the UHI effect. Therefore the main aim of this study is to compare various form variations according to the same plan decisions to search for better solutions to mitigate UHI intensity.

In this framework, the main research problems can be stated as follows:

- How can the adaptation of UHI studies into parametric modelling provided?
- Which morphological indicators can be redefined within parametric modelling for analyzing UHI effect in actual urban areas?
- Can various form compositions and configurations be generated by parametric modelling to mitigate the UHI intensity with regards to the settled (parametric) indicators of development planning system in Turkey (i.e. height, FAR, coverage, setback distance)?
- How can the integration of analysis and design processes be provided as an effective and flexible tool in urban design and planning practices?

1.3. Method of the Research

The research stands on a model proposal as a synthesis of analysis and simulation

processes via parametric modeling tools, which are incorporated into Rhinoceros and Grasshopper softwares. Parametric modelling can be defined as a computational design approach based on evaluation and generation of form compositions and design alternatives by controlling input and output parameters. This generative tool allows designers and researchers to build up and develop algorithms for analyzing and generating form variations depending on their design problems.

In this research, the proposed model aims to achieve the combination of Sky View Factor (SVF) calculation, which is described as the ratio of the visibility of the sky from a point on the urban surfaces depending on the interception of the near located urban structures, by analyzing morphological components, and form generation by maximizing the obtained SVF values in order to mitigate heat island intensity. To that end, a wide range of literature on the UHI studies, the effect of urban geometry on the UHI development and calculation methods based on geometrical features of urban areas is reviewed in order to come up with an original SVF calculation method as the main part of the research study.

Following the literature review, the first phase of the proposed model, which is named as the analysis phase, is constructed in the parametric modelling software by defining algorithmic setting of morphological indicators to develop SVF calculation algorithms. Then, in the second phase, a set of computational algorithm is defined for the simulation process to generate form variations by maximizing SVF values to achieve minimum heat island intensity. Consequently, the research method aims provide a new technique to simulate UHI effect in different urban design scenarios that will enhance the discussion on the typological formations in this regard.

1.4. Structure of the Research

This research is composed of five chapters. It begins with an introductory chapter on the main research problem of this study, which is a model proposal as a synthesis of analysis and simulation for urban design, while giving research questions and methodological approach to draw the framework of the thesis.

Chapter 2 starts with a comprehensive literature review on the Urban Heat Island (UHI) phenomenon, and summarizes the process of the formation of UHI effect, main causes of the heat island intensity and its relation with urban geometry. After explaining the characterization of urban geometry indicators, the UHI calculation methods based on urban geometry are examined. A comparison between the different methodologies is made to decide which calculation method to be used in this research. Also, by means of a critical review of the previous studies, their methodologies has been discussed to specify the major components of the proposed model.

In the following chapter, the model proposal for the mitigation of UHI effect is introduced by defining computational framework of this study. Algorithmic setting of analysis and simulation processes are given in detail along with the explanation of the application on hypothetical urban canyon, which is defined as a basic unit of urban surfaces, and characterizing urban areas by its repetition. For the demonstration of the applicability of the proposed parametric model, and for the integration of parametric modelling with urban design and urban planning practices, Chapter 4 gives the detail of the application of this proposal on an actual urban context.

CHAPTER 2

URBAN HEAT ISLAND PHENOMENON

2.1. Definition of Urban Heat Island

Today, more than half of the world's population living in urban areas has been growing more rapidly than the world population growth rate. Within the next two decades, the growth rate of urban population, which is 1.8, is expected to double while the growth rate of world population is 1 (UN, 2001).

According to the results of United Nation's (2017) world population projection, the world has roughly 7.6 billion inhabitants and it will reach 8.5 billion by the end of 2030. Estimations show that while the urban population will continue to increase from 54% to 60% by 2030, the rural population will gradually decrease. In developed countries, the majority of the population (74%) lives in urban areas, so the growth rate of these countries is expected to increase slowly rather than less developed countries (UN, 2016).

Table 2.1: World's population by size of settlement, 2016 and 2030 (Source: UN, 2016)

	2016			2030		
	Number of settlements	Population (millions)	Percentage of world population	Number of settlements	Population (millions)	Percentage of world population
Urban	..	4034	54,5	..	5058	60,0
10 million or more	31	500	6,8	41	430	8,7
5 to 10 million	45	308	4,2	63	434	5,2
1 to 5 million	436	861	11,6	558	1128	13,4
500.000 to 1 million	551	380	5,1	731	509	6,0
Fewer than 500.000	..	1985	26,8	..	2257	26,8
Rural	..	3371	45,5	..	3367	40,0

As a result of the increase in population and urbanization, urban settlements have expanded and sprawled on the outskirts of cities and thus, land use has changed. Following this alteration, human activities and industrial developments increased energy demand and fossil fuel consumption, which lead to production of waste and air pollutants. The emissions of CO₂ and greenhouse gases in the urban environment has risen significantly between industrial revolution and modern period. By 2010, the emission concentrations had risen from 260 ppm to 400 ppm (UN, 2011).

With regard to growth of the cities many problems emerged. To illustrate, air pollution and global temperatures increased, approximately 50% of wetlands and forests of the world were lost, many lands were altered to agriculture field, and many countries destroyed their green areas for urban development (MEA, 2005). For instance, in New York City, 20% of forestlands were eradicated because of increasing urban density during the 1990s (Santamouris, 2004). Thus, urbanization became responsible for the pressure on the environment and climatic conditions of Earth.

Urban areas dramatically affect not only global but also local climates. The expansion of the boundaries of the urban areas on their environs causes modification on surface cover of rural characteristics. In addition to the change of surface cover, such as establishing impermeable surfaces instead of vegetation, increase in urban roughness also affects the circulation of heat, water vapor and greenhouse gases, which leads to climatic differences between urban areas and its surroundings (Yüksel, 2005).

Cities create new environmental conditions by changing the parts of nature where they were located. They alter the geographical, ecological and atmospheric characteristics of the region, so the city acquires its own, specific climatic environment which is called 'Urban Microclimate' (Akay, 1996). In other words, it can be defined as a shift from natural environment to man-made environment.

As Givoni (1989) states,

“The climatic conditions in a man-made urban environment may differ appreciably from those in the surrounding natural or rural environs.. each urban man-made

element: buildings, roads, parking areas, factories, etc.. creates around and above it a modified climate with which it interacts.”

Urban microclimate, which is formed by the complexity of morphological conditions of urban areas, influences temperature, air pressure, wind, humidity and precipitation of the prevailing region climate (Yılmaz, 2013). Krusche et al. (1982) revealed that, in urban areas, the average annual precipitation is 5-10% higher, humidity is 6% lower, air temperature is 1-2°C warmer, wind speed is 20-30% lower, cloudiness is 5-10% higher and level of atmospheric pollution is 10 or 25 times greater than their rural surroundings (Yüksel, 2005). In addition, sunshine duration is 10-20% lower (Landsberg, 1981).

The differentiation in air temperature, which can be observed as higher values in the urban areas, has been the subject of many studies as an Urban Heat Island phenomenon since it had negative impacts on thermal comfort and human health. In the 17th century, the rise of health concern stemming from increase of heat and air pollution conducted to detection of air temperature difference between urban and rural areas. However, at the beginning of the 19th century, the need for observation and indication of temperature and how it is affected by urban areas was brought up in a study by Luke Howard. He recorded daily temperature data for more than two decades in urban and rural areas of London and generated a basis for UHI definition from examination of highest and lowest daily temperatures. Afterwards, he associated heat difference to urban density by determining that densely located buildings are warmer than widely spaced ones and revealed the spatial distribution and variation of temperature (Stewart, 2011).

The UHI studies spread from Europe to other regions of the world, such as North America and Japan, following Howard’s findings. In fact, in the 1900s, the foremost reason for disseminating heat island knowledge is the growth of urbanization. The shift of the most of the world population to urban areas has raised the consciousness about the effect of human being on climatic environment (Stewart, 2011). In other words, the literature shifted its focus to the anthropogenic effects on heat island. For example,

Kalma (1974) developed a map of Sydney showing the spatial distribution of anthropogenic heat flux.

In the modern period of UHI investigation, progress in understanding of heat island formation provided by Oke's studies. Oke (1988a) linked the magnitude of heat island effect to the energy balance of urban areas, and improved the knowledge of the association with the urban microclimate. He has also conducted numerous studies about physical causes of the formation of UHI, and thus has correlated it to the urban population, weather condition, thermal properties of surface materials and urban canyon geometry. Following his studies, several researchers have contributed to the field as providing estimation of heat island intensity and mitigation strategies for that.

As a result of all these studies, warmth characteristics of surface and air temperatures in the environment are described according to urban areas and its surroundings. The temperature difference between them is called as Urban Heat Island (UHI) intensity. It has been explored in certain ways, such as thermal image capturing by remote sensing, data collection from weather stations and ground-based measurements. In urban areas, the mean air temperature is determined be minimum 1 to 3°C warmer than suburban or rural areas, and it can be reach up to 10 - 12 degrees (EPA 2008; Oke, 1973). The magnitude of the heat island intensity may vary from to day/night time, winter/summer period, tropical/arid climate or other weather conditions. Nevertheless, the best time for the measurement is cloudless and calm sky conditions in the summer period because of the warming effect of the solar radiation can be observed in maximum level. For example, in Gothenburg, Sweden, the UHI effect was estimated 3.5°C in winter and 6°C in summer time (Santamouris et al., 2001). Oke and East (1971) observed that nocturnal heat island intensity in Montreal, Canada was nearly 10.5°C. Sani (1973) also conducted a study for heat island effect of Kuala Lumpur in different sky conditions, and found that the city was warmer 2 - 2.2°C in cloudy day, but under clear sky it was close to 5°C.

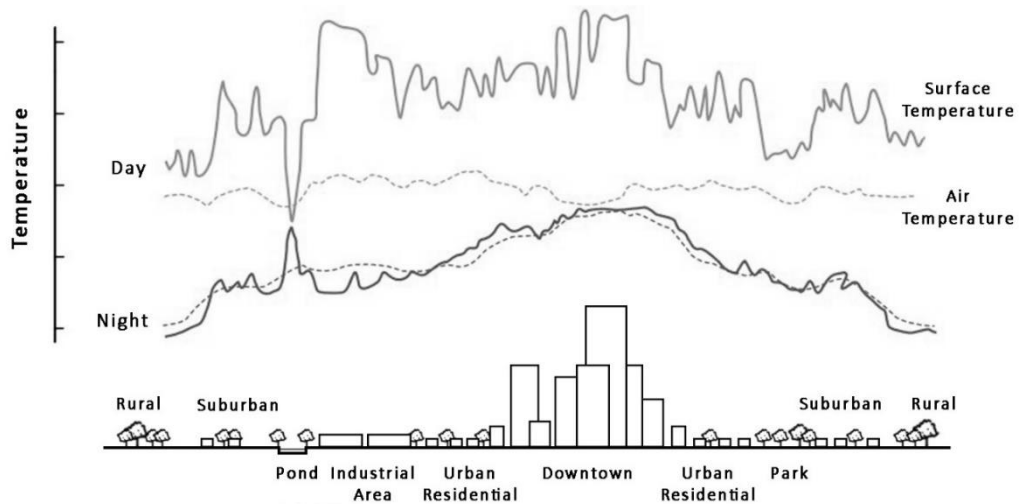


Figure 2.1: Spatial distribution of surface and air temperatures (Source: EPA, 2008)

The well-known temperature fluctuation in terms of urban heat island as to urban development is given in Figure 2.1. This schematic heat island pattern shows that there is a sharp heat increase in the transition from rural area to suburban area, and then it was followed by smooth increase until the highest temperature level at the downtown area of the city (Voogt, 2004). To illustrate, daily heat island effect was observed 15°C in the central area of Athens, and the rest of the urban areas' temperature was recorded close to 10°C. In addition, in the suburban area, temperature ranged from 2 to 6°C (Santamouris et al., 2001).

2.1.1. Formation of UHI

Energy balance is the main driver behind the ambient air and surface temperature differences between built and natural environment. Impermeable surface materials with a low reflectance, limited sky view due to urban geometry, lack of vegetation and water bodies as a result of urbanization features all cause disparity in heating and cooling capacity. As a consequence, heat storage capacity of cities increases through absorption and storage of solar radiation in higher amount. Moreover, with the high level of surface emissivity, more heat is being gained because of inadequate reflection of incoming radiation. As a result of the energy flux, when the thermal balance of the

environment turns into positive, the heat of the environment increases and it conduces to development of Urban Heat Island effect (Erell et al., 2011; Oke, 1988a; Santamouris et al., 2001).

2.1.1.1. Physical Principles of Energy Balance

Principles of energy balance system are based on Thermodynamics Law (Ashrafizadeh and Tan, 2018). In Einstein’s words, “Energy cannot be created or destroyed, it can only be changed from one form to another.” It means that the incoming energy flux can only be converted to outgoing energy and stored energy (Santamouris et al., 2001).

$$Energy\ input = Energy\ output + Energy\ storage$$

In the environment, energy is transferred from natural and artificial surfaces to the atmosphere and vice versa (Oke, 1988a). Energy gains of surfaces consist of absorption of both short-wave and long-wave radiation. Especially, from the short-wave radiation, surface materials can get a huge amount of heat (Brunt, 1952; Tymkow et al., 2013). However, it also depends on the ability of reflection. As seen in Figure 2.2, some of the rays from the sun are trapped and some are reflected. The less reflection ratio becomes, the more absorption amount becomes. Thus, substances warm up (Erell et al., 2011). According to the physics laws, when a substance heats up, the ambient air temperature increases (Bergman et al., 2011). Higher air temperature in the urban environment can be explained by overheated urban surfaces, such as roofs, pavements and facades, causing heat transmission to the air (EPA, 2008). 2008).

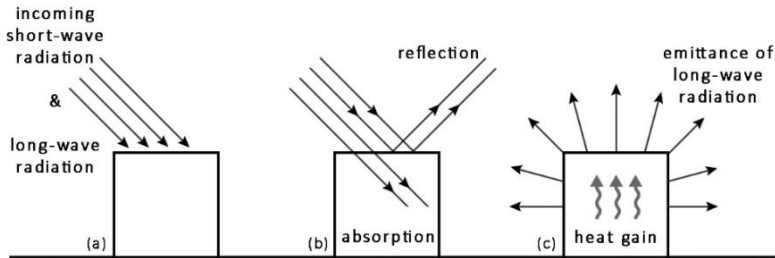


Figure 2.2: Energy conversion system in the environment (Source: personal drawing)

As a result of increased warmth of surfaces, objects emit long-wave radiation which is measured as a level of emissivity (Oke, 1988a). Warmer surfaces radiate more infrared energy, which explains fundamentals of remote sensing (Mather and Koch, 2011; Oke, 1987). Infrared scanners on thermal remote sensors sense surface temperature differences between urban and rural areas. Therefore, satellite images of cities have been used to quantify surface UHI intensity (Dousset, 1992; Voogt and Oke, 2003). Apart from energy gain, energy can be lost from surfaces via convection, evapotranspiration and advection. Convection is a process of heat transmission through flow of fluids from surfaces (Bejan, 2013). In urban areas, convective heat transfer from impermeable and dry surfaces causes rising air temperature. However, energy lost by evapotranspiration from moist surfaces does not result in more heat increase (Erell et al., 2011). In evapotranspiration, vegetation areas use stored energy to release heat in the form of water vapor (Suomi, 2014). Energy losses can also be caused by advection, which is defined as horizontal air flow transporting heat or moisture between different land covers (Erell et al., 2011; Santamouris et al., 2001). In brief, all these energy gains and losses can be expressed in an equation of energy balance (Oke, 1988a):

$$Q^* + Q_F = Q_H + Q_E + \Delta Q_S + \Delta Q_A$$

Where:

Q^* = Net all-wave radiation

Q_F = Anthropogenic heat flux

Q_H = Convective sensible heat flux

Q_E = Latent heat flux

ΔQ_S = Net storage heat flux

ΔQ_A = Net horizontal heat advection

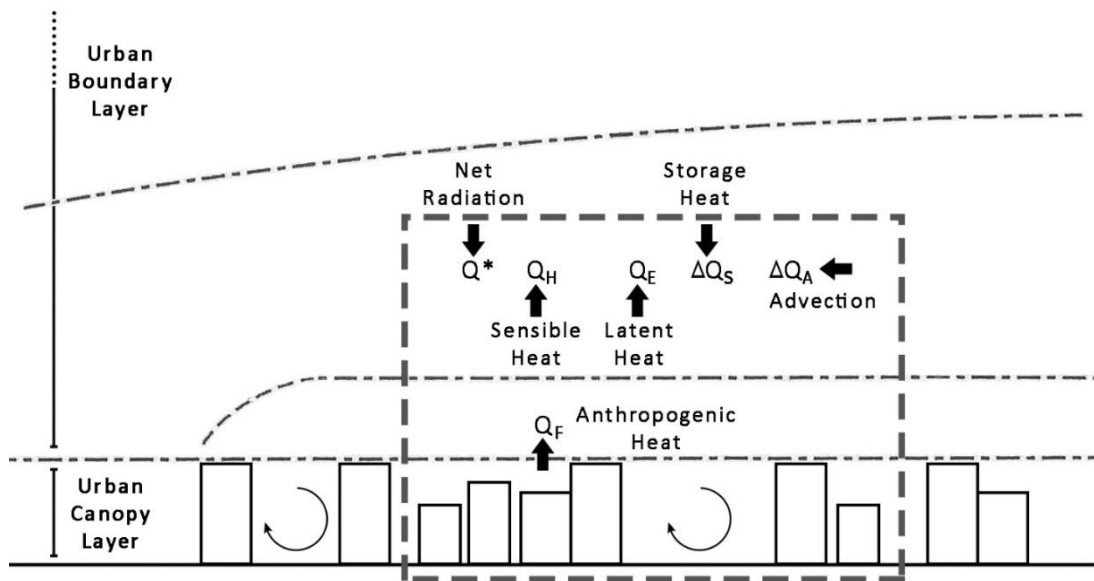


Figure 2.3: Schematic depiction of energy balance components (Source: Erell et al., 2011)

Figure 2.3 illustrates energy balance is provided by the transfer of its components between urban surfaces and different layers of the atmosphere. Oke (1976) classified them into two main layers in relation to different types of UHI formation. Firstly, Urban Canopy Layer (UCL), which is observed between the buildings and limited by their heights. Secondly, Urban Boundary Layer (UBL), which extends from the top of the UCL to a distance where urban areas effects cannot be perceived. Due to spatial variations of urban surfaces, wide spectrum of energy fluxes occur above UCL (Oke, 1988a).

In detail, net radiation (Q^*) is comprised of subtraction of emitted radiation from the sum of received solar radiation. Thus, the amount of net radiation depends on thermal properties of surface materials (Erell et al., 2011; Santamouris et al., 2001). In addition to radiation-caused heat, human activities also contribute as anthropogenic heat flux (Q_F) to warm up. It can be quantified by per capita energy consumption (Oke, 1988a). In general, the role of anthropogenic heat and net horizontal heat advection (ΔQ_A) are considered negligible in the calculation of energy balance (Cleugh and Oke, 1986). Convective sensible heat flux (Q_H) and latent heat flux (Q_E) are most significant components of energy balance in respect of UHI development. Sensible heat is

convection process from dry urban surfaces (concrete buildings, asphalt pavements, etc.) to the atmosphere when they have temperature differences between them. In built-up areas, absorbed radiation is converted to sensible heat because of limited evaporation surfaces that results in air temperature increases. On the contrary, moist urban surfaces, such as vegetated and irrigated lands, convert energy as latent heat through evapotranspiration (Erell et al., 2011; Oke, 1988a; Pearlmutter et al., 2009). Oke et al. (1999) have demonstrated that latent heat composed only 4% of the net radiation in central area of Mexico City. Nonetheless, 58% of the net radiation is stored as heat by urban fabric, and remain amount, which is 38%, is released as sensible heat due to lack of available moisture. Therefore, the equilibrium between sensible heat and latent heat fluxes depends on permeability and humidity of urban environment.

Additionally, another important component is net storage heat flux (ΔQ_s), which is storage of surplus energy as heat by urban fabric during daytime (Erell et al., 2011). The high level of storage heat is based on surface types and their thermal properties. For example, the heat storage capacity of impervious surfaces, such as pavements, is higher than green spaces' capacity (Grimmond and Oke, 2002). Such surfaces trap energy easily all day and store them. They have small changes in their surface temperatures during night, so the heat is maintained (Oke, 1988a).

2.1.1.2. Energy Balance Differences between Urban and Rural Areas

Energy balance of urban areas differentiates from rural areas because of the impacts of urban development on energy fluxes. Due to low evaporation rates and high level of absorption by impermeable surfaces, different amount of energy fluxes, such as sensible heat flux, latent heat flux and storage heat flux, have emerged (Cleugh and Oke, 1986; Oke, 1988a; Santamouris et al., 2001). For instance, heat storage flux, which is a significant indicator about air temperature, was observed in a rural area as one-third of an urban area. Nevertheless, the amount of latent heat of rural area was indicated three times as high as urban area (Suomi, 2014).

In addition, energy fluxes not only differentiate between urban and rural areas but also can vary according to land use. In urban centers, particularly, heat release slows down, energy lost cannot occur in a significant level, and then heat goes up. As Clarke et al. (1982) state, sensible heat shows an increase from approximately $140\text{-}150\text{ W/m}^2$ for a rural area to 200 W/m^2 for an urban residential area and to 300 W/m^2 an urban commercial area, which is the most built-up site. As a result of these changes in energy fluxes, air temperature becomes higher in urban areas rather than rural areas so all cause UHI formation.

Temperature differences between urban and rural areas can be explained by two main reasons for improving better understanding of UHI development. Firstly the type and amount of energy transfer from surfaces can change depending on land cover, permeability of surfaces, availability of moisture, urban geometry and thermal properties of urban surfaces. Despite the fact that both urban and rural areas receive the same amount of solar radiation, urban areas store higher amount of heat while rural areas release higher amount of latent heat (Erell et al., 2011; Santamouris et al., 2001). Cleugh and Oke (1986) have demonstrated that rural and suburban areas have different energy flux densities between them. As seen in Figure 2.4, the net radiation gain of suburban area is greater than rural. The reason is that natural surfaces of rural area release latent heat and sensible heat instead of storing energy as heat. On the contrary, in suburban area, buildings and other dry surfaces store huge amount of heat. Therefore, air temperature can be sensed higher in suburban area.

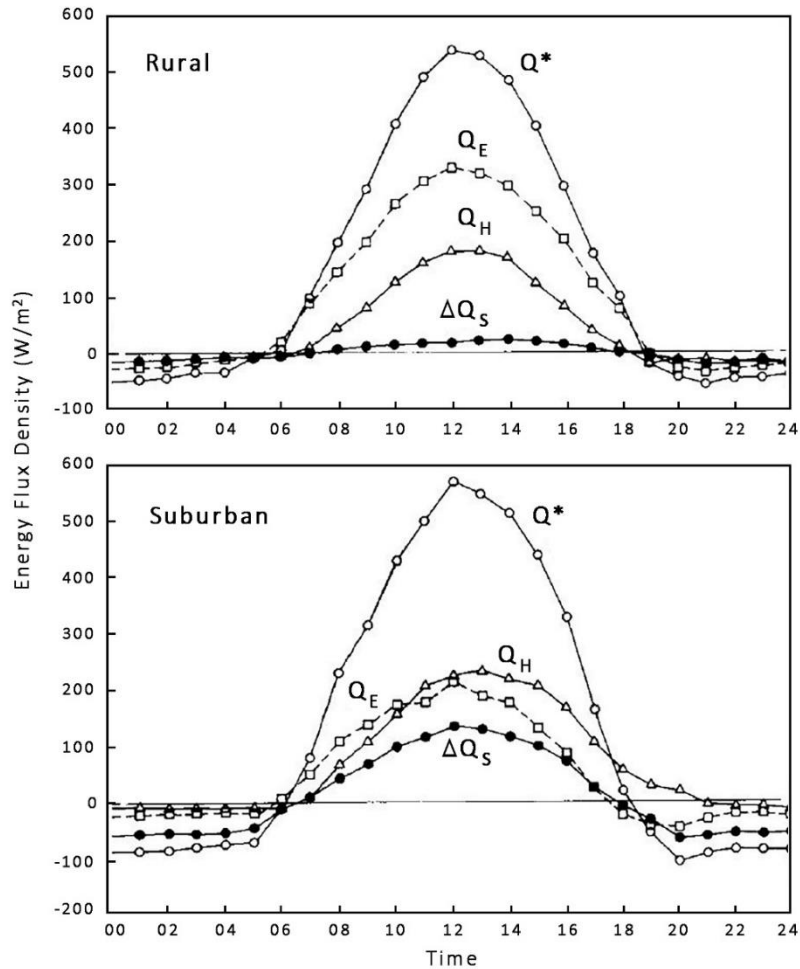


Figure 2.4: Energy balance of rural and suburban areas (Source: Cleugh and Oke, 1986)

On the other hand, the second reason is based on energy transfer speed. In other words, urban and rural areas have different heating and cooling rates because of their surface varieties (Oke, 1982; Yilmaz, 2013). In general, during daytime, urban surfaces store huge amount of heat and release sensible heat. It can be considered as positive net radiation. After sunset, surfaces started to reach a balance with storage heat loss, and it goes on during a night. Day after, energy balance become positive again with recharging of heat storage (Erell et al., 2011). The important thing in energy transfer process is to cool of surfaces in a short time before heat gain in the next morning.

Oke (1982) have shown that the foremost reason for increasing air temperature in urban areas is that rural areas cool faster than urban areas. In the afternoon, the heat

balance between urban and rural areas seems steady as given in Figure 2.5. As the sun's effect decreases, rural area is cooling down when urban area preserves its warmth. After, both areas continue to release heat during night but they have maximum temperature difference at that time, which is called UHI intensity (ΔT_{u-r}). In fact, nighttime formed UHI intensity is known as nocturnal UHI.

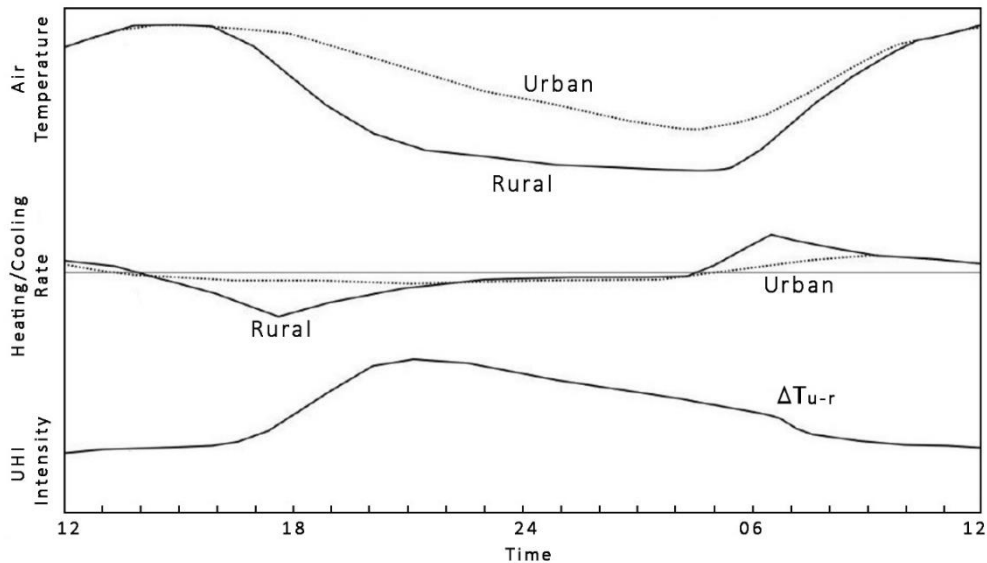


Figure 2.5: Daily heating/cooling rates and air temperature changes in urban and rural areas (Source: Oke, 1982)

2.1.2. Causes of UHI

In the formation of UHI, changes in the thermal balance of the environment can be defined as the main influential factor. The magnitude of the heat island intensity may vary to the climate, geographic location and urban layout of the cities. In particular, outcomes of the urbanization, such as densely built-up areas, radiative urban geometry, increased human activities due to population growth, anthropogenic heat release via energy consumption, the replacement of natural ground coverages by low reflective surfaces, demolition of moist surfaces or vegetation areas, and reduced wind speed within the streets, cause temperature increase and make cities warmer than their

surroundings. These modifications in urban areas create complex radiation exchange between the surfaces and the atmosphere, and thus contribute to more intensive heat island effect (EPA, 2008; Oke et al., 1991; Santamouris et al., 2001).

2.1.2.1. Urban Population

The growth of urban population leads to increase in the air temperature due to dense urban areas and surface materials of built-up areas (Oke, 1976). Therefore, population size is used as a criterion to determine heat island effect. Many studies examined the effect of population on the magnitude of UHI. According to Chandler (1964), a relation between them does not exist. However, Sundborg (1950) demonstrated a relevance for the first time (Oke, 1973). Because of certain limitations of Sundborg's model, Oke's proposal has been the most well-known model.

Oke (1973) established a strong correlation between the logarithm of the population and temperature differences for North American and European cities. Minimal temperature increase, which is at least 1 degree, was observed even in 1000 habitant villages. This increase may further was recorded to be as high as 12°C depending on the growth of population size. According to these observations, new equations were formulated for calculation of the UHI intensity for different regions.

The equation for North American cities is as follows:

$$\Delta T_{u-r} = 2.96 \log P - 6.41$$

The equation for European cities is as follows:

$$\Delta T_{u-r} = 2.01 \log P - 4.06$$

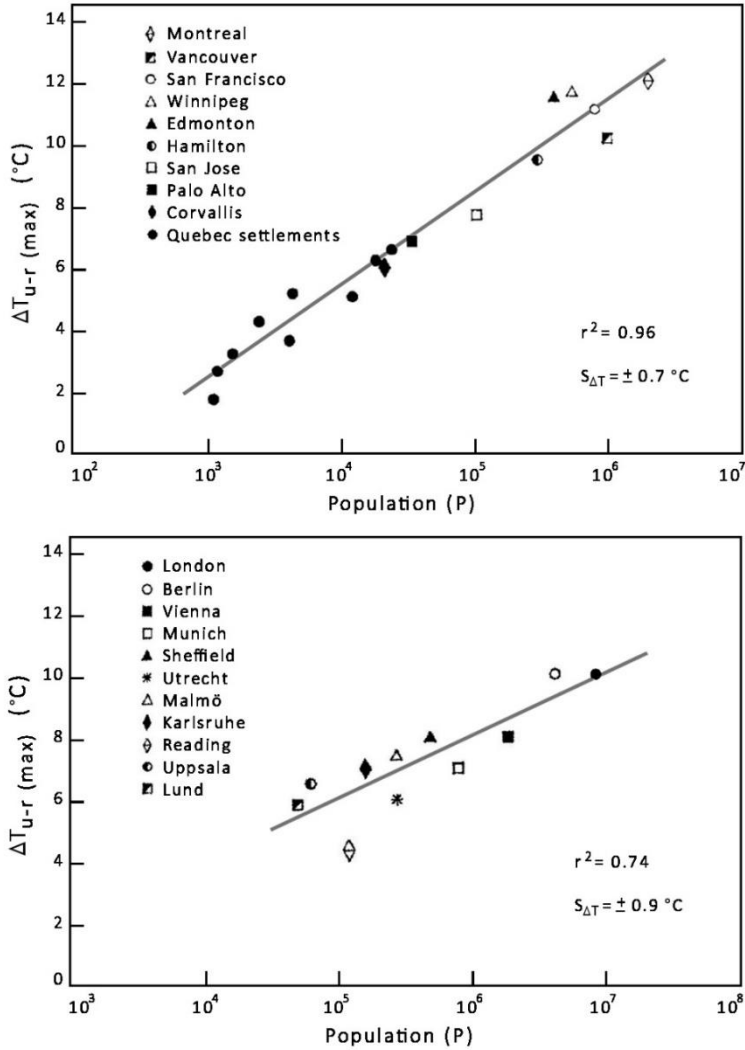


Figure 2.6: The relation between UHI intensity ($\Delta T_{u-r(max)}$) and population ($\log P$) for North American (a) and European (b) cities (Source: Oke, 1973)

2.1.2.2. Urban Geometry

Urban geometry is defined as one of the most important reasons for the development of heat island effect. In particular, form, location, orientation, height of the buildings and spaces between them are the main parameters of the urban geometry. It has also been characterized by the repetition of urban canyons, which are consist of horizontal and vertical elements of urban fabric. Such building implementations as an urbanization features are responsible for the alteration both on the microclimate and

the energy balance of the environment.

Urban canyon is recognized as a basic unit of urban surfaces, and thus it has been the subject of numerous studies. The energy balance of urban canyons, which consist of building surfaces, canyon floor and the air volume between the buildings, is mainly influenced by its own geometry. As the depth of the urban canyon (length of the canyon and height of the buildings) has changed, energy fluxes on the surfaces directly affect the air temperature in the canyon (Nunez and Oke, 1977; Santamouris et al., 2001). Therefore, heat island intensity is getting greater with the repetition of this effect throughout the city. For the first time, Nunez and Oke (1977) evaluated a model of energy balance in the urban canyon and its formulation as a result of the measurement on an experimental canyon during a summer period in Vancouver. According to this measurement, the main influential factors on the heat gain are found as canyon geometry and canyon orientation.

The energy balance of an urban canyon is written as:

$$Q^* = Q_H + Q_E + Q_G$$

Where:

$$Q^* = \text{Net all-wave radiation flux } (W/m^2)$$

$$Q_H = \text{Sensible heat flux to the air } (W/m^2)$$

$$Q_E = \text{Latent heat flux } (W/m^2)$$

$$Q_G = \text{Subsurface heat flux } (W/m^2)$$

The ratio between the main parameters of urban canyon that mentioned before as height (H), width (W) and length (L) are defined to determine the depth level of the canyon. To illustrate, a shallow canyon is considered as below 0.5 H/W ratio while a deep canyon has H/W ratio over 2. In addition, length of the canyons are also defined with the use of L/H ratio (Bakarman and Chang, 2015; Shishegar, 2013).

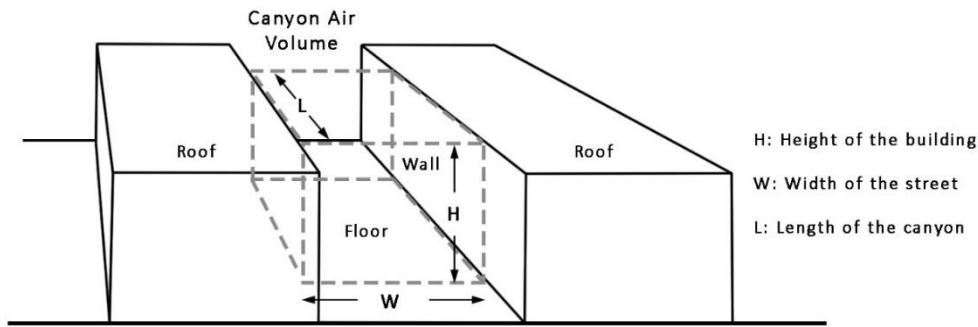


Figure 2.7: Schematic depiction of an urban canyon (Source: Nunez and Oke, 1977)

Many studies clearly showed that the surface temperature in the urban canyon is higher by 10-13°C than the air temperature. Moreover, the air volume inside the canyon has a greater temperature compared to the air flow, which has an unchanged wind speed by any obstruction above the canyon. During the day-time, the net radiation balance of an urban canyon becomes positive so the air in the canyon is warmed up. Additionally, due to the geometry of the canyon, limited sky view and heat release through emissivity, a remarkable heat loss cannot occur. As the canyon gets deeper, the rate of heat loss is slower, and the air temperature is sensed higher (Santamouris et al., 2001). According to Pearlmutter's (2009) study, when the canyon depth is doubled (from single building height to double height), the density of net radiation flux (Q^*) is increased by 50 W/m^2 showing that heat is stored in there.

In general, the effect of urban geometry on the magnitude of UHI effect can be explained by two main reasons. Firstly, a high amount of absorbed radiation by urban structures causes a rise in the air temperature. Increased irradiated surface area, configuration of buildings and rugosity of roof level have a significant impact on that increase. Before urban development, surfaces were exposed to the same amount of solar radiation, and they could directly reflect the incoming rays. However, the addition of new horizontal and vertical surfaces in urban areas, such as building walls and roofs, increased the total surface area. Their warming effect is exponentially greater because these surfaces trap not only incoming short-wave radiation from the atmosphere but also reflected radiation from building surfaces. This transition of radiation between

buildings is called as multiple reflection, which is mainly caused by configuration of buildings. In built-up areas, when high-rise buildings are located too close to each other or deeper canyons are arranged, reflected incoming radiation is absorbed again and again by building surfaces instead of released to the atmosphere as seen in Figure 2.8 (Erell et al., 2011; Yilmaz, 2013).

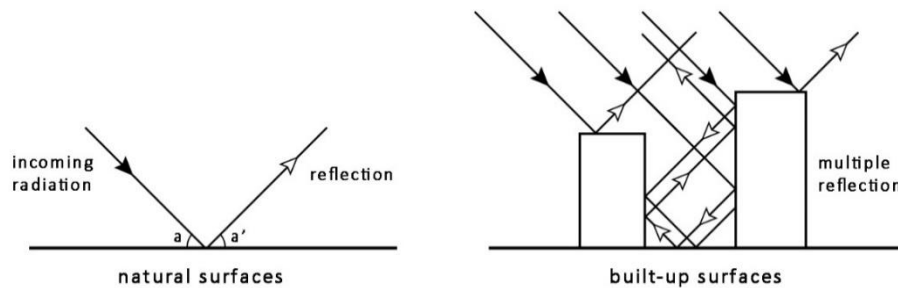


Figure 2.8: The reflection of incoming radiation from different surfaces (Source: personal drawing)

On the other hand, created various heights by buildings increase the roughness of urban surfaces that result in high level of absorption. To avoid interception of reflection by another facade, uniformity of roof level should be provided like North African cities with same height buildings and flat roof level. In brief, all these multiple reflections and absorptions result in an increase in both surface temperature of the buildings and air temperature between them (Erell et al., 2011).

Secondly, another impact of urban geometry is that weakened ventilation throughout canyons. In heat island studies, the continuity of prevailing wind for providing heat extraction or advection from canyons has gained importance. Generally, wind has a certain speed and flow pattern over the terrain until it encounters with an urban structure. Any change in an urban canyon, such as alteration in building height or street width, causes extreme modifications in the direction and cooling effect of the air flow (Santamouris et al., 2001; Shishegar, 2013). To ensure the cooling effect, Oke (1988b) has specified threshold wind speeds for different air flow patterns, which are characterized by H/W ratios. The velocity inside the canyon should be higher than the threshold value that is calculated approximately between 1.5-2 m/s for medium

($H/W < 2$) canyons. Many investigations with the use of air flow simulations or field measurements demonstrated that the wind speed is significantly decreased in the deeper canyons. Even shallow canyons have a negative impact on that.

Moreover, the importance of wind direction that can be parallel or perpendicular to the canyon is established by many studies. For instance, Arkon and Özkol (2013) have estimated that perpendicular wind angle to the canyon axis caused 3 m/s decrease in the velocity. According to Priyadarsini and Wong's (2006) parametric study on the modification of urban geometry and air flow, when high-rise buildings were located strategically, the temperature decreased by 1°C with parallel air flow and 90% increase in the velocity. For perpendicular flow, the velocity was also increase and the air temperature decreased by 1.1°C in an urban canyon which has a larger H/W ratio.

2.1.2.3. Thermal Properties of Urban Surfaces

Thermal properties of urban surface coverages are differentiated from rural ground coverages. In fact, surface materials are characterized by their heating and cooling capacity, thermal conductivity, emissivity and reflectivity due to their impact on energy balance of the environment. The reflectivity of incoming solar radiation of surfaces, which is called albedo, is one of the most important consideration in heat island studies. All these thermal properties have an influential role in the formation of surface temperature. Higher surface temperatures are responsible for the increase in the air temperature and UHI effect because of the use of inappropriate materials in urban areas (EPA, 2008; Santamouris et al., 2001; Erell et al., 2011).

One of the thermal characteristics of surface materials is defined as thermal conductivity, which is an amount of energy that substances can store during daytime. The level of thermal conductivity determines heating or cooling capacities of surfaces (Oke, 1987). The combination of thermal conductivity and heating capacity of materials constitute a measure of thermal admittance showing the reaction of surfaces to the incoming radiation. Materials with high level thermal admittance denote small changes in their surface temperature because of the heat is stored by the substances

(Oke, 1988). In brief urban surfaces have high level of thermal conductivity/admittance than rural areas that indicates the reason of the air and surface temperature differences between them. Another thermal property is the level of emissivity that taken into less consideration due to it has smaller impact on heat island intensity than other parameters (Santamouris et al., 2001). Oke et al. (1991) demonstrated that increase of emissivity level from 0.85 to 0.1 results in 0.4°C increase in the UHI development. Unlike this effect, differentiated thermal admittance of urban and rural surfaces causes 2°C increase in the heat island intensity.

Apart from other thermal parameters, the albedo of artificial and natural materials influences their energy fluxes according to reflectivity levels (Erell et al., 2011). Albedo can be defined as a fraction indicating that the reflectance of solar radiation from surface to the atmosphere. Due to the main forces behind the energy balance in the environment is amount of absorption or reflection of solar radiation, any small changes in albedo value can alter the heat balance (Banihashemi, 1995). As the albedo increases, the reflectivity increases, and thus the surface is not overheated. It means that lower surface temperatures caused by higher albedo values.

The albedo value is within a range of 0 to 1, where represent all incoming solar radiation is absorbed whereas 1 means that radiation is completely reflected. In other words, these values denote black and white colors, respectively. (Şimşek, 2013; Banihashemi, 1995). Because of that albedo and surface temperature may vary in a wide range when surface coverages are in different colors, for example, white facades were found to be 3°C colder than the other different colored facades (Parker and Barkaszi, 1997). Taha et al. (1992) documented a report about albedo values and temperatures in different surface materials in summer period. They found that white covered surface has an albedo of 0.72 is 45°C cooler than black covered one, which has an albedo close to 0.08. Moreover, another white surface (0.62 albedo) is just 5°C warmer than ambient air temperature while darker surface (0.09 albedo) is 30°C warmer.

Many investigations are conducted about the range of albedo values in relation to air

and surface temperatures, and their main focus was on the pavement and roof materials. Table 2.2 gives compiled results of studies about albedo values of different materials and ground coverages in urban areas. Accordingly, conventional paving materials have an albedo of 0.05 to 0.35 (asphalt and concrete) so it means that they can reflect only 5 - 35% incoming radiation. However, their reflectivity can change by turning lighter color overtime because of the weather condition or pollution (EPA, 2012). In addition, the surface temperature of asphalts is measured 5-8°C higher than other pavement materials, such as concrete and slab (Asaeda et al., 1996; Santamouris et al., 2001).

Table 2.2: Albedo values of surface materials (Source: Santamouris et al., 2001)

Surface	Albedo	Surface	Albedo
Pavements		Paints	
Asphalt	(fresh) 0.05 - (aged) 0.2	White	0.50-0.90
Concrete	0.10-0.35	Red, brown, green	0.20-0.35
Whitewashed stone	0.80	Black	0.02-0.15
Light-colored brick	0.30-0.50	Ground coverages	
Red brick	0.20-0.30	Light-colored sand	0.40-0.60
Dark brick	0.20	Dry sand	0.20-0.30
Limestone	0.30-0.45	Wet sand	0.10-0.20
Roofs		Dark cultivated soils	0.07-0.10
Tile	0.10-0.35	Deciduous plants	0.20-0.30
Slate	0.10	Grass and leaf mulch	0.05
Corrugated iron	0.10-0.16	Dry grass	0.30
Highly reflective roof	0.6-0.7	Wood (oak)	0.10

To increase reflectivity and thermal performance of roof surfaces, light colored tints are tended to use as roof coatings. Thus, albedo of conventional roofs can be increased from 0.2 to 0.7, and its temperature can be reduced by a significant amount (Akbari et al., 2006). To quantify surface temperatures of different colored coatings, Backenstow (1987) measured panels' heat under clear and cloudy sky conditions. As a result of that the highest temperature is determined for black colored (70°C) in high heat absorption day, which is a cloudless day. As given in Figure 2.9, surface temperature of darker panel is followed by beige and white colored surfaces that are approximately 55°C and 40°C, respectively. Despite the reduction in the amount of incoming radiation due to weather conditions, both measurements show that grey or black surfaces have always higher temperatures than lighter colored ones (Taha et al., 1992; Santamouris et al., 2001).

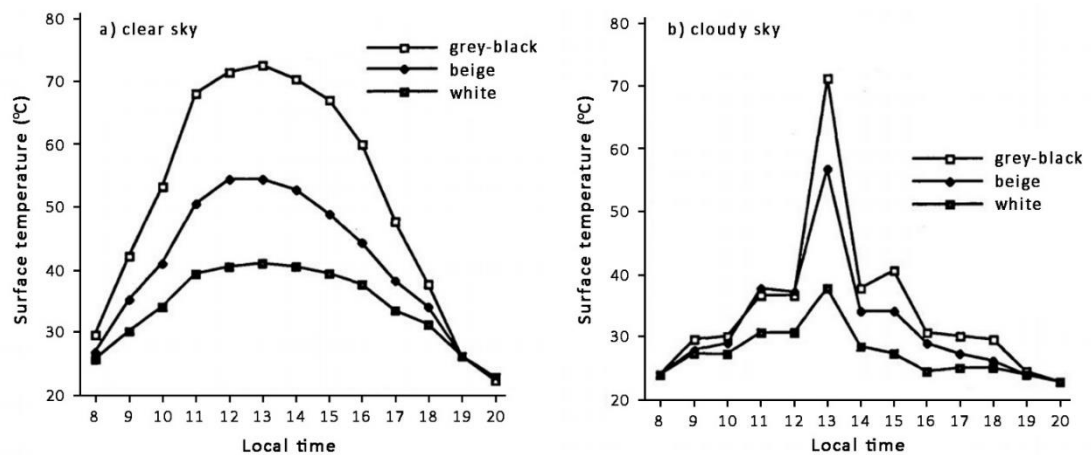


Figure 2.9: Daily surface temperatures of different colored panels (Source: Taha et al., 1992)

In many research, the mean albedo values of urban and rural areas were measured by remote sensing correspondingly heat island effect, instead of measuring one by one surface materials of albedo. For example, urban areas have nearly 0.14 albedo because of the domination of darker surfaces compared to rural areas, which have 0.05 lower value. Moreover, American, European and North African cities have different albedo values according to their density, urban geometry and roof color. In general, American and European cities are tend to use dark colored roofs so their albedo in within a range of 0.10-0.20. On the contrary, dense, low-rise and white colored buildings/roofs with African cities have change in 0.30-0.45 (Taha, 1997; Erell et al., 2011).

2.1.2.4. Lack of Vegetation Areas

Green areas have a significant role as a natural cooling mechanism in the urban environment. They contribute to creating lower temperatures through evaporative heat loss. However, in urban areas, vegetation areas are considerably reduced because of the replacement of natural surfaces by artificial ones. Undoubtedly, urban areas can be considered as dry fields due to domination of concrete buildings and asphalt pavements. In the absence of vegetation areas, urban surfaces exhibit moisture-reducing characteristics. As a consequence, diminished latent heat release by moist surfaces induce UHI development (Akbari et al., 1992; Sailor, 1994; Santamouris et

al., 2001; Erell et al., 2011).

The effect of vegetation areas on air and surface temperatures is related to the energy balance of the environment, and is compound of two main causes. One of them is that they reduce penetration of incoming solar radiation to surfaces by shading. In other words, they provide solar protection to areas and prevent surface heating during summer period (Santamouris et al., 2001). Otherwise, radiation can be absorbed by surfaces, and thus it contributes to the increase of air temperature by releasing sensible heat, instead of absorbed by trees (Erell et al., 2011). Another reason is based on energy transfer to the latent heat flux by evapotranspiration. In vegetated surfaces, high level of evaporative cooling effect causes an increase in the release of latent heat while decreasing sensible heat (Santamouris et al., 2001; Akbari et al., 1992).

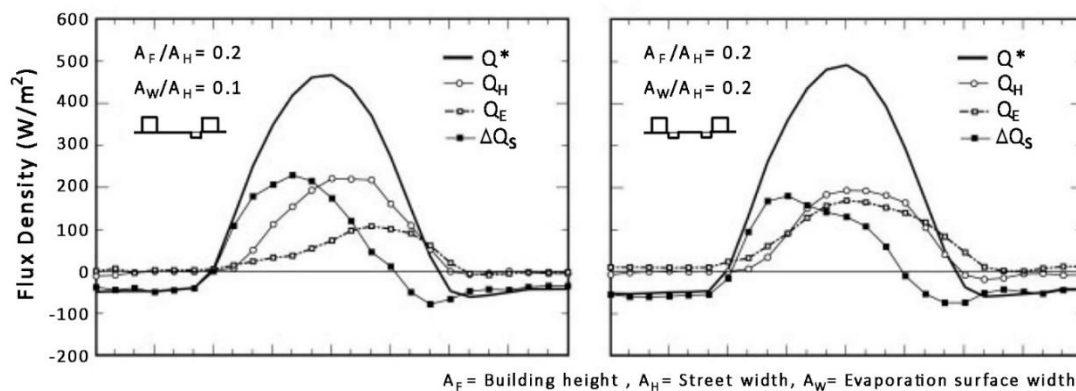


Figure 2.10: Daily energy fluxes for two configurations of canyon depth and evaporation area (Source: Pearlmutter et al., 2009)

Pearlmutter et al. (2009) found that latent heat flux is increasingly growing with the addition of evaporation surfaces to the fixed depth urban canyon. As seen in Figure 2.10, storage heat flux also decreases while latent heat increases steadily. These changes in energy fluxes result in different surface temperatures in the urban areas. Due to such surfaces have lower temperatures than dry surfaces, the air is cooled near them (Santamouris et al., 2001; Erell et al., 2011).

All in all, urban vegetation can provide many benefits, such as mitigation of UHI

effect, reduction of energy demand for cooling and improvement of air quality (Sailor, 1994; Erell et al., 2011). Many studies have been performed about the cooling effect of vegetation and have shown that, in urban areas, parks are generally 2-8°C cooler than their surroundings (Duckworth and Sandberg, 1954; Huang et al., 1990; Akbari et al., 1992; Taha et al., 1991). For instance, in Montreal, urban parks have 2.5°C lower temperature than nearby areas (Santamouris et al., 2001). Moreover, Alavipanah et al. (2015) identified remarkable cooling effect according to proportion of vegetation cover which is between 70-80% per square kilometer. The temperature difference between vegetation areas and fully covered (100%) built-up areas is observed 4.5°C in 2012. In another study, shading and evaporative cooling effects of trees on temperature reduction are calculated by computer simulations. In these simulations, which are shown in Figure 2.11, tree coverage is increased by 10% and 25%, and thus decrease in temperature in Sacramento is estimated approximately 2-5 °C (Akbari et al., 1992).

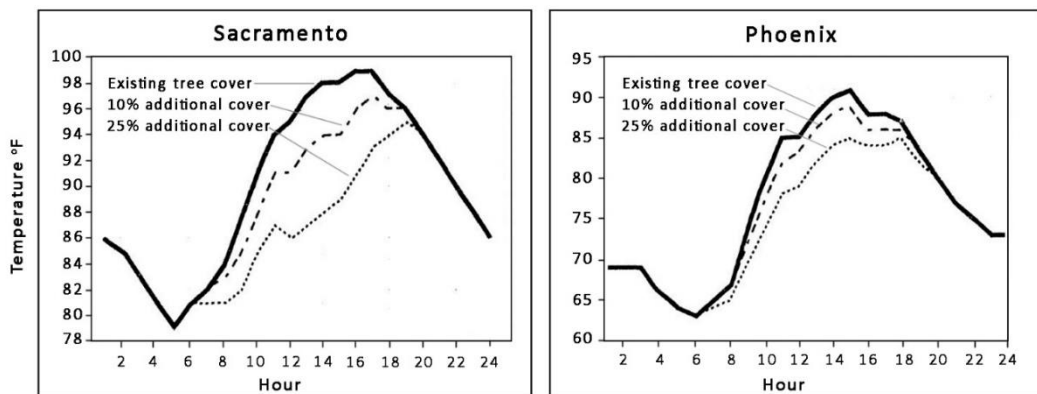


Figure 2.11: Temperature reductions in Sacramento and Phoenix with additional tree cover in summer period (Source: Akbari et al., 1992)

In addition, the magnitude of the cooling effect of green areas generally depends on plants type, vegetated field size and its location. Their effect on air temperature can be observed from nearest plot area to wider urban areas within the framework of UHI effect. According to Jauregui (1990), the cooling effect of an urban park in Mexico, with an area of 500 ha, has an impact on city-scale which is about 2 km. However,

Honjo and Takakura (1991) reported that when the wind speed is weak, cool air can only be perceived up to 300 m. Similarly, Takebayashi (2017) conducted a study about a measurement of the change in air temperature in regard to distances from vegetation areas. Estimations show that the range of rise in the air temperature is related to both distance and wind speed. As shown in Figure 2.12, the most significant rise in air temperature is occurred in the lowest wind speed in spite of being close to the vegetation area. Furthermore, the increase in ambient air temperature of urban areas has become stable when the distance from the green area is more than 30 meters.

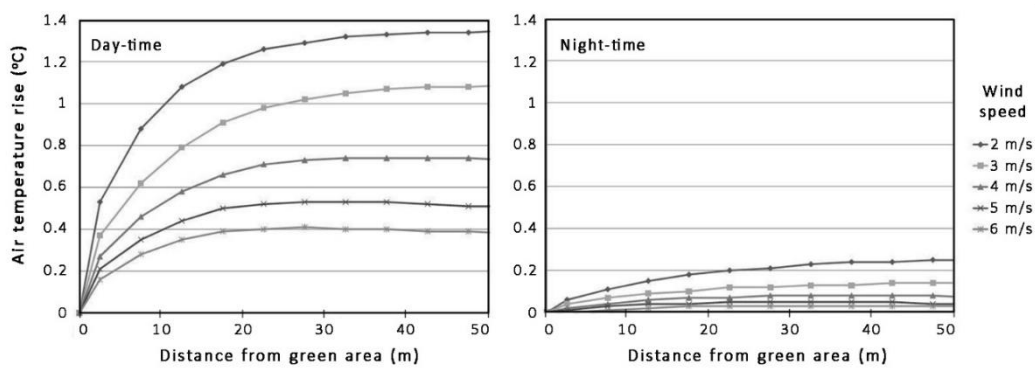


Figure 2.12: The rise in air temperature in proportion to the distance from green area during day-time and night-time (Source: Takebayashi, 2017)

According to Bilgili (2009), when the park sizes are similar, their cooling distances may vary according to the plant types. As a result of his research on cooling effects of green areas in Ankara, he found that the cooling effect from Kurtuluş Park reached about 200 meters, while Gençlik Park was limited to a distance of 50 meters. Although the vegetation areas are spatially equivalent in both parks, types of plants are differently arranged. While Kurtuluş Park is composed of broadleaf tall trees, Gençlik Park is dominated by grasses, which have reduced cooling distances than tree canopies. As Shahidan (2011) reported, tree density have an influence on microclimate and thermal balance of the surrounding urban environment. Instead of small green areas and grasslands, the variation of tree canopies can create different and effective cooling distances.

Apart from urban parks, in local scale, green roofs also have an impact on UHI

mitigation. Green roofs are used to reduce heat storage instead of standard roofing materials. For instance, a mesoscale modeling of green roof indicates that the ambient air temperature, which is reached 30°C on a hot summer day, is lowered by 1°C through reduced sensible heat flux by 52% compared to the darker roof (Scherba, 2011). Conventional roof surfaces with low reflectivity can heat to 65°, while the air temperature reaches 35° during the summer (Karaosman, 2006). These roofs are always warmer than ambient air temperature in their environment. In contrast to that, green roofs can prevent air and roof surfaces from getting warmed by providing moisture balance. In other words, they provide protection against overheating, and thus the heat transfer between outside and interior of the building is delayed. Therefore, they can be considered as an increased vegetation areas in urban areas that helps to reduce heat island effect (Zareiyan, 2011).

2.1.2.5. Anthropogenic Heat Release

Urbanization is responsible for artificial heat release due to energy demand of human activities. The magnitude of anthropogenic heat release mainly related to heating or cooling of buildings, industrial activities, fuel combustion from vehicles (or in general, transportation system) and human metabolism, which is considered less important (Oke, 1988; Santamouris et al., 2001; Erell et al., 2011). The heat release from these sources in urban areas contributes to increase in air temperature and UHI effect. Taha (1997) estimated that anthropogenic heat can increase UHI intensity by 2-3 degrees.

To quantify anthropogenic heat release, population density or energy consumption data of building sector or transportation system are regarded. In comparison of energy usage in Seoul, Incheon and Gyeonggi, Lee et al. (2008) found that anthropogenic heat fluxes are 55, 53, and 28 W m⁻², respectively. Moreover, it depends on climate zones and spatial organization of cities. Firstly, climate zones play a determinant role in energy consumption. Anthropogenic heat varies dramatically between low-latitude and mid-latitude cities because of their warm and cold seasons are completely different from each other (Suomi, 2014; Heiple, 2007; Chrysoulakis and Grimmond, 2016). In low-latitude zone, tropical and arid climates prevail in cities where warm weather is

sensed all months (Money, 2000). Such cities have largest anthropogenic heat release in summer due to exceeded cooling need or their magnitude can remain in high level throughout the year (Suomi, 2014; Quah and Roth, 2012). Nevertheless, in mid-latitude cities, which are dominated by cold winter, increased heating demand that causes greater amount of anthropogenic heat rather than cooling demand in summer for the same city (Sailor and Lu, 2004). To illustrate, the anthropogenic heat rates in US cities in the summer and winter seasons are estimated 20-40 W/m and 70-210 W/m, respectively (Hosler and Landsberg, 1977).

In brief, largest anthropogenic heat values can be defined differently as wintertime or summertime fluxes according to cities. Apart from climate conditions, another factor is associated with urban land-use distribution. In general, anthropogenic heat release is observed dramatically high level in the city centers, and it gradually decreases to the outskirts of the city. For instance, in London, heat flux exceed 400 W/m² in the city center, but in the fringe of the city the value is estimated 60 W/m². Additionally, the impact of anthropogenic heat on UHI is quantified in central London 1-1.5°C for different seasons (Bohnenstengel et al., 2014). According to Cao et al. (2018), highest daily temperatures in the downtown of Guangzhou City in China caused by anthropogenic heat release which is more remarkable in high density residential area, and it is followed by commercial/industrial area and lastly low density residential area. On the contrary, in Singapore, estimation results of anthropogenic heat variability in common land use types show that commercial area has the most significant anthropogenic heat flux. The maximum values of commercial area, high density residential area and low density residential area are measured around 113 W/m², 17W/m² and 13 W/m², respectively. In addition, because of the cooling demand, the major source of heat flux is determined as buildings in each area (Quah and Roth, 2012).

2.1.3. Negative Impacts of UHI and Need For Mitigation

The development of larger heat island intensity, due to growth of urban density, unsustainable urban development, and release of human related heat and greenhouse

gas emissions to the atmosphere from urban areas, causes climate modifications from local to global scale. At least 1°C rise in air temperature of cities has a knock-on effect on the global warming. In fact, this warming trend has negative impacts on the environment both ecological and economical, and on the human health. In particular, high temperatures in urban areas are responsible for the increase in energy consumption, air pollution and for the decrease in thermal comfort in public space. Moreover, it poses a risk for human health because of the respiratory effects of air pollutants and morbidity or mortality risks of extreme heat waves. Therefore, mitigation of UHI effect should be taken into consideration as a necessity for the community well-being (Erell et al., 2011; Santamouris et al., 2001; Shahmohamadi et al., 2010).

One of the negative effects of the UHI is that higher urban temperatures exacerbate energy consumption due to their effect on outdoor conditions influence the indoor climate, especially in the summer period of hot climates. Although, in hot-arid climates, heat island intensity reduces energy demand for heating in winter seasons, cooling demand induces more energy consumption in summer (Santamouris et al., 2001; Wong and Chen, 2009). On the contrary, as a result of a climatic simulation that shows changes in heating and cooling energy demands for European cities to increase in the global warming by 2°C, the electricity consumption for heating will be reduced up to 5.2%. Because of the domination of continental climate in Northern Europe countries, heating demand is more than the need for cooling in there (Damm et al., 2017). Moreover, in tropical climates, the magnitude of heat island and the amount of building energy consumption are crucial concerns because of the cooling demand continues throughout the year (Wong and Chen, 2009). Typical building energy consumptions in tropical climates were estimated that the most dominant was air conditioning, which comprised of 56% of the total consumption (Katili et al., 2015). In addition, Tham (1993) demonstrated that a reduction of 2°C with air conditioning in the building, in Singapore, caused 11.8 % more energy consumption. As a result of the development of UHI effect, increased cooling demand requires more energy production, which has several side effects, such as higher energy cost, thermal pollution and toxic gas emission from power plants (Arnab et al., 2013).

Another negative impact is that increased air temperatures influence concentration and dispersion of air pollution. While pollutants are released from combustion of fossil fuels, power plants and industrial activities, warm air accelerates photochemical reactions between them. Once these reactions occur, they tend to be trigger for more reactions, to contribute to the formation of smog, to increase ozone concentration and heat intensify. Therefore, higher air temperatures and air pollutions can aggravate each other (Santamouris et al., 2001; Wong and Chen, 2009). Besides that, release of emissions to generate electricity is the major problem for the environment and human health. The main emissions are carbon dioxide, carbon monoxides, nitrogen oxides, sulphur dioxide, etc. are considered to increase greenhouse gas effect and global warming (Arnab et al., 2013). They can also directly affect human health through respiration. For instance, according to a study about the relation between air pollution and patient registration in Athens, it was found that when the air pollution increased three times, the number of patients who applied for respiratory disorders doubled (Santamouris et al., 2001).

In addition to health problems related to air pollution, the magnitude of UHI can lead to heat-stress injuries and heat related mortalities. Several studies have focused on heat related mortality with few cases. One of them is that heat-related deaths in summer period of 1999 in Chicago were associated with risk factors, and it was found that 47% of them were over 65 years and most of them were living alone (Naughton et al., 2002). In France, 2003, the extremely hot summer caused a dramatic increase in mortality. Fouillet et al. (2006) reported that deaths were directly related to heat wave, and also respiratory and cardiovascular disorders conduced to a high death rate. Moreover, Stafoggia et al. (2006) compared mortality datasets from hospital to meteorological data (temperature and humidity) and documented that heat waves increased the risk of mortality by 34% in Italy.

Because of all these negative effects, the UHI intensity should necessarily mitigated, especially both in hot-rid and tropical climates. Reducement of surface and air temperatures in urban areas may provide many benefits to the entire community, such as saving in electricity consumption with reducement of cooling demand, decrease in

smog accumulation and decrease in the risk of heat related diseases and deaths. The mitigation of heat island effect can also provide enhancement of thermal comfort in open urban spaces that may attract more people to use and get social interaction with each other.

2.2. The Relation between UHI and Urban Geometry

Urban geometry has a certain effect on the urban microclimate and on the development of the UHI intensity. During a day, incoming short-wave radiation is absorbed by urban structures and stored as heat in them. After the sunset, daytime warmed up urban surfaces start to emit long-wave radiation and to release heat during a night. However, urban geometry have a crucial role in the heat loss rate of the gained heat. When the components of urban canyon geometry (building height, street width, etc.) generate deep canyons, sky view becomes limited, and thus radiation loss occurs lower than open spaces. In other words, as a result of restricted long-wave radiation and heat loss by 3D geometrical configuration of urban fabric, residual heat contributes to the formation of nocturnal heat island (Hammerle et al., 2011a; Lopez et al., 2016; Oke, 1981; Unger, 2009). Therefore, these energy exchanges can be linked to the variables of urban canyons, and canyon geometry can be characterized by three main indicators, which have been demonstrated to have a significant impact on the UHI by several studies, that are aspect ratio, sky view factor and building orientation.

2.2.1. Characterizing Indicators of Urban Geometry

2.2.1.1. Aspect Ratio (H/W)

Among many factors that induce to the UHI development, one of the most important causes is urban geometry is mainly measured by the aspect ratio. Because of urban canyons are composed of building blocks and linear spaces (streets) between them, aspect ratio of a canyon, or in other words, building height to street width (H/W) ratio has been found to be a significant factor contributing to UHI intensity (Bakarman and

Chang, 2015; Takkanon, 2016).

In heat island studies, three-dimensional urban geometry data are transformed to the two-dimensional sections to calculate H/W ratio. For symmetrical canyons, only the ratio of mean building height to the street width is considered, but length of the building should be regarded for the evaluation of asymmetrical canyons (Goh and Chang, 1999; Takkanon, 2016). The calculations of H/W ratio for different canyon configurations are given in Figure 2.13-15.

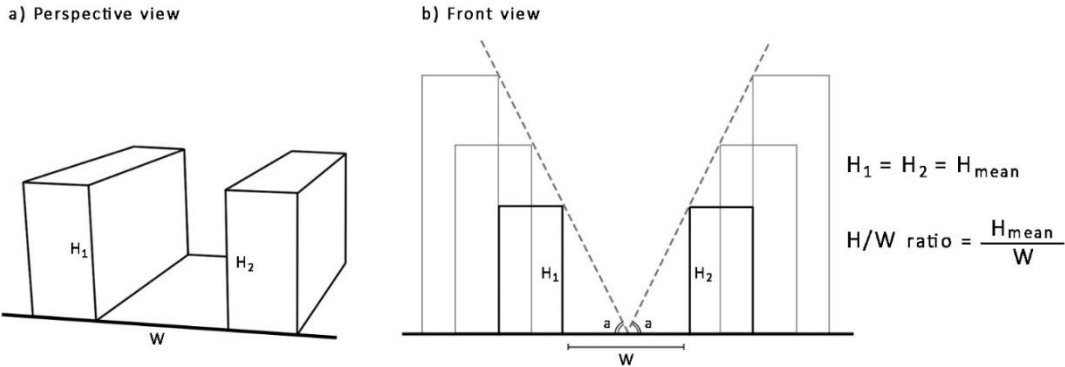


Figure 2.13: The calculation of H/W ratio for a symmetrical canyon (Source: personal drawing)

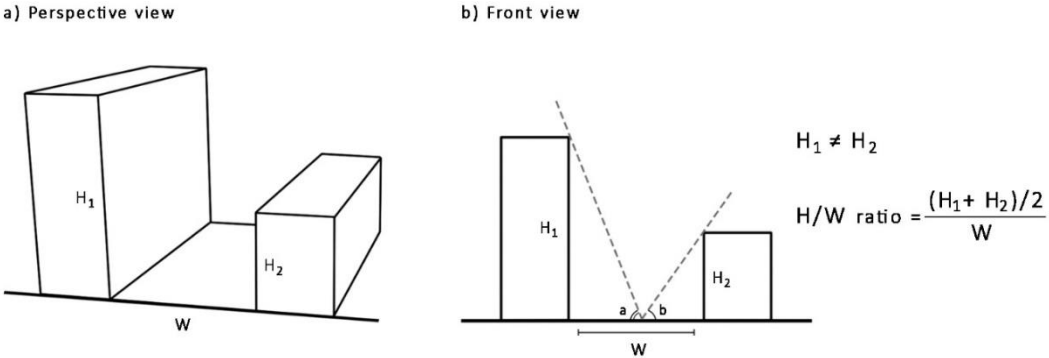


Figure 2.14: The calculation of H/W ratio for non-uniform buildings (Source: personal drawing)

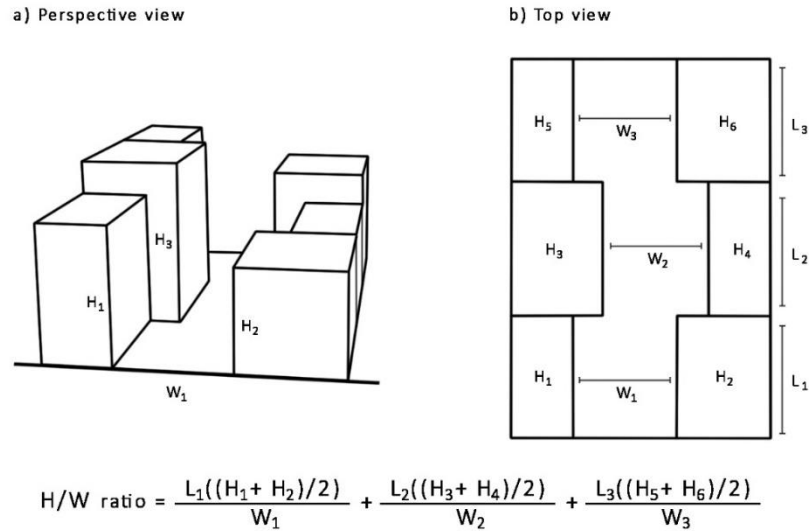


Figure 2.15: The calculation of H/W ratio for an asymmetrical canyon (Source: personal drawing)

In general, an increase in the H/W ratio as a result of created deep canyons in urban areas, contributes to development of UHI effect. Oke (1981) demonstrated a strong and linear relationship between H/W ratio and heat island intensity. As seen in figure 2.16, when height-to-width ratio of an urban canyon was measured as 2, the UHI intensity had reached up to 12 degrees. However, the temperature difference due to H/W ratio may vary according to climate zones and weather conditions of cities. In fact, in tropical and continental (mid-latitude zone) climates, high H/W ratio causes an increase in heat island intensity. On the contrary, in hot-arid cities, deep canyons ($H/W > 2$) can conduce to decrease in the air temperature and the heat island effect.

Oke (1981) simulated this relation for European and North American cities, and his estimation has been approved by many studies. One of them is Nakata and Souza (2013) conducted a study for five selected sites from central area in Brazil. According to this study, the ambient air temperature in the highest H/W ratio (0.5) canyon was measured 5.5°C higher than the rural area. To define this relation between them a new formulation was developed which estimates that as a canyon gets deeper and narrower ($H/W > 2$), the temperature difference may rise to 10 degrees. The other is based on a developed formulation for tropical cities, but the results are quite consistent with Oke's

estimation. To illustrate, in Bangkok, weather data were collected from different urban canyons both in wet season (July) and cool season (December). As a result of this study, Takkanon (2016) reported that when the H/W ratio was within a range of 0.20 to 0.30, intensity of heat island was observed to be between 5°C and 8°C. Moreover, UHI intensity was measured 9°C for a canyon with a H/W ratio of 1. Therefore, the relation between them was established with a linear model which gives R^2 values for both wet season and cool season as 0.49 and 0.45, respectively. It means that the magnitude of UHI effect is depended on urban geometry (aspect ratio) by 45 to 49%.

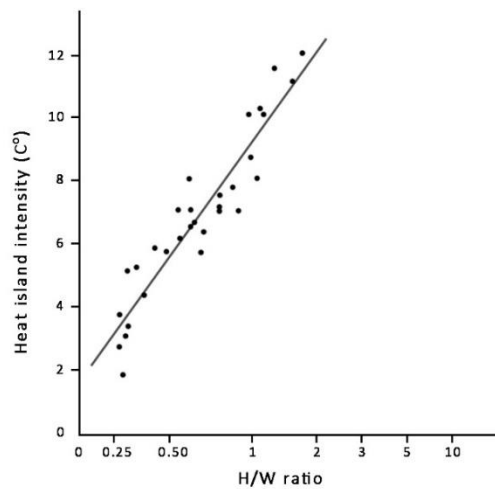


Figure 2.16: The relation between H/W ratio and UHI intensity (Source: Oke, 1981)

Apart from this general view of enhancing effect of deep canyons on UHI, Bakarman and Chang (2015) demonstrated that, in the hot-arid climates, deep canyons in compact urban fabric have a cooling effect due to its shade-providing configuration. In the city of Riyadh, Saudi Arabia, it was found that while the air temperature in the shallow canyon was 52°C, which was 15% higher than the rural area, deep canyon's temperature was measured as 47°C as seen in Figure 2.17. Because of shallow canyons in urban forms, which are characterized by low-rise buildings and wide streets, are exposed to extreme level of incoming solar radiation, ground surface in there warmed quickly and reached by 66°C as a peak value. As the canyon profile gets deeper, directly incoming solar radiation to the ground coverage is restricted, and thus a

decrease in the air and surface temperatures can be observed during a day.

In addition, a change in the height-to-width ratio of urban canyons influences the formation of diurnal and nocturnal heat islands. For instance, shallow canyons absorb greater amount of incoming radiation that leads to an increase in the diurnal UHI effect. On the contrary, deep canyons store huge amount of heat due to trapped radiation through multiple reflection, and that results in the intensification of nocturnal heat islands (Bakarman and Chang, 2015; Montavez et al., 2008).

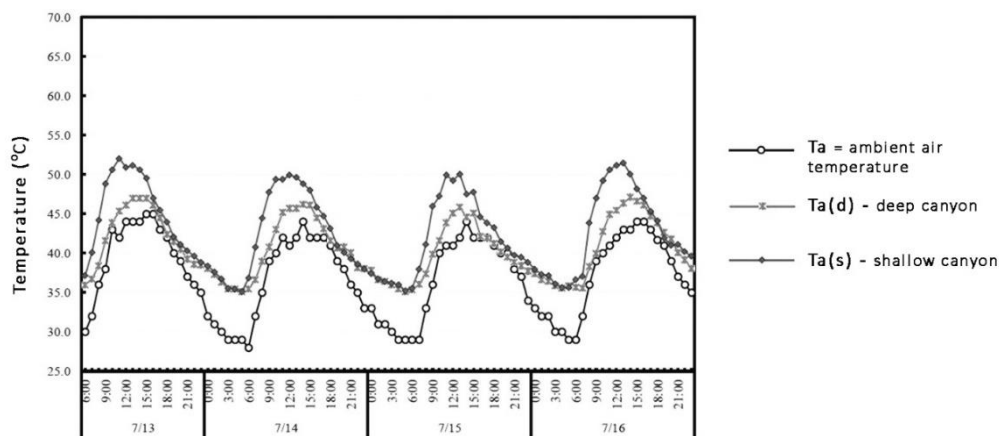


Figure 2.17: The hourly variations of the air temperature in different canyon profiles (Source: Bakarman and Chang, 2015)

2.2.1.2. Sky View Factor (SVF)

The Sky View Factor (SVF) is widely used as an important measure of urban geometry for the estimation of UHI effect. It determines the ratio of emitted long-wave radiation from urban surfaces to the atmosphere. Therefore, the fraction of the visibility of the sky from a point on the urban surfaces depending on the interception of the near located urban structures, is represented as a SVF values, which is within a range of 0 to 1. The SVF value of 1 means that the sky is unobstructed and completely visible, but if it is 0, the sky is completely blocked. For example, Unger (2009) measured SVF values both for relatively open area (0.97), which is surrounded by low-rise buildings, and for

more closed area (0.57) where the bordering buildings are quite high and the street width is low. In brief, as the SVF value decreases due to high-rise buildings and narrow streets (Figure 2.18), in addition to the multiple reflection, long-wave radiation loss is restricted, heat is trapped, and thus heat island effect is increased in urban canyons (Canan, 2017; Hammerle et al., 2011a; Unger, 2009).

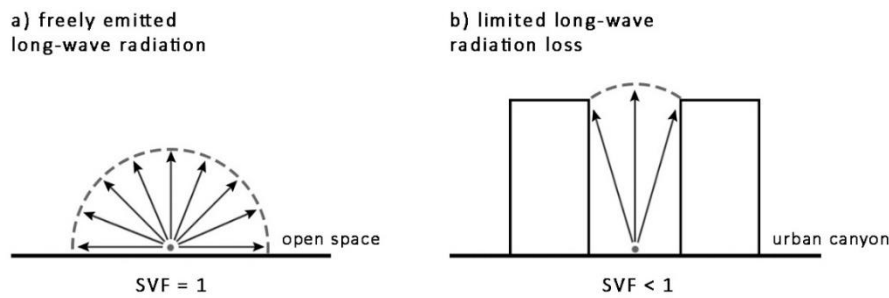


Figure 2.18: The relation between SVF values and emitted long-wave radiation (Source: personal drawing)

The basic principle of the calculation of the SVF value for a specific point on an urban area is based on the projection of each building shapes, which are seen from the point as obstruction, to the sky vault. Figure 2.19 illustrates limited part of the sky due to projected building surfaces on the hemisphere. The ratio of the remain part is considered as the SVF value, and it is basically formulated by subtracting from 1 the sum of all view factor values of building surfaces (Unger, 2009). To calculate the view factors (VF_S) of these geometric arrangements, elevation angle (β), which is defined by vertical extension of rectangle (S), its distances from the view point, and rotation angle (α) can be used. These calculations are simplified and described by Oke (1987) in few equations as follows:

$$SVF = 1 - \sum VF_S$$

$$SVF = 1 - \cos^2 \beta = \sin^2 \beta$$

$$VF_S = \cos^2 \beta (\alpha / 360^\circ)$$

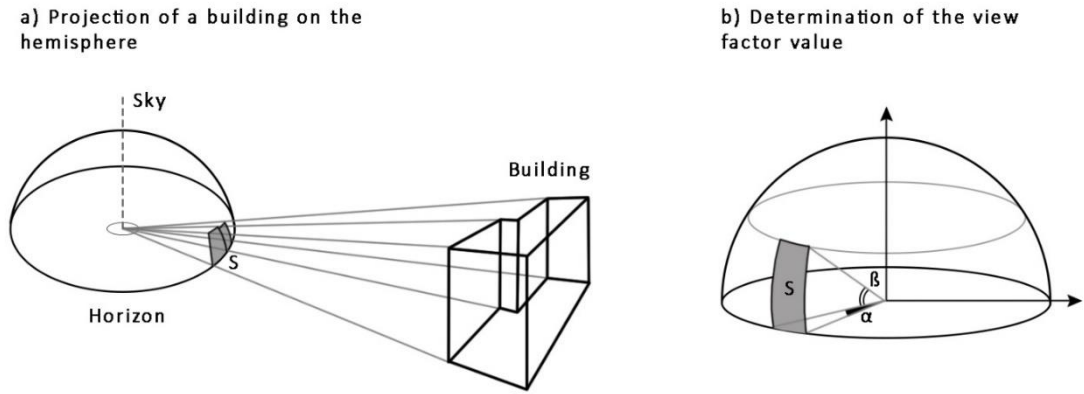


Figure 2.19: Schematic depiction of the SVF calculation (Source: Unger, 2009)

Apart from Oke's (1987) formulation, a more exact analytical model was developed by Johnson and Watson (1984) that defines SVF value by analyzing geometric features and radiation fluxes of urban canyons. This calculation is based on the fraction of long-wave radiation that reaches to the sky vault from canyon surfaces (Chen et al., 2012; Cheung et al., 2016). It can be given by an equation:

$$\Psi_S = \frac{1}{\pi R^2} \int_{S_v} \cos\varphi dS$$

Where:

Ψ_S = The sky view factor

R = Radius of the sky hemisphere (m)

S_v = The sky vault seen from the canyon ground

φ = The angle between the canyon ground and the sky vault radius to area

dS = Area of the sky seen from the canyon ground (m²)

To calculate the SVF values in urban areas, several image-based manual and computational methods have been developed by many researchers. Image-based methods for identifying the SVF require the use of fisheye lenses to obtain hemispherical photographs. Two-dimensional images of an urban canyon can be

captured from the center of the canyon and 1-1.5 meters above the street surface to represent how the sky is seen from there (Cheung et al. 2016; Hammerle et al., 2011a; Liao and Cavaleri, 2014). Otherwise, if photos are taken on different sides of horizontal plane or on the ground level, calculation of SVF values may give inaccurate results. For example, Cheung et al. (2016) investigated effects of different measurement points on the SVF results. They found that when the canyon was very symmetric, SVF values of each point, which are left side (0.126), center (0.190) and right side (0.126) of the canyon, were similar. However, in the asymmetric canyon, remarkable differences between them were observed. Also, as the height of the measurement point was close to the ground level, SVF was calculated lower than the upper measuring point's value, but there was no essential difference between them.

Image-based methods have been evolved from manual to digital calculating processes. The most basic one is called as Steyn method, which is based on manually annulus counting in a divided fisheye image by polar grid and their summation. On the contrary, Rayman method processes digitized fisheye images through pixel counting. That type of pixel calculators designate darker colors for shapes, which are perceived as obstacle to the sky view, and the remain area is colored to white. Therefore, selected white pixels can be used for the calculation of SVF values in a specific urban area (Hammerle et al., 2011b; Liao and Cavaleri, 2014). To illustrate, CCL model in MATLAB software converts images to only black and white colored pixels (Cheung et al., 2016). As seen in Figure 2.20, all urban structures, such as buildings, trees and street lights, are represented as black and visible part of the sky is shown as white. Also, to calculate SVF, photos can be converted to the grayscale and be separated black and white pixels carefully by graphic softwares, then geometric variables can be calculated by GIS software (Shaker and Drezner, 2010).

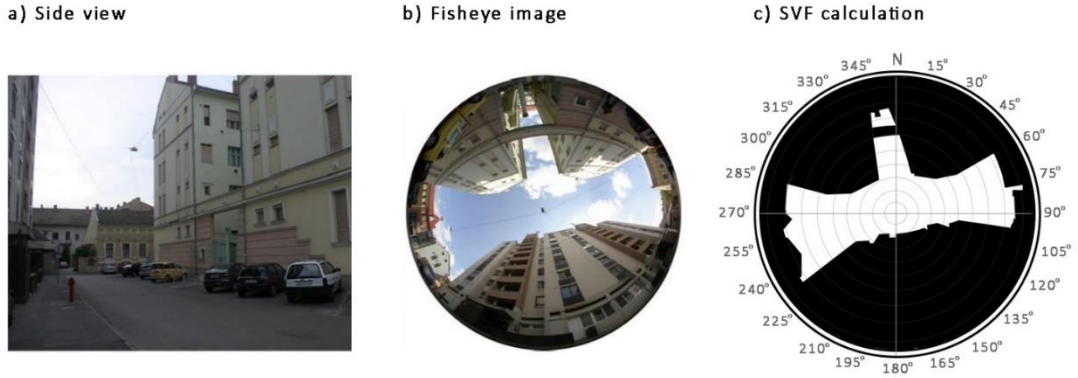


Figure 2.20: Image-based SVF calculation process (Source: adjusted from Hammerle et al., 2011b)

Additionally, fisheye images can be completely evaluated by using of ArcGIS software. The design of ArcView Script is based on Steyn method, so the basis of the calculation is adjusted to the count of annular rings (Hammerle et al., 2011a). The steps of the SVF calculation can be expressed as follows:

$$SVF_{maxi} = \frac{\pi}{2} \sin\left(\frac{\pi(i - 0.5)}{2n}\right) \cos\left(\frac{\pi(i - 0.5)}{2n}\right)$$

$$\alpha_i = (T_{total} - T_{obs}) / (\pi r_2^2 - \pi r_1^2)$$

$$SVF_i = SVF_{maxi} \frac{\alpha_i}{2\pi}$$

Where:

SVF_i = Result of the total SVF value

SVF_{maxi} = Maximum SVF value

α_i = Obstructed angle in ring 'i'

T_{total} = Total area of annular ring

T_{obs} = Obstructed area in the same ring

r_1 and r_2 = Radii of the inner and outer limits of the ring

i = Number of actual rings

n = Count of annular rings

Apart from image-based methods, computational methods using 3D building database

are more widely preferred (Matuschek and Matzarakis, 2010). In addition to the SVF calculation, software tools also provide climatologic analyses, such as sunshine duration, thermal comfort and radiation fluxes of the urban environment. By using 3D urban geometry data, SVF values can be rapidly estimated for each selected view point in an urban area. For example, Sky Helios, which is one of the most well-known softwares, can be considered as a developed model of the Rayman method. This tool generates a virtual fisheye image from a chosen view point, and then it calculates SVF values like Rayman's workflow by using graphic processor (Hammerle et al., 2011a). Additionally, SOLWEIG software is widely used for the estimation of SVF values and spatial variations of mean radiant temperature in urban areas. It also provides a simulation interface for the effect of sky view factor on the temperature distribution (Lau et al., 2015). The other one is that Townscope software is basically designed for sky visibility and solar access analyses. For instance, by using Townscope, Kakon and Nobuo (2009) calculated average SVF values for selected roads and the amount of solar radiation being exposed.

As a result of many research, a strong linear correlation between the SVF and the UHI effect has been proven. Comparison of collected air temperatures at different urban sites and calculated SVF values shows that urban geometry has a significant impact on the distribution of the average air temperature (Svenson, 2004). In addition, Yuan and Chen (2011) confirmed the effect of sky view factor on the mean air temperature in their study in Hong Kong. It was demonstrated that when the SVF value was calculated as 0.10-0.15, the air temperature was measured to be 30.5°C. However, in selected urban sites where the sky view factor increased to 0.85, the ambient air temperature decreased to 27.5-28°C. The relation between them was defined as a 0.1 increase in the SVF value results in a 0.4°C decrease in the mean air temperature (T_{mean}). Also, a new equation was developed for the calculation of T_{mean} in tropical climate cities that is stated as:

$$T_{mean} = 3.82 SVF + 31.02$$

Moreover, Cheung et al. (2016) conducted a study about intensity of heat islands in the central area of Manchester city. The data of selected canyons were used to confirm the importance of the SVF as a determining factor in the heat island development. They reported that the smallest SVF value (0.271) of the canyon had the largest UHI intensity (6-6.4°C). Nevertheless, SVF values were not low in all of the canyons where the heat island intensity was detected in high level. Therefore, this study did not fully agree with the Oke's (1987) empirical equation about the UHI estimation, but it was seen that when the SVF values were lower than 0.65, 63% of the variation in heat island intensity depended on sky view factor.

2.2.1.3. Orientation

The role of the urban geometry indicators on the thermal comfort and heat island effect is also controlled by the building orientation, or in other words, canyon axis orientation. The level of the solar access to the canyon, especially to the building facades, is highly determined by the orientation to the azimuth angle, which shows that the direction of the incoming solar radiation to the ground. Moreover, the cooling effect of the air flow throughout the canyon is also affected by that indicator. Therefore, orientation induces changes in the radiation fluxes and air temperatures that can be evaluated by two main parameters.

Firstly, the direction of the canyon axis, such as north-south (NS) or northwest-southeast (NW-SE), influences the amount and duration of the exposed solar radiation. Thus, canyon surfaces having high level of energy flux density cause an increase both in the air and surface temperatures inside the canyon. To illustrate, Nunez and Oke (1977) conducted a study on the experimental urban canyon which was oriented in the NS direction. They recorded diurnal energy balances of canyon surfaces and reported the importance of the orientation on the solar irradiance. As given in Figure 2.21, when the energy flux of the canyon floor reached to the maximum value, west and east facades had peak value earlier and later than, respectively.

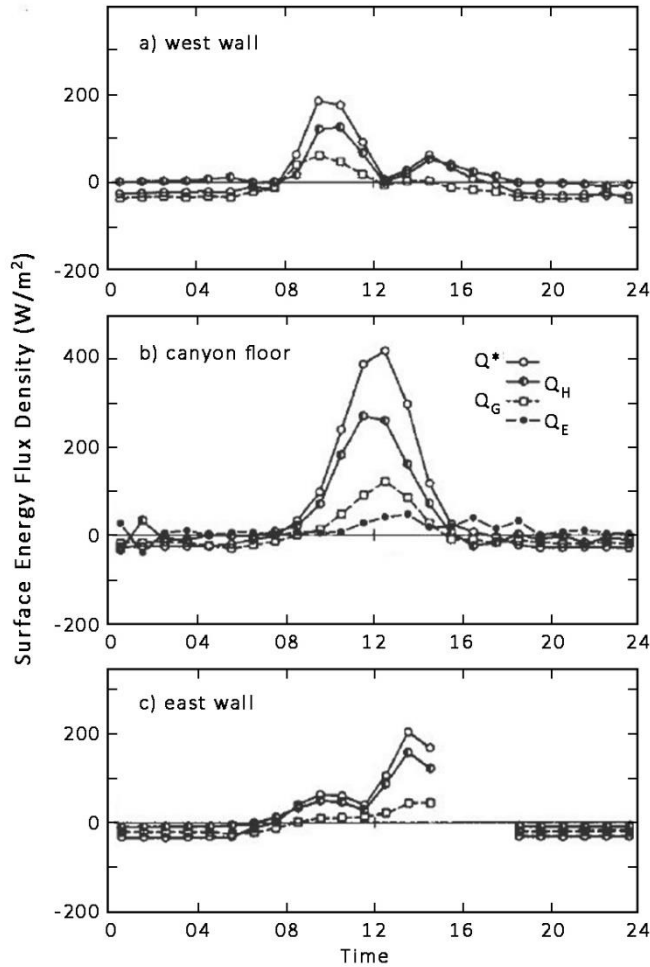


Figure 2.21: Energy balances of canyon surfaces based on hourly measurements (Source: Nunez and Oke, 1977)

In addition, Lau et al. (2015) investigated the effect of canyon orientation on the spatial variation of mean air temperature (T_{mean}). Urban canyons were simulated in the different rotation angles, such as 0°, 22.5° and 45°. In the non-rotated canyon, the highest air temperature (near 60°C) was observed on the south-facing building surfaces, and the lowest temperature, which was below 50°C, was estimated along the north facades. Moreover, the result of the comparison of the canyon directions shows that while NE-SW oriented canyon had the highest air temperature (58.1°C), NW-SE oriented one had the lowest value (52°C).

Secondly, street orientation has a significant impact on the temperature reduction through air flow. The air flow, with a specific speed and direction coming from the external environment, interacts with canyon surfaces or passes through to the end of the canyon. The warm air can be transported into the canyon or out of from there by means of advection, which is highly depended on the air flow patterns inside the canyon. The air flow possibilities can be categorized into three types that are parallel flow, cross-angle flow and perpendicular flow. For the case of parallel flow, Nunez and Oke (1977) estimated the importance of the wind direction for the NS (north-south) oriented canyon. Figure 2.22 shows that when the warm air blows from the south, advection occurs at the low level, but heat transport from the canyon air volume increases with the cooling effect of the northern wind.

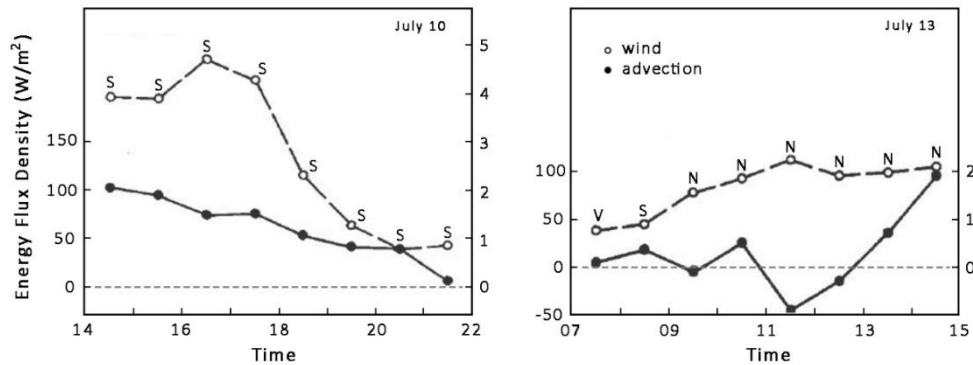


Figure 2.22: Advection of the canyon air volume due to the wind direction: N-north, S-south, V-variable (Source: Nunez and Oke, 1977)

In addition to the advective transport from the canyon air volume, surface heat can also be removed from building facades by convenient wind speed and direction according to the canyon orientation. Gülten (2014) simulated building orientation to calculate heat island potential in different cases of wind speed and direction. For the WE (west-east) oriented canyon, when the wind direction was west, heat island potential was estimated near 30°C even the wind speed was high (5.85 m/s). On the contrary, northwestern wind at low speed (3.4 m/s) had a greater cooling effect than the west wind that resulted in the estimation of air temperature as 20°C.

Another simulation result based on the hourly estimation shows that parallel wind flow with the speed of 6.25 m/s had not any effect on the air temperature inside the canyon. After an hour, despite being at the same wind speed with the parallel flow, cross-angle flow approximately dropped surface and air temperatures by 10 and 5 degrees, respectively. Figure 2.23 illustrates that how the orientation effects the temperature reduction by modifying air flow. According to the simulation, parallel flows cannot reduce both surface and air temperatures due to wind does not interact with the canyon walls. When the canyon axis oriented to the cross-angle flow, for example NS oriented canyon with NE wind direction, the wind firstly hits on the north-facing facades, and then move on to the south-facing surfaces. Therefore, a decrease in the surface temperature can be occurred by the interaction of wind and building facades, also this effect will be greater with an increase in the wind speed.

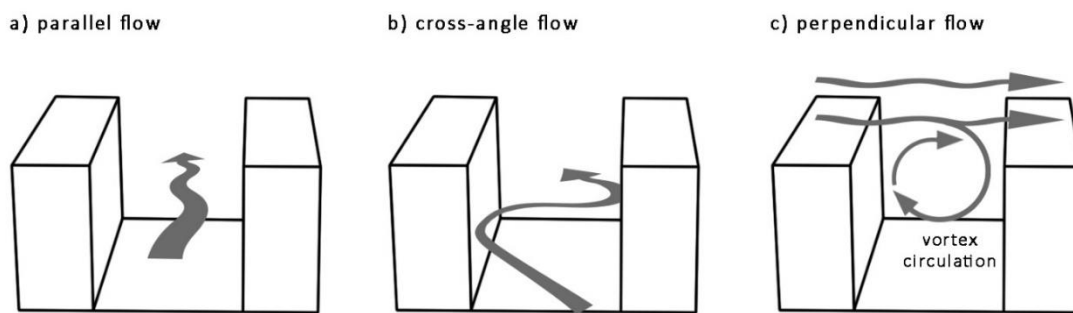


Figure 2.23: Schematic depiction of flow patterns (Source: personal drawing)

On the other hand, Gülten (2014) found that a perpendicular flow, which means wind blows perpendicular to the canyon axis, does not have any cooling effect in the canyon air volume. To illustrate, for NS oriented canyon, the east and west winds lose their velocity when they try to get into the canyon. At that time, as the amount of absorbed solar radiation increases, the air temperature of the canyon rises in spite of the wind flow. However, Nunez and Oke (1977) stated that perpendicular wind flow over the canyon develops a vortex circulation between the buildings that may leads to remove of the heat from the canyon air volume. Therefore, Nunez and Oke's prediction may be substantiated if the wind speed is above a threshold value.

2.2.2. Calculation of UHI Intensity based on Urban Geometry

To calculate UHI intensity ($\Delta T_{u-r(max)}$), measurement or simulation based mathematical models have been developed by using urban geometry parameters, such as height-to-width ratio (H/W) and sky view factor (SVF). Firstly, Oke (1981) modelled a scaled urban environment to simulate the impact of the urban geometry, which was represented as H/W ratio, on the formation of UHI intensity. In his experiment, only the effect of building blocks on the air and surface temperatures of the canyon was taken into consideration, so other factors, such as thermal properties of different materials, air flow or evaporative surfaces, were neglected. Therefore, the result of this experiment was written in a new equation as follows:

$$\Delta T_{u-r(max)} = 7.45 + 3.97 \ln(H/W)$$

After Oke (1981), Goh and Chang (1999) established a new statistical model representing a relation between H/W ratio and nocturnal heat island intensity for tropical cities due to Oke's model was mainly developed for mid-latitude cities. After the determination of spatial variation of heat island intensity, results of the study were compared with the predictions of the model of Oke as seen in Figure 2.24. Because of the remarkable difference between them, a new heat island formulation was constructed as:

$$\Delta T_{u-r(max)} = 0.952 \text{ median } H/W - 0.021$$

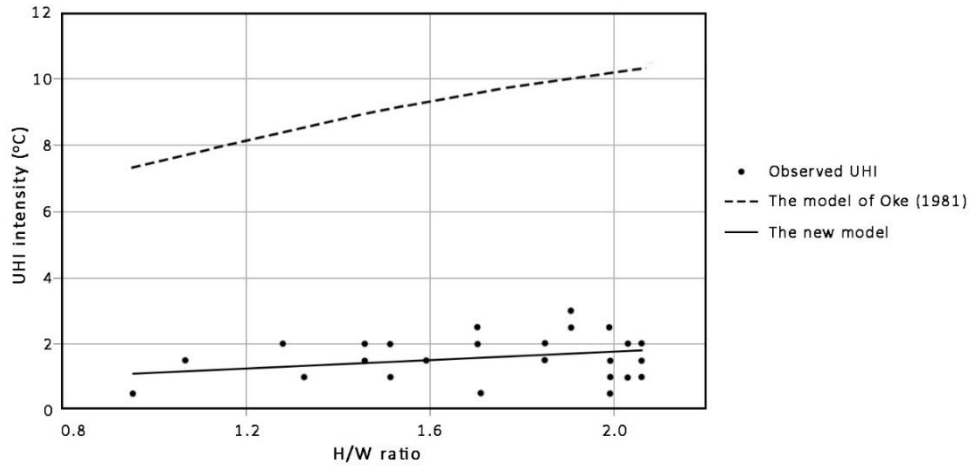


Figure 2.24: UHI intensity distribution according to the model of Oke (1981) and to the new statistical model (Source: Goh and Chang, 1999)

Apart from that a research of Nakata and Souza (2013) showed relevance with Oke’s (1981) finding. Also, they suggested a new model as an adjustment of Oke’s model according to measurement results in the city of Sao Jose do Rio Preto. After the application of both models, their results were compared to validate the applicability of the new model. Figure 2.25 illustrates that the results of the calculation of UHI intensity by the adjusted model are considerably similar to the measurement results. Additionally, the temperature difference between Oke’s model and the adjusted model can be reached at the highest level (1.6°C) when the height-to-width ratio is within a range of 0.25 to 0.5. The lowest level of the heat island intensity difference (0.2°C) can be observed in urban canyons where the H/W ratio is between 1 and 2, respectively. The equation for adjusted model as follows:

$$y = 0.802x + 1.4574$$

Where:

y = The result of the adjusted model

x = The result of the Oke’s model

$$y = 0.802 [7.45 + 3.97 \ln(H/W)] + 1.4574$$

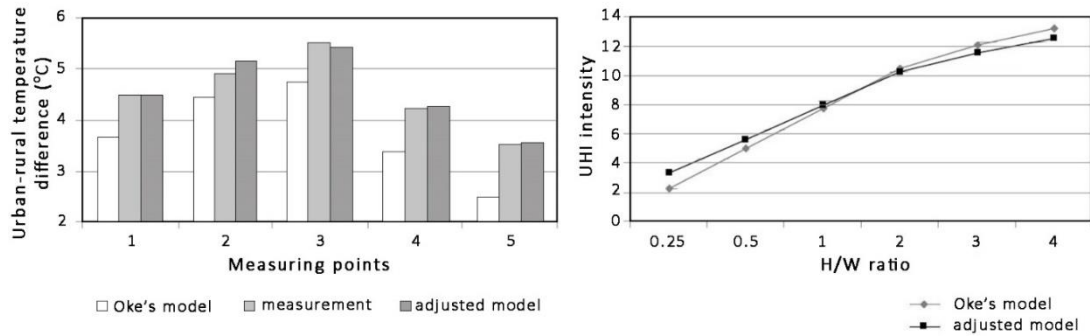


Figure 2.25: Comparison of estimated heat island intensities by different models (Source: Nakata and Souza, 2013)

In addition to the use of H/W ratio as an urban geometry indicator in the calculation of the UHI intensity, sky view factor (SVF) is also used due to it's a significant determinant factor depending on the context of the study. To demonstrate the correlation between them, Oke (1987) formulated a new equation using SVF (ψ_{sky}) as a measure:

$$\Delta T_{u-r(max)} = 15.27 - 13.88 \psi_{sky}$$

Among many studies which have been conducted to confirm the influence of view factor on the development of UHI, Cheung et al. (2016) found that a linear relation between them for both in summer and winter seasons. Moreover, they suggested a new equation to obtain stronger linearity with a higher coefficient of determination (R^2) value that corresponds to measurement results. Equations for the estimation of the maximum heat island intensity in summer and winter periods are compatible with the results of Oke's (1987) model that can be expressed as:

$$UHI(max)_{summer} = 6.75 - 3.03 SVF$$

$$UHI(max)_{winter} = 4.25 - 2.39 SVF$$

2.3. Evaluation of UHI Related Studies in the Literature

2.3.1. Previous Studies on UHI

Because the UHI effect induces many problems in the urban environment, several studies have been conducted to provide a comprehensive understanding about urban characteristics affecting the development of heat island intensity. The associated factors of UHI have been investigated in many aspects, and analyzed their effect on air and surface temperatures. All these studies were performed from the macro scale to micro scale. To illustrate, in macro scale and meso scale studies, for the assessment of the surface urban heat island (SUHI), spatial and temporal variations in surface temperatures and contributed factors were defined by using statistical datasets and remote sensing images. The use of satellite images to analyze land use, total area of vegetation covers or surface temperatures indicate the sensitivity factors of UHI parameters. Accordingly, many studies validated that urban expansion with an increase in the total area of impervious ground covers has a remarkable effect on the increase in surface temperatures.

Apart from surface temperature determinations, many studies also have been analyzed daily (diurnal and nocturnal), seasonal or annual air temperature differences with related to thermal properties of surface materials, vegetation areas, land use (residential, commercial and industrial areas), building density and canyon geometry in local or micro scales. To demonstrate the effect of these parameters on the air temperature and UHI intensity, measurement-based studies have been conducted. On the other hand, to estimate negative effects for different urban scenarios, to examine the relation between urban geometry indicators and heat island, and to develop a model, from estimation to implementation, for the mitigation of UHI effect simulation softwares have been preferred. Therefore, UHI studies within the scope of urban geometry can be categorized into two main part as measurement-based studies and simulation-based studies.

2.3.1.1. Measurement Related Studies

Measurement-based studies are fictionalized to investigate the effect of urban geometry indicators, such as height-to-width (H/W) ratio and sky view factor (SVF), on the formation of UHI intensity. To determine the influential factor of geometrical features, urban canyons with different H/W ratios and SVF values are selected, carefully. As a result of several regression analyses of these dependent and independent variables, a linear relation between urban geometry and heat island intensity is validated with fairly high coefficient of determination (R^2) values.

Table 2.3: Examination of measurement-based studies

Author	Urban Geometry Indicator	Method	Findings
Bakarman and Chang (2015)	H/W ratio (shallow canyon: 0.42) (deep canyon: 2.20)	Measurement of air (from roof and inside the canyon) and surface temperatures (walls, roofs, floor) with sensors.	Determination of an increase in the air and surface temperatures due to a decrease in the H/W ratio.
Cheung et al. (2016)	SVF values (within a range of 0.3 to 0.9)	Calculation of SVF values with the use of fisheye images in MATLAB.	Determination of the max. UHI intensity (6°C) with the min. SVF value (0.3) in summer nights, and correlation of a linear relation between them. ($R^2=0.63$)
Takkanon (2016)	H/W ratio (within a range of 0.06 to 0.95)	Measurement of the hourly air temperatures by a mobile weather station along the roads.	Demonstration of a linear relation between H/W ratio and nocturnal UHI intensity. (for wet season $R^2=0.49$) (for cool season $R^2= 0.47$)
Yuan and Chen (2011)	SVF values (within a range of 0.15 to 0.85)	Calculation of SVF values with 3D building data in ArcGIS.	Demonstration of a linear relation ($R^2=0.73$) between SVF and UHI intensity, and estimation of 0.4°C decrease in the air temperature due to 0.1 increase in the SVF value.

2.3.1.2. Simulation Related Studies

Apart from real-time measurement studies in urban areas, many researchers have conducted simulation studies to develop an estimation tool for UHI intensity to investigate the influence of urban geometry on air temperature for different scenarios, and to generate various form configurations to mitigate the UHI effect. Generally, for the simulation process, or related to the case study, for the optimization process, morphological indicators are used to be input data, and thus the output data, which has been reached from the modification of input parameters, provides many estimations for the development of UHI effect.

One of these studies, Gülten (2014) evaluated urban heat island effect in high density urban areas by using a computational fluid dynamics (Ansys Fluent) software. Simulations were made for different scenarios, which are determined to height-to-width ratio (0.5, 1 and 2) and orientation of urban canyons. In order to define the impact of velocity, traffic flow, vegetation, and surface material properties on the magnitude of heat island intensity, each variable was added to the simulation one-by-one. Therefore, estimation results were compared with each other, and their effect on the UHI development were discussed on their own terms.

One of these studies, Chokachian et al. (2017) proposed a generative method to determine the relation of UHI and solar access with urban forms by developing a tool in Grasshopper software, which is defined as a visual programming interface. To generate urban forms (600 form samples) with some limitations, set of geometric circumstances, such as block size, floor number and floor height, were defined, first of all. Then, after the simulation, identified H/W ratios are used to calculate UHI intensity using Oke's (1981) formulation. The application of developed method shows a strong relation between floor area ratio and heat island intensity, and thus a new equation is suggested as follows:

$$UHI = 7.45 + 3.97 \ln \left(3.2 FAR \frac{(1 + \frac{w}{x})^2}{w} \right) \cong 12.08 + 3.97 (\ln FAR + 2 \ln (1 + \frac{w}{x}) - \ln w)$$

Where:

FAR = Floor area ratio

w = Canyon width

x = Building size

The other one is Hu et al. (2016) developed a parametric modelling to mitigate the UHI effect through optimization of SVF values in urban areas. This method was evaluated with the use of genetic algorithm in Rhinoceros software. Firstly, to represent the compact urban form, various form distributions were generated according to some restrictions, such as plot number, plot size, range of the floor area ratio and certain length of building setbacks. Secondly, as seen in Figure 2.26, the optimization process proceeded on these form configurations (around 1275 samples) to find the max. SVF value which represents min. magnitude of the UHI intensity. As a result of this simulation, optimum solution for the mitigation of UHI effect was emerged as a rough urban form. Because of the overall design algorithm was based on the maximization of average SVF value in the experiment area, high-building density in the central area with low SVF value was recommended. Therefore, the periphery area high SVF value conduced an increase in average SVF value of the whole area.

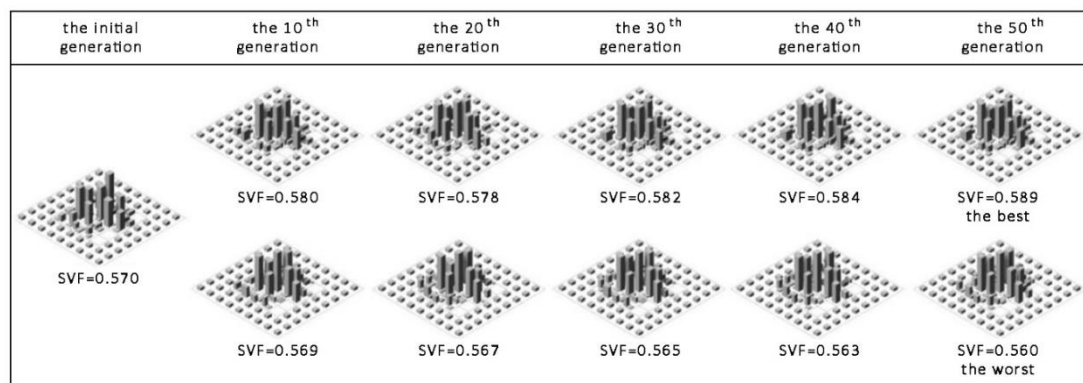


Figure 2.26: Generated form samples based on the best density distribution (Source: Hu et al., 2016)

Table 2.4: Examination of simulation-based studies

Author	Urban Geometry Indicator	Method	Findings
Chokachian et al. (2017)	- H/W ratio - FAR (floor area ratio)	Development of a mathematical generative methodology to calculate UHI intensity by using urban form in a software.	Estimation of a relation between geometric parameters (building height, street width, FAR) and UHI intensity.
Hamdi and Schayes (2008)	- H/W ratio (0.43 and 1.50) - SVF values (within a range of 0.47 to 0.70)	Simulation of diurnal variations of the UHI intensity through TVM model.	Estimation of a decrease in UHI intensity with high H/W ratio, and 0.4°C decrease in UHI due to each 0.1 increase in SVF.
Hu et al. (2016)	SVF values	- Calculation of SVF values with the shadow projection method for a large number of urban form samples. - Optimization of SVF values of urban forms to mitigate UHI intensity	Generation of a compact density distribution form in the center of the experimental area to produce high SVF value of the whole area.
Lau et al. (2015)	- H/W ratio (0.5 - 1 - 2 - 3 - 4) - Street orientation (rotation angle: 0° - 22.5° - 45°)	Simulation of the mean air temperature according to geometrical features by using SOLWEIG.	- Determination of the highest air temperature (58.1°C) in the lowest H/W ratio (0.5) canyon and 45° rotated canyon. - Exemplification of the importance of urban geometry to exposure to solar radiation.
Montavez et al. (2008)	H/W ratio (within a range of 0.11 to 5)	Simulation of an energy transfer process of urban canyon models	- Determination of a high potential of the urban geometry to generate UHI intensity (4-12°C)
Nakata-Osaki et al. (2015)	H/W ratio (within a range of 0.25 to 2.02)	- Simulation of a hypothetical scenario by the recognition of input data. - Computation of the model and application of the algorithm through GIS tool	Suggestion of a developed tool to simulate UHI intensity in different urban scenarios.

2.3.2. The Overall Critics on Existing Methods of UHI

Literature review on the Urban Heat Island (UHI) studies shows that several research projects are based on the measurement of air and surface temperatures, energy fluxes, and other artificial and natural environmental conditions to establish their effects on the magnitude of heat island intensity. Actually, the main purpose of these studies can be interpreted as a search for a set of knowledge to mitigate the UHI effect in urban areas. Defining influential indicators and estimating relations between these indicators and heat island magnitude provide data for the future studies, and also suggest mitigation strategies by controlling these causing factors. In addition to the measurement-based studies, simulation-based ones help designers to evaluate the impact of variables (components of urban geometry, climatic conditions, material properties, etc.) on the UHI intensity. Moreover, simulation softwares can estimate air and surface temperatures for different urban scenarios that provides a foresight before the design and planning processes. However, estimation results are not enough to produce better solutions and form configurations to mitigate heat island intensity, particularly in the field of urban geometry. Since the tested scenarios are set by users with limited number of morphological features, the acquired evaluations from the simulation softwares are inadequate to offer alternative design recommendations. Briefly, the overall critics on existing methods of UHI in the context of urban geometry related studies can be defined as follows:

- Estimation results as a decrease or increase in heat island intensity with specified geometrical features (height-to-width ratio, SVF value and orientation degree) are limited with a few scenarios
- Simulation softwares generally evaluates specified conditions by designers, and thus they tend to establish alterations in the air temperature in regard to restricted samples
- For mitigation of the UHI effect, previous studies suggest only strategies or specific rates that based on their case areas instead of achieve better form solutions
- Simulation-based studies have the lack of searching design proposals from a wide range of geometrical features to achieve a minimum heat island intensity

CHAPTER 3

PARAMETRIC MODELLING FOR THE ANALYSIS AND SIMULATION OF UHI: A MODEL PROPOSAL

3.1. Methodical Approach

Evaluation of the overall critics on the existing methods of urban geometry based UHI studies shows that simulation-related methods are insufficient in generating form compositions to mitigate heat island intensity. Instead of measuring geometrical features to estimate the UHI effect with a limited number of scenarios determined by the designer, such as 0.5-1-2 height-to-width ratios, the search for UHI mitigation requires new methodical approaches to achieve alternative scenarios, which will be produced beyond the designers' limits. To meet this demand, parametric modelling can be considered as an effective tool that allows designers to response their own needs. By using parametric modelling, many geometric components can be analyzed and form configurations can be generated in regard to design problem through a customized set of algorithms. Thus, in this context, a parametric model is developed to response the research problem of this study.

The methodological approach of this study stands on a synthesis of analysis and simulation processes. To mitigate UHI intensity in urban areas, the proposed model provides the combination of SVF calculation by analyzing morphological components, and form generation by maximizing the obtained SVF values at the same platform. In other words, designers will be able to proceed analysis and design process by running a set of algorithm in the parametric modelling software. By means of this proposal, the effect of urban geometry on the UHI development can be revealed, and measurement

results can be utilized to produce design solutions that mitigate heat island intensity. Also, this proposal offers urban designers and planners a set of possible design outcomes that is more than producing an optimal solution.

The proposed parametric model consists of analysis and simulation phases. Figure 3.1 illustrates the workflow of the model with detail explanations of each step. As mentioned earlier, literature review indicates that urban geometry indicators have a strong relationship with the magnitude of the UHI effect. To calculate heat island intensity, a few equations were developed by using geometrical parameters, such as height-to-width ratio (H/W) and sky view factor (SVF) value. Because H/W ratio is a representation of three-dimensional building data as two-dimensional sections, the use of H/W ratio in the analysis would not be an accurate selection for the parametric approach that is based on 3D modeling. Therefore, SVF calculation for the estimation of heat island intensity is determined as a main part of the methodology. Additionally, to calculate UHI intensity by using average SVF value, Oke's (1981) equation will be used. Briefly, at the first phase, the layout of the design area will be defined according to their component, and then will be analyzed to calculate SVF value and UHI intensity.

As seen in Figure 3.1, at the second phase, which is named as simulation, Genetic algorithm will step in to generate form alternatives by maximizing SVF value or minimizing UHI intensity. As a result of the simulation, a list of maximized SVF results with their design proposals will be given by the algorithm. Since the simulation tends to find much better solutions, designers will be able to choose any design alternative from the wide range of proposals.

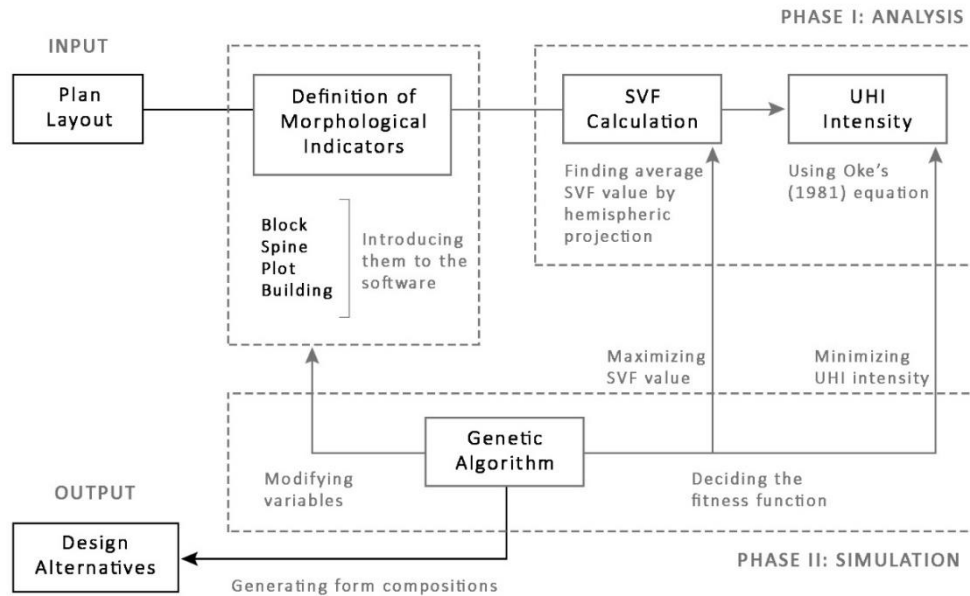


Figure 27: Schematic depiction of the workflow

3.2. Parametric Modelling: Tools and Techniques

The complex conditions of architectural design and urban design necessitate the emergence of new approaches and tools in the design process with the development of computational systems. Up to the present, decision making mechanism of the design process has static and solid structure. After the emergence of parametric modelling, the understanding of design principles has been shifted to the more flexible and generative process. As Schumacher (2014) states that the new form of design process is based on generation and selection from a set of created alternatives via parametric modelling. This new era of the design field that provides the formation of alternative solutions, generation of many design forms, manipulation of design entities by using a set of specified parameters and algorithms (Dino, 2012).

As opposed to conventional design process, parametric modelling provides designers to specify parameters in regard to their design concepts, and allows to make changes by controlling input and output parameters interactively. Because the modelling software is principally created as a responsive system, as any changes on the

parameters are made by designers, the whole design can be updated automatically by the model.

Parametric modelling can be defined as a computational design approach that is principally based on algorithmic settings. A set of instructions need to defined as an algorithm to compute input values, and transform them to produce output values. Using parameters and algorithms, to generate geometric forms with mathematical operations, and to create a finite set of possible solutions, forms the ground of parametric thinking. It provides an ability of searching better solutions, sorting the findings, generating alternative from configurations, and operating all of them in a connected platform (Dino, 2012). Therefore, parametric modelling can be taken into consideration as a fast-growing and a powerful method, which produces new architectural and urban morphologies in a constant diversity, and enhances design variations beyond the limits with the creativity level of designers.

Parametric modelling tools provide flexibility, diversity, and efficiency by form generation with generative and adaptive design system. Designers have an ability to manipulate parameters in any condition, and test generic options for different design scenarios. Due to defined parameters are connected with each other, they can interact easily in any change and reflect the new results according to the manipulation. Also, designers can improve the design process by searching and producing new shapes and forms. One of the outcomes of the generative design system is the formation of countless complex compositions, which cannot be produced easily by other design softwares. Thus, parametric modelling tools help designers to improve their imagination, and various form generation capacity.

Rhinoceros and Grasshopper softwares are utilized for parametric modelling. Rhinoceros is a 3D-modelling program, which visualizes algorithmic scripts as a three-dimensional model. Grasshopper is a visual interface, which is built inside Rhinoceros software. In other words, Grasshopper is a developed plug-in for algorithmic design scripting, and it can be used through Rhinoceros application. These tools control geometrically defined the urban environment by introducing them to written

algorithms and mathematical operations. Creating algorithms is only allowed on the Grasshopper canvas via its component tab, as seen in Figure 3.2. The component tab includes all parameters, mathematical operations, geometrical elements, and optionally attached add-ons that provide to create geometries by algorithms. The canvas is, in this context, a workplace where designers can create a set of algorithms, and control all the scripted design algorithms to form geometrical components. Also, canvas requires to set a connection between components in order to make transaction data.

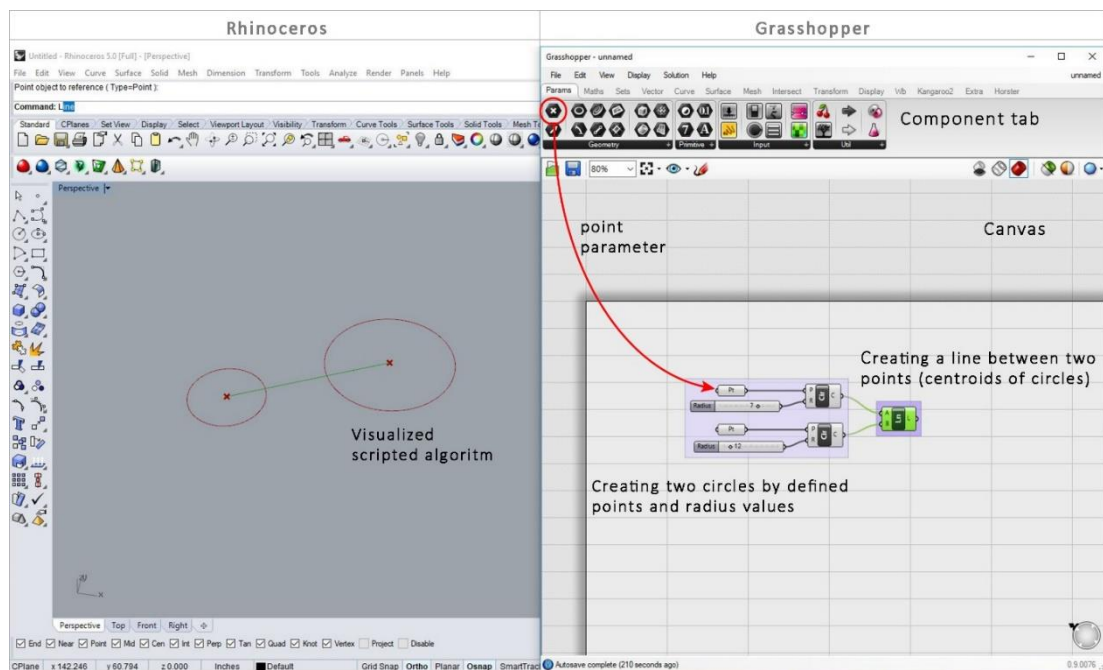


Figure 3.2: Rhinoceros and Grasshopper softwares with basic explanations

Parametric design tools contain numerous plug-ins and add-ons, which are constantly created by designers. For example, DIVA is a developed plug-in for Rhinoceros by members of Graduate School of Design at Harvard University. This plug-in offers a daylighting and energy modelling for buildings and urban landscapes. Another environmental performance provider add-on is named as Ladybug tool. Ladybug allows designers to import and analyze weather data, and to run radiation, sun-path and daylighting simulations. Apart from environmental analysis tools, one of the most important tools of Grasshopper softwares is Galapagos, which can be defines as

Genetic Algorithm that provides from generation and optimization. The basic proceeding principles of Genetic Algorithm can be described as follows:

- Distributing a population over the specified domain set
- Testing this domain in regard to achievement minimization or maximization
- Generating a population with selected solutions from test results
- Applying the fittest selection on the manipulation
- Using last generation results to create the next generation (Musleh, 2012)

Due to the nature of Genetic Algorithm, it tends to find fittest genomes to achieve better solutions, and thus Galapagos tries to optimize the test results at each generation. As seen in Figure 3.3, the fitness process can be observed by the Galapagos editor. This editor window shows, at the top of the screen, the number of generations on the x-axis, shows the fitness level on the y-axis, and represents average fitness value with red line for each generation results. Additionally, yellow and orange colored buffer zones give an information about the strongest/weakest genomes and standard deviation for each generation, respectively. The light purple rectangle, which can be moved by user, shows selected generation. To illustrate, to get maximized values from the simulation results for first generation, this rectangle should be moved to 1 on the x-axis. At the bottom of the window, selected genomes and the list of maximized or minimized results are represented. In the fitness process, from the test of first generation to the last generation, the fittest genome is tried to select from the gene pool. While the selected genomes have not been optimized in the first generation, the fittest genome has been reached for each population test at the eight generation. Therefore, towards to end of the process, the yellow and orange colored zones are getting smaller because of the maximization results are reduced to almost a single or similar set of values by the optimization process.

Depending on the context of the design problem, Galapagos tends to run for indefinite duration, so users have to put some limitations by specifying indicators. To illustrate, for an urban area, when a designer wants to maximize the building density, building height should be determined within a range of values. Also, Galapagos allows

designers to use selection and mutation operations, and to control the number of population per generation, number of generation and duration of the simulation according to the problem solutions. Because Galapagos has an ability to solve complex problems by testing any changes in each parameter, to achieve fittest solutions, and to generate alternative form configurations, this tool has been widely preferred by designers. Genetic Algorithm offers designers to explore new design compositions and different configurations by investigating as much as possible amount of arrangements with defined input parameters. Thus, designers can select better or fitter solutions from a list of full of alternatives, at the earlier stage design. Having a real-time feedback from the software also improves and steers designers' decisions through the process (Musleh, 2012).

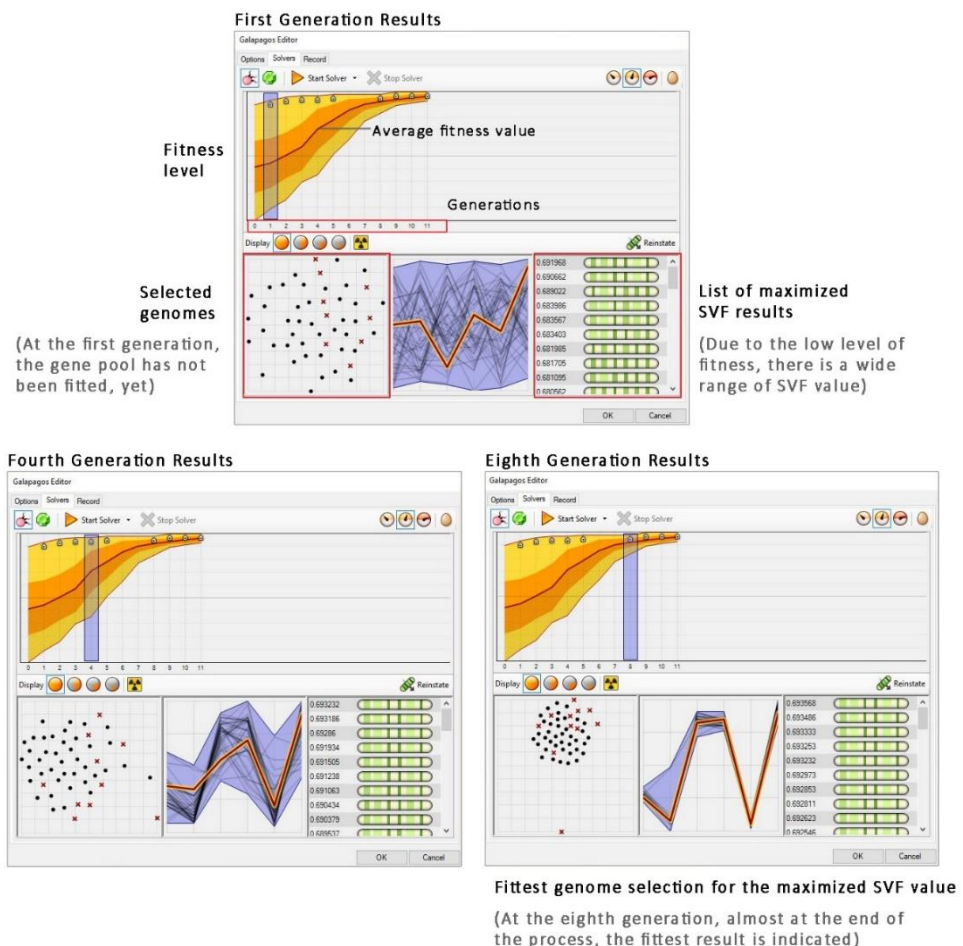


Figure 3.3: Fitness process of the Galapagos tool

3.3. Definition of Computational Framework for the Mitigation of UHI

3.3.1. Algorithmic Definitions of the Morphological Indicators of UHI

To define a relationship between basic components of urban geometry and UHI effect, and to fully understand the process of heat island mitigation, is necessary to construct algorithmic framework and to use these morphological indicators for parametric modelling. To analyze the effect of urban geometry on heat island intensity through SVF value, to manipulate morphologic entities, and to generate forms by simulation, parametric modelling requires a definition of main morphological components, which are named as block, plot and building.

Previous studies on the relationship between sky view factor and heat island intensity have considered the height of the buildings, the distance between buildings, the distance between measurement point and buildings, and the size of the buildings as main influential factors on the UHI effect. As shown in Figure 3.1, the variation in the main parameters of urban geometry (height, distance and size) induces an obstruction of the sky view in different sizes. When the height of the building ($h_2 > h_1$) increases, the obstructed area also increases. However, an increase in the distance ($d_2 > d_1$) between test point and buildings results in a decrease in the obstruction of the visibility within the condition of same building height. Moreover, the size of the building (building coverage area or building volume) has a directly proportional effect on the increase in SVF value. Therefore, in this study, morphological components of urban areas (block, plot and building) will be associated with measuring instruments as geometric parameters, and will be defined algorithmically to initiate parametric discussion on the morphological indicators of UHI.

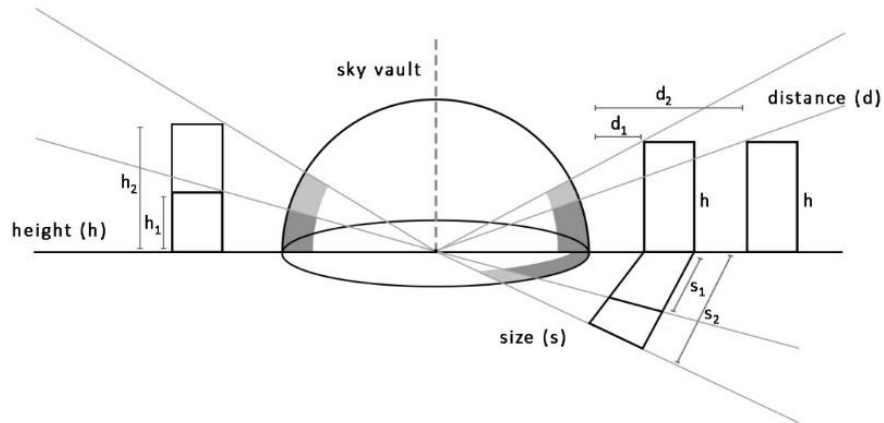


Figure 28: Schematic depiction of the effect of morphological parameters on the visibility of sky

Parametric modelling necessitate an algorithmic transformation of each design units, which are imported as layouts to Rhinoceros software or completely drawn at there, to set up algorithms for computations of design areas. Hence, to be able to analyze geometric features, to search, select and sort a set of values, and to manipulate or generate forms, morphological components of urban areas should be introduced to Grasshopper software through specification of their basic element, such as surface, edge, centroid and corner. This transformation of knowledge from two-dimensional drawings to the algorithmic tools allows the designers to have a control over the design process, and makes this process more flexible and interventional. Figure 3.5 illustrates the algorithmic definitions of basic elements within this study's framework. Blocks are defined by surface (area) and corner (point), plots are defined by surface (area) and centroid (point), and buildings are specified by surface (area), corner (point) and centroid (point). Street layout is not specifically taken into consideration due to the space between the blocks can provide the measurement information of street width, but the midline of the street, which is named as spine, is defined by line and segments (point).

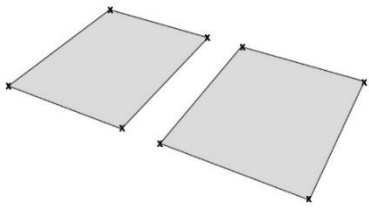
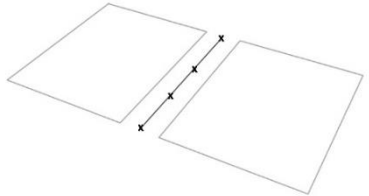
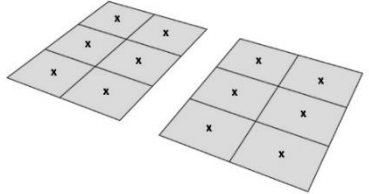
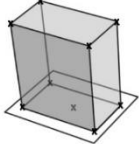
Components	Notation	Elements
Block		<ul style="list-style-type: none"> - Surface (area) - Corner (point)
Spine		<ul style="list-style-type: none"> - Line - Segment (point)
Plot		<ul style="list-style-type: none"> - Surface (area) - Centroid (point)
Building		<ul style="list-style-type: none"> - Surface (area) - Corner (point) - Centroid (point)

Figure 3.529: Definition of basic elements of morphological components

One of the parametric modelling tools is that Genetic Algorithm requires definition of a set of operations regarding morphological parameters for the simulation. Determination of the effect of parameters on the SVF value, simulation of different scenarios, and generation of forms in order to mitigate UHI effect can be operated via algorithmic attributions, which are the basic tools of Grasshopper software. These tools (extrude, move and scale) work with the direction of x-y-z coordinates, and make alterations on the height of the buildings, location of the buildings and size of the buildings.

Parameters			
Tools			
Algorithm	<p>Extruding a building 12 meters on the z-axis</p>	<p>Moving a building on the x-axis and y-axis</p>	<p>Scaling a building with a certain scale factor</p>

Figure 3.6: Schematic depiction of algorithmic attributions

Searching form configurations and better solutions in the context of heat island mitigation, defined limitations or controller indicators are crucially necessary due to the nature of Genetic Algorithm. Therefore, firstly, morphological parameters can be classified as variable and stable components. To illustrate, building height, floor area of the building, building volume, and distances between buildings are considered as variables, while the main layout of an urban area, block and street organization, street width, block size, and building numbers are defined as stable ones. Thus, this categorization may help designers to cope with the design complexity.

Secondly, morphological indicators to control these parameters are determined referring to the regulations of Turkish planning system. In Turkey, planning regulations for 1/1000 scaled urban areas are enforced through Implementation Development Plans. These plans include 3 essential metrics, which are Building Coverage Ratio (BCR), Floor Area Ratio (FAR) and Hmax, providing a control mechanism over the building density in urban areas. One of them is that Building coverage Ratio (BCR) can be detailed as the ratio of the building coverage (footprint) area to the plot area. In other words, that ratio helps to calculate the purposed building area within the total gross area. The other one is that Floor Area Ratio (FAR) represents

the ratio of total building floor area to the plot area. Since FAR is determined by the measurement of the horizontal (surface) area and its vertical distribution, that ratio can inform designers about the building density of three-dimensional urban environment. Apart from BCR and FAR, the other metric, Hmax also indicates the urban density through providing a limitation on the building height.

In this study, BCR and FAR are determined as controller indicators in the simulation process for generating many design alternatives to achieve increases SVF value to mitigate heat island intensity. For different scenarios, to modify the measurement of height, distance and size, Building Coverage Ratio and Floor Area Ratio are algorithmically defined as given in Figure 3.7.

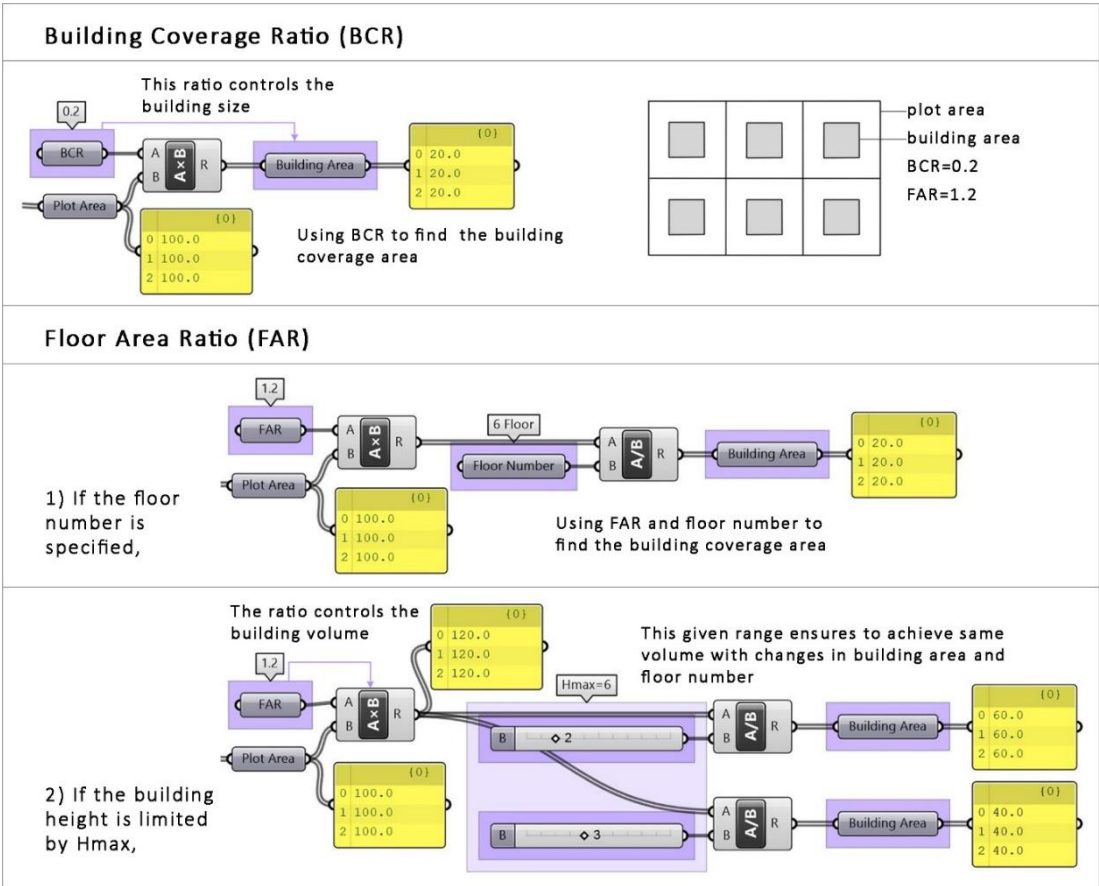


Figure 30: Algorithmic definition of Building Coverage Ratio (BCR) and Floor Area Ratio (FAR)

3.3.2. Algorithmic Setting of Analysis

To calculate SVF value in urban areas, a new technique that is based on algorithmic calculation of geometric features is developed through Rhinoceros and Grasshopper softwares. Geometric components of urban areas were quantified by specialized algorithm, and then for each viewpoints SVF values were computed depending on hemispheric projection of buildings. With the help of this algorithmic model, visibility factors of urban canyons, distribution of SVF values in the complex urban environments, and the magnitude of UHI intensities at those areas can be evaluated and compared with each other easily.

The proposed analytical model is constructed on a hypothetical urban layout that consists of two blocks, and its plot and buildings. Thus, users are required to import layout of a site as an input data to run this analysis in order to import 3D model to Rhinoceros. Nevertheless, 3D building database can be introduced easily to the algorithm, as well. This proposal calculates SVF values with three main steps, which are *detection* (measuring points and areas), *projection* and *extraction* (SVF values).

The first phase is that **detection** can be defined as a decision-making algorithm for selecting the measurement points, the plots and the buildings that are visible to test point where the SVF calculation is to be made in the urban areas. Figure 3.8 illustrates the process of Phase 1, which is composed of measurement point detection, frontal facade detection and closest buildings selection steps. Firstly, to define the test point for the measurement, a spine is generated through the exact center of the buildings due to the calculation of SVF values may give more accurate results when they are observed from the center of the canyon. To ensure the uniformity of the distribution of all SVF measuring points in the area, the spine is divided into equal distances instead of equal segments. Additionally, to avoid the positive influences of empty spaces on the visibility of sky, end points of the spine can be removed. Therefore, the remaining points on the spine are used as measuring points. Also, these ground level test points are selected to obtain more precise projection on the hemisphere, because there is no essential difference between the ground level measurement and 1-1.5 meters above the

ground measurement SVF results.

Secondly, because of the SVF values are only measured between the buildings that border the canyon axis, the visible areas from the measurement point should be detected. Therefore, within this step, detection of frontal facades is generated by the algorithm due to restraining of unwanted plots and buildings selection. Detection of frontal plots is formulated by the splited comparison of the distance between two blocks, and the distance between measurement point and plots. Thus, the closer than the specified distance plots are selected. After the plot detection, as a final step, closest buildings to the test point are defined due to reduction of the buildings that are out of calculation. In addition, since the formulation is based on the amount of closest points to the test point, the generated algorithm enables users to choose number of buildings for SVF calculation.

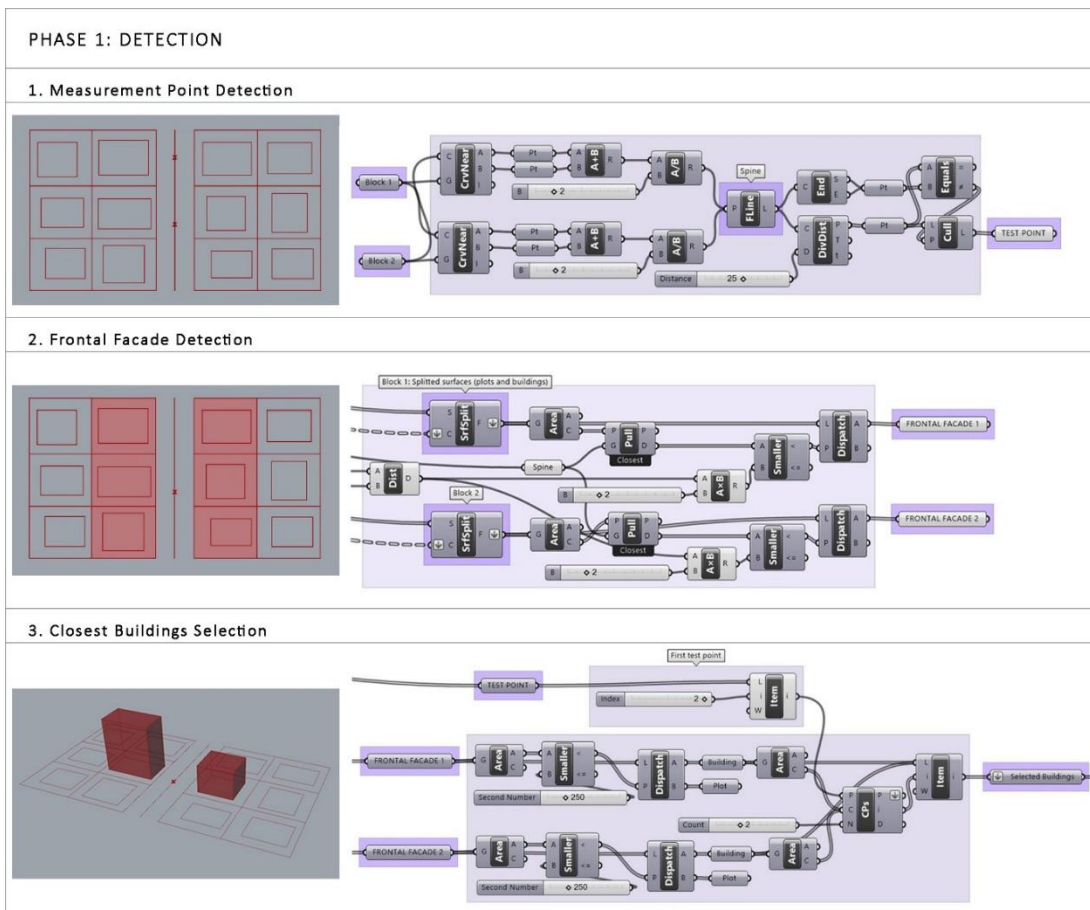


Figure 3.8: The detection process of the measurement point and areas (Phase 1)

As the second phase, **projection**, is basically designed as a preparation phase for the SVF extraction. In this process, firstly, a hemisphere is generated at the center of the urban canyon. For this purpose, a circle with a radius of 7 meters, which is a half of the street width, centered on the measurement point is created. After that the hemisphere is generated by creating circle-based algorithm series. As opposed to the previous studies, the hemisphere is not divided into segments or slices with refers to the rotation angle (the angle between buildings and test point). The reason for that, the ratio of surface areas (obstructed and visible sky areas) is to be utilized in SVF calculation instead of angle-based formulations.

Secondly, with the use of buildings, test point and hemisphere input parameters, projection lines are generated from the measurement point to the edge of buildings. Once the lines get their directions, the intersection of lines and the hemisphere gives a set of points that helps to produce buildings projection on the hemisphere. As a result of that operation, the obstructed area on the sky vault by buildings is represented.

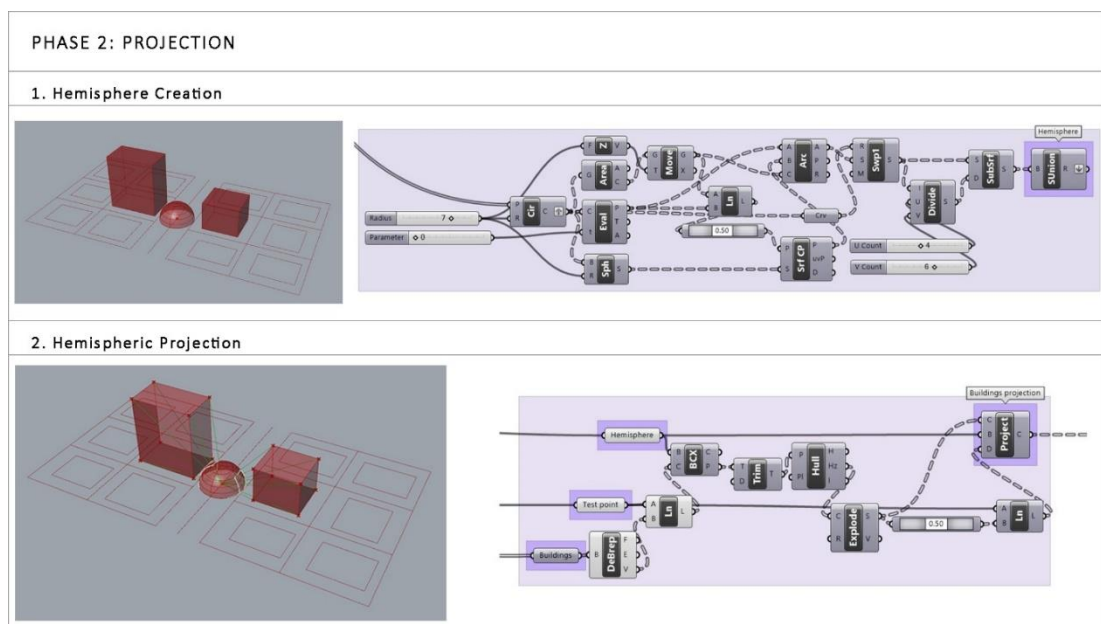


Figure 3.9: The projection process of the buildings on the hemisphere (Phase 2)

After the projection process, at the third phase, to calculate SVF values two extraction models are developed. One of them is a fisheye image extraction via projection of

buildings on a flat surface, and the other one is a hemispherical SVF extraction from a 3D model. The first model is that fisheye image extraction represents a flat image showing the visibility of the sky like image-based SVF calculation methods. The SVF (ψ_{sky}) value can be computed by the subtraction of the ratio of circle area, which represents an unobstructed and clearly visible sky, and the total area of projected buildings from 1. Then, the UHI ($\Delta T_{u-r(max)}$) intensity can be calculated with the use of Oke’s (1987) formulation, which is given as follows:

$$\psi_{sky} = 1 - A_{obs}/A_{total}$$

$$\Delta T_{u-r(max)} = 15.27 - 13.88 \psi_{sky}$$

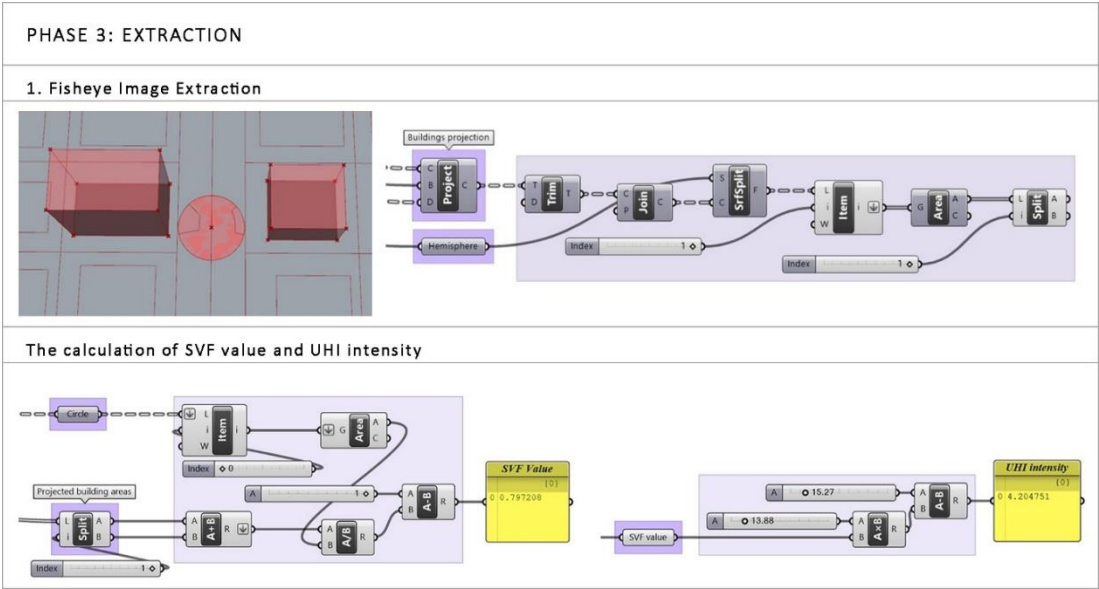


Figure 3.10: The SVF extraction from the fisheye image model (Phase 3)

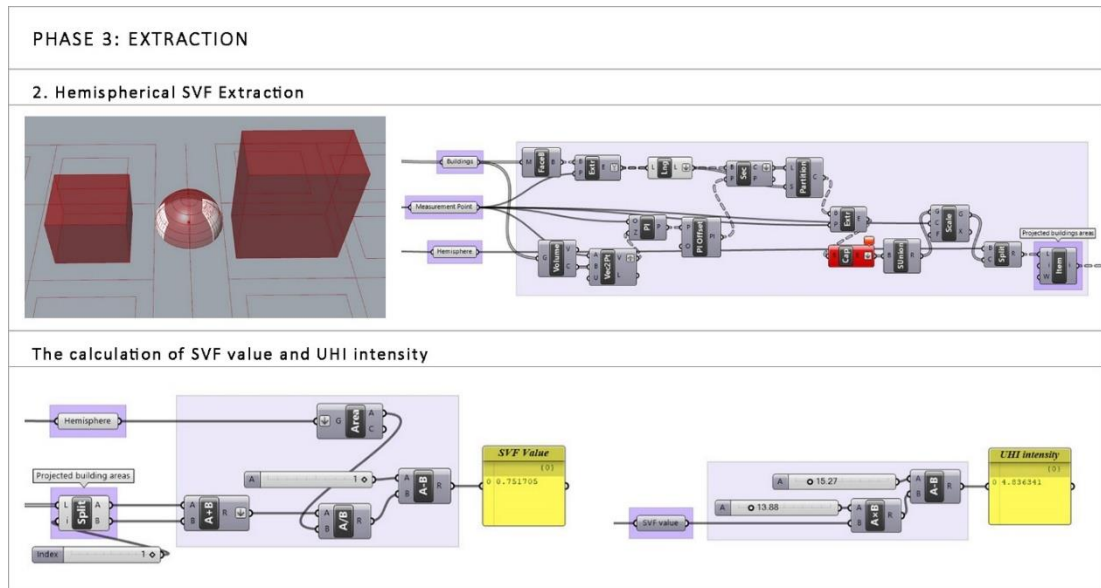


Figure 3.11: The SVF extraction from the hemispherical projection model (Phase 3)

The second developed model to quantify SVF values is based on the hemispherical extraction that can achieve more accurate results than the fisheye image model. Because of the nature of two-dimensional images of projected urban areas (fisheye images), the sky vault (hemisphere) is represented as a 2D circular flat area. Therefore, surface areas of the hemisphere ($2\pi r^2$) and the circle (πr^2) are differentiated from each other, and thus their sky view factors and heat island intensities result in different values.

The results of the area calculations, sky view factor and heat island intensity computations of produced two models are compared in Table 3.1. In the fisheye image extraction model, the obstructed area by buildings is measured as 31.21 square meter while the hemispherical model calculates the obstructed area with the same buildings is 76.44 square meter, however the projection surfaces (circle and hemisphere) also increase in a similar manner. As a result of the calculation, 0.04 unit difference between SVF values and 0.63 degree difference between UHI intensities are detected within this experiment. The evaluation of generated models improves the understanding of the accuracy of different SVF computation models. Although fisheye image extraction model is not completely accurate for the SVF and UHI

determinations, this model offers a possibility to calculation of SVF values in urban areas like capturing real fisheye-photography, and to compare SVF result from other image-based studies, which are widely preferred by researchers.

Table 3.1: The comparison of SVF extraction models

	Fisheye Image Model	Hemispherical Model
Building 1	20.90 m ²	45.71 m ²
Building 2	10.31 m ²	30.73 m ²
Total area of buildings	31.21 m ²	76.44 m ²
Projected surface area	153.93 m ² (circle)	307.87 m ² (hemisphere)
SVF value	0.79	0.75
UHI intensity	4.20 °C	4.83 °C

Furthermore, this experimental model is defined by analyzing the nearest two buildings to the measurement point for the hypothetical urban area. Therefore, heat island intensity is calculated by using a single SVF value measured in the canyon, but when the algorithm for the analysis is implemented to an actual urban area, UHI intensity should be calculated by averaging the SVF values of each measurement point. Additionally, this algorithmic setting of SVF analysis offers a flexible testing opportunity to users via changing in the number of buildings to be measured with a simple move on the number slider.

Figure 3.12 illustrates the differentiation of the building amounts according to their distances to the measurement point. When the slider is moved from 2 to 6, closest six buildings to the test point will be automatically selected, and the analysis runs immediately. In other words, in a short time, additional buildings are projected on the hemisphere and the new SVF value is calculated. For example, the SVF value for two buildings selection was calculated as 0.75, but with the addition of four buildings the SVF result decreased to 0.56. Briefly, this algorithmic model on Grasshopper is designed to be open to intervention by users, and thus parameters, such as the number

of measurement points, distances between these points, and the number of plots and buildings, for the calculation of sky view factor and heat island intensity, depends on users' decisions.

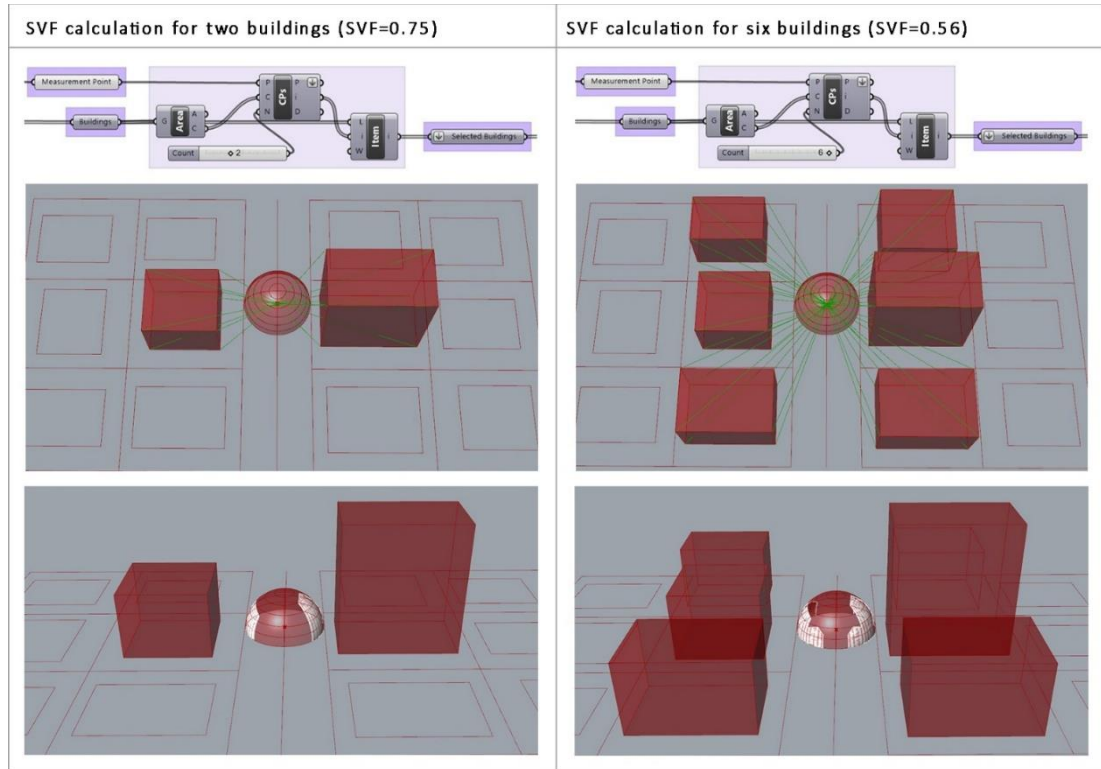


Figure 3.12: The comparison of SVF measurement results of the different number of buildings

3.3.3. Algorithmic Setting of Simulation

Proposing a parametric model, to find better form configurations and to get most achievable SVF values for the mitigation of UHI intensity, requires an algorithmic setting of the simulation performance. In order to do that, Galapagos, the evolutionary solver, is used to test input parameters and to generate alternative or better geometric forms. Algorithmic sets are organized into two steps, which are differentiated from each other by the addition of limitations. The first step is principally designed to evaluate morphological parameters (height, distance, size) via Genetic Algorithm. For each parameter, simulation is set to run for searching the effect of each change in the value of the parameters on the visibility of sky. To illustrate, the simulation tool

(Galapagos) slightly changes the number slider, which connects to the height measurement, and finds out which building height is better for the maximization of the SVF value. Therefore, appropriate and various design results can be obtained according to the changes in the urban geometry parameters.

The second step is a developed set of algorithm that originated from the first step for providing an integration between parametric modelling and enforced planning regulations, and improving the applicability of this simulation tool on the actual urban areas. Thus, the definition of Building Coverage Ratio (BCR) and Floor Area Ratio (FAR) are transformed as a limitation into an algorithmic script. The addition of these algorithms will limit the Genetic Algorithm tool to generating form configurations, and will ensure that changes on the parameters will stick to the specified building density ratios by Implementation Development Plans.

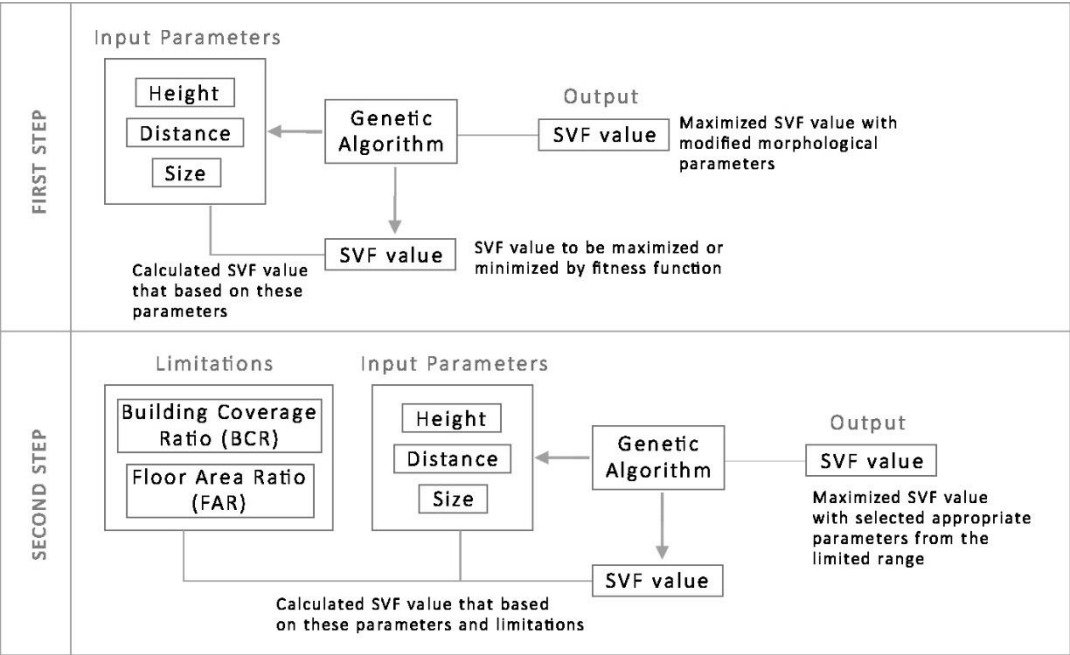


Figure 3.13: Workflow of the algorithmic setting of the simulation

Simulations of morphological parameters are designed separately from each other to establish their influences on the sky view factor one-by-one. One of these parameter is that height has a remarkably effect on the visibility of sky, which is demonstrated by the simulation. Galapagos tries to find most appropriate building height to maximize SVF value with a given range of height. As a result of this simulation, best genomes representing the lowest building height (approximately one-storey building height) are selected to achieve the maximum value (SVF=0.80). According to the determined population number for the simulation, Genetic Algorithm sorts a list of better genomes as many as the population number. The worst genome, which is located at the bottom of the list, shows the minimum SVF result (SVF=0.62) among the better ones.

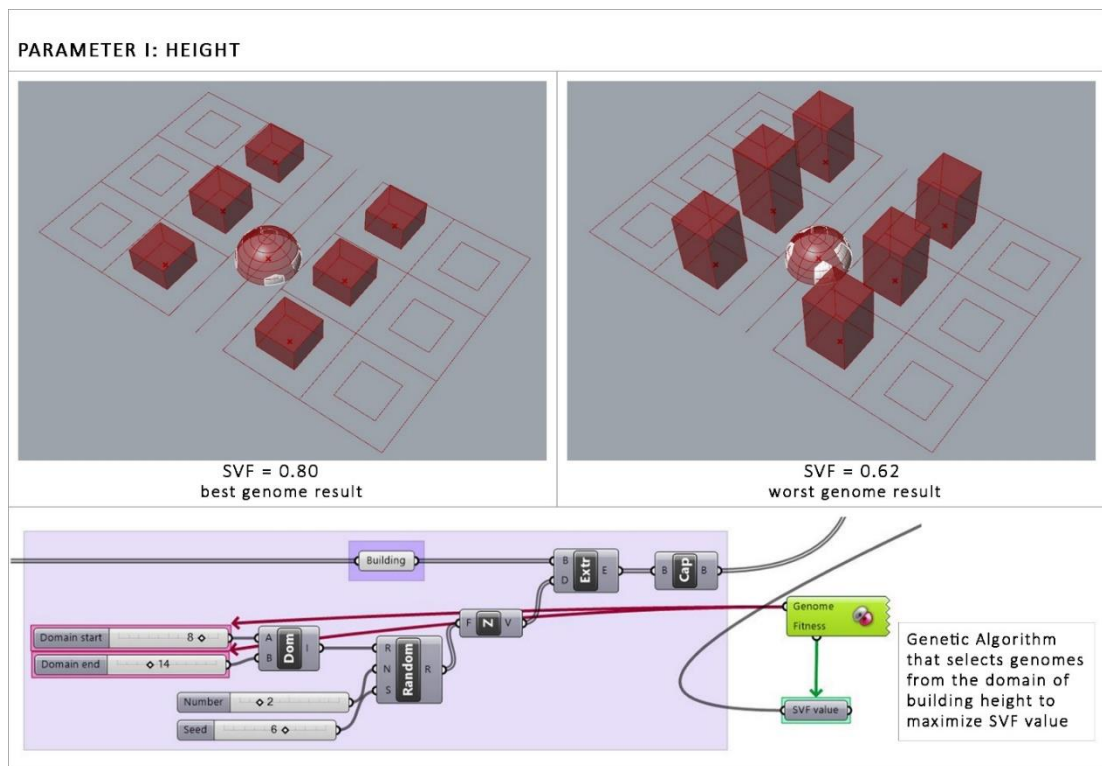


Figure 3.14: The SVF simulation based on the building height

Another parameter is the distance between measurement point and buildings is simulated according to the movements of the buildings on x and y coordinates. The alteration in each building location results in different SVF values, which is estimated by many iterations via Galapagos tool. When the population number of each generation is tested, the best and worst SVF results can be obtained from the list. As seen in Figure 3.15, simulation results show that even small differences in the distance of buildings to the test point causes significant increase in the SVF value such as from 0.66 to 0.75.

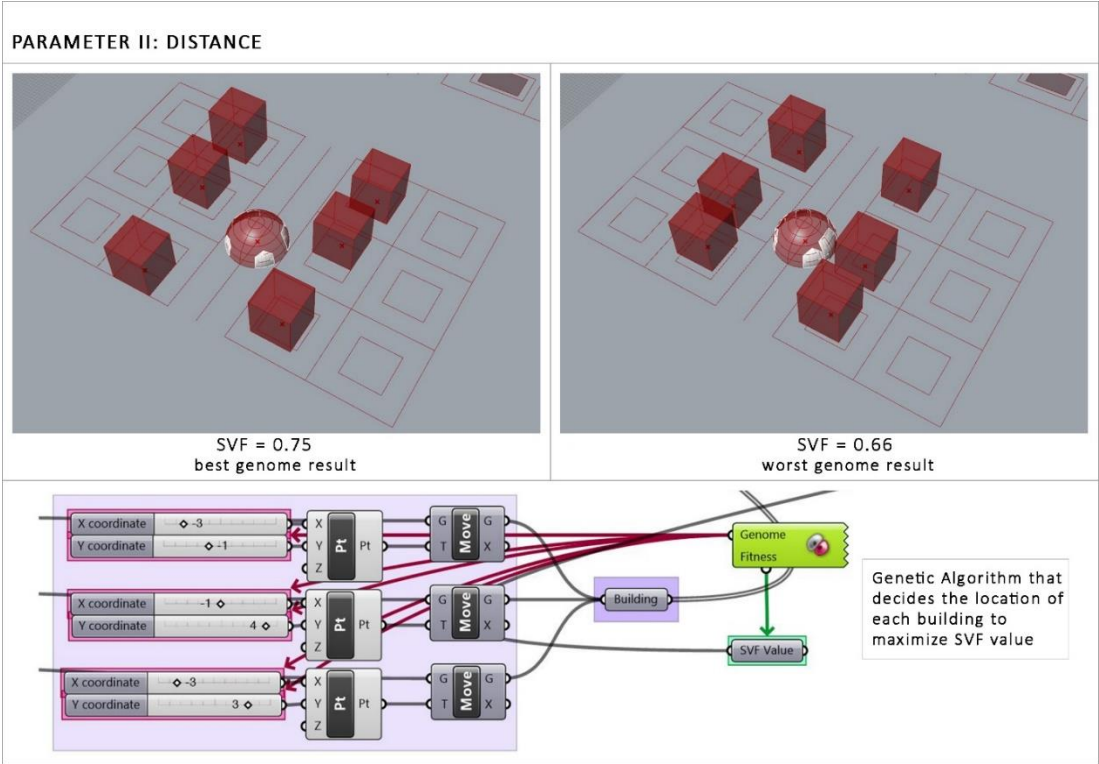


Figure 3.15: The SVF simulation based on the distance parameter

In addition to the establishment of the maximized SVF value with the most appropriate distances for buildings, Figure 3.16 illustrates the richness of the form configurations for the same SVF value. Because of the nature of Genetic Algorithm, Galapagos tends to create a list of better solutions from tested different values like every meter increase or decrease in the building height. Thus, this genome list may be filled with similar SVF results, but they do not represents the same form findings. As given in Figure

3.16, as a result of the distance simulation, the building-plot relations according to the location of buildings is represented with different solutions for the same SVF (0.70) value.

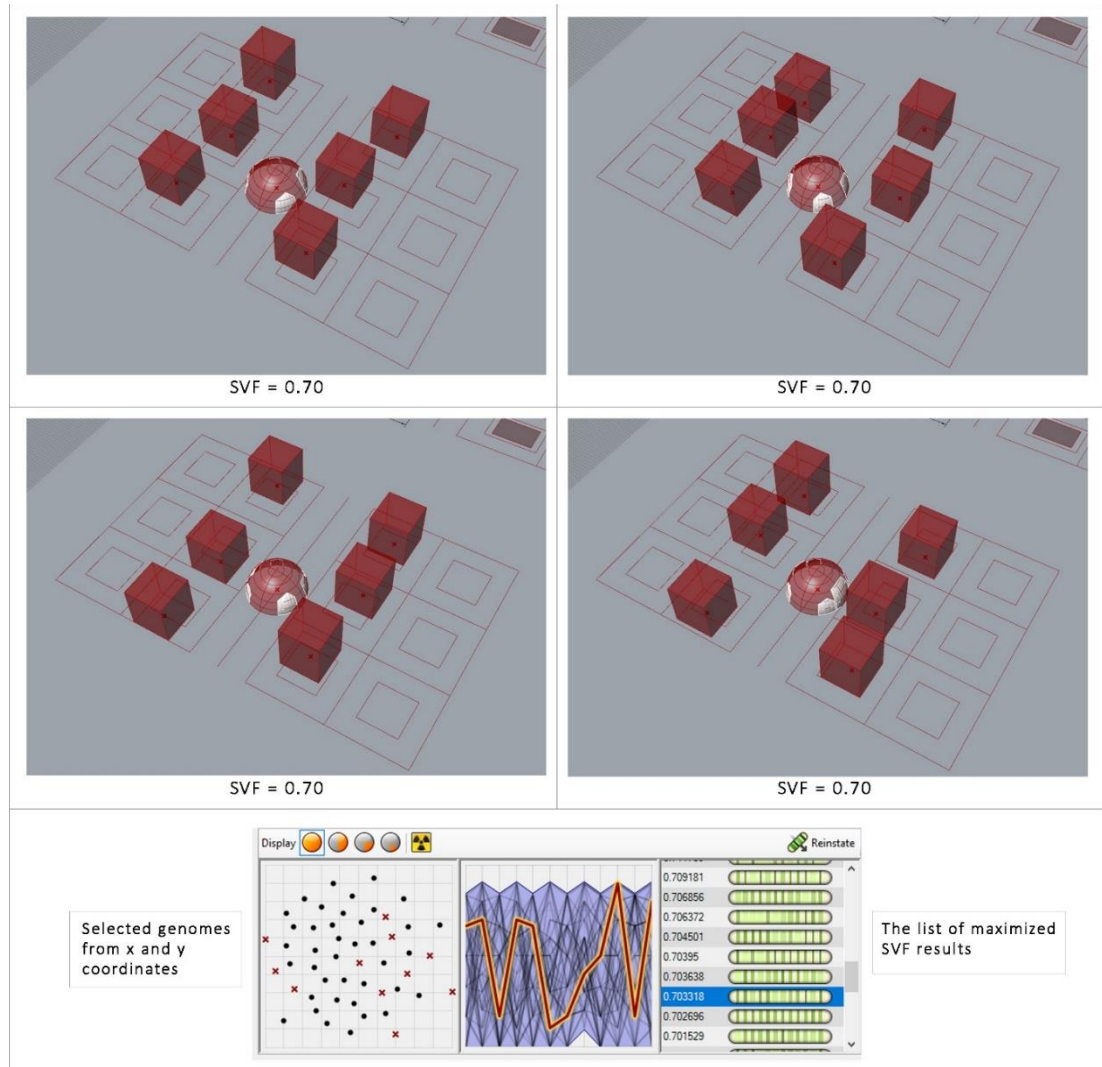


Figure 3.16: Different form configurations for the same ‘distance simulation’ result

Changes in the building coverage area, which is defined as a size parameter, is also simulated for getting a wide range of SV results. Due to the height of the buildings is fixed in a certain value, an increase in the floor area of the buildings directly affects their volume that results in a decrease of SVF value. The main logic of this simulation is based on a scale tool that can control the size of the building with a specified scale

factor. In order to increase the number of test values, the scale factor is determined by a set of value, but it is also limited by the ratio between building floor area and plot area to prevent the development of the building on the entire parcel area. Hence, for the first generation, the simulation estimated the maximum and minimum SVF values for different building volumes as 0.79 and 0.61, respectively. Figure 3.17 shows that the increased building size causes an increase of the obstructed area on the sky vault.

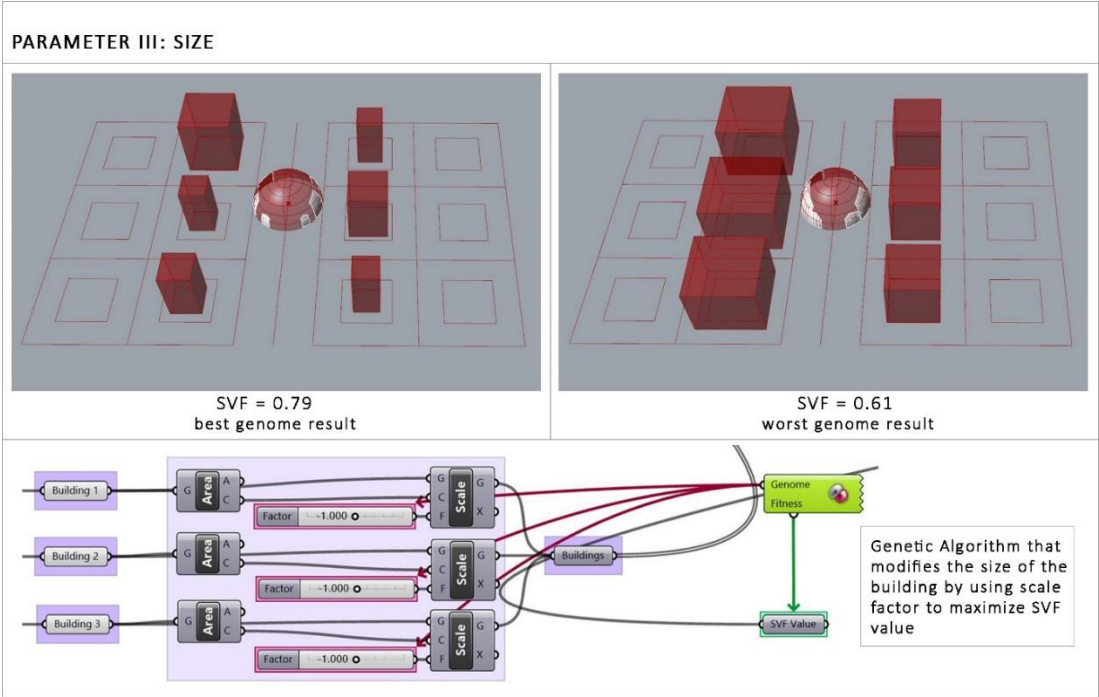


Figure 3.17: The SVF simulation based on the building size

As a second step of the algorithmic setting of simulation, Building coverage Ratio (BCR) and Floor Area Ratio (FAR) are added to the earlier scripted algorithm. By the addition of these limitations, building heights and their coverage area will be changed depending on the density ratios. Since the BCR keeps the building coverage under control, this ratio is already used as a limitation in the previous simulation where the building height is manipulated. Therefore, in this simulation, FAR is used as a controller indicator for making alterations on the building height and size. In other words, to provide a certain Floor Area Ratio, as the building height increases, the floor area will decrease, and vice versa. Thus, the building volume will remain during the

simulation process.

As seen in Figure 3.18, the algorithm is defined for building groups, which are located in the same block. Hence, the height and size of the buildings are modified en masse for those who want to create a more homogenous form with uniformity. As a result of the simulation, the best SVF (0.69) value is obtained from the building typology, which has the lowest height and the widest floor area. Also, simulation results show that the narrowest and highest buildings cause the worst SVF (0.66) value when the building volumes are kept constant.

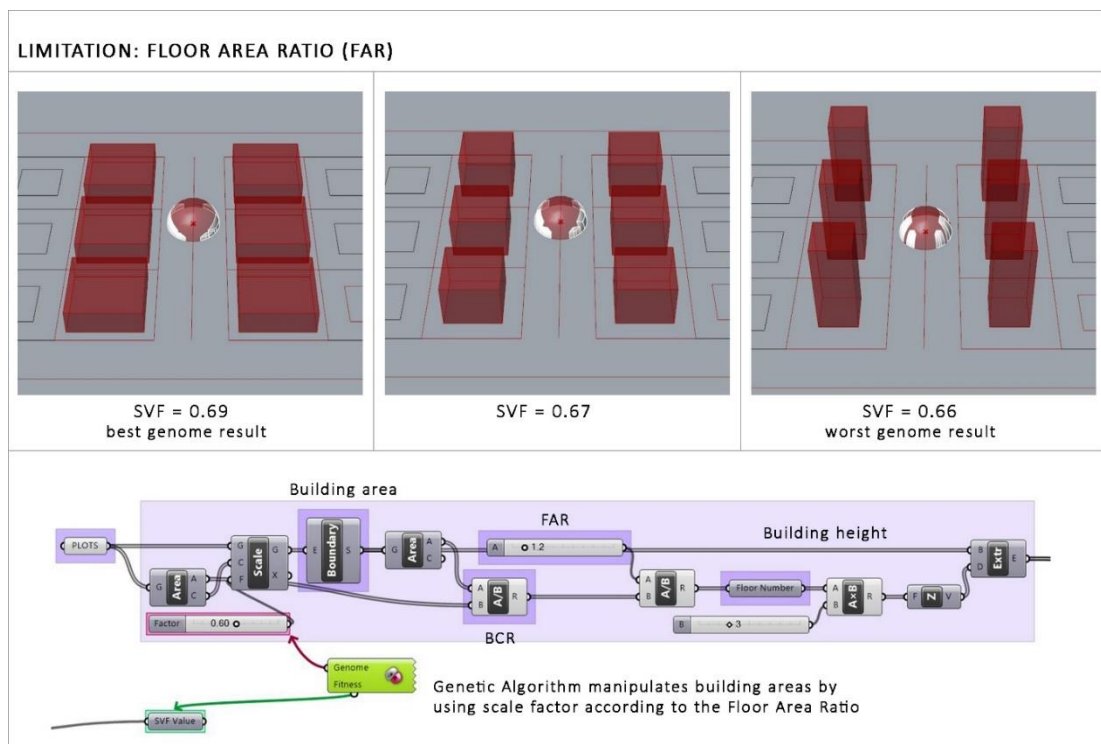


Figure 3.18: The SVF simulation based on the Floor Area Ratio (for all buildings)

When the algorithm of the simulation is manipulated for the implementation of this script to the each building in the study area, a wider variety of proposals has been obtained. Because of the calculation of the SVF value is based on the projection of the buildings on the hemisphere, any changes on the height and size of the buildings result in different SVF values. Thus, Genetic Algorithm tries to find which arrangement will

be better for obtaining the maximum SVF value by investigating the height and size values given in a certain range. As seen in Figure 3.19, the simulation result represents preferable form configuration for the best SVF (0.69) value. According to the simulation, the fittest SVF result can be achieved when the nearest buildings to the measurement point are higher and narrower than the other buildings. The comparison of these two from alternatives shows that, even if the building volumes are the same, the height and width of the buildings cause better SVF values according to buildings location.

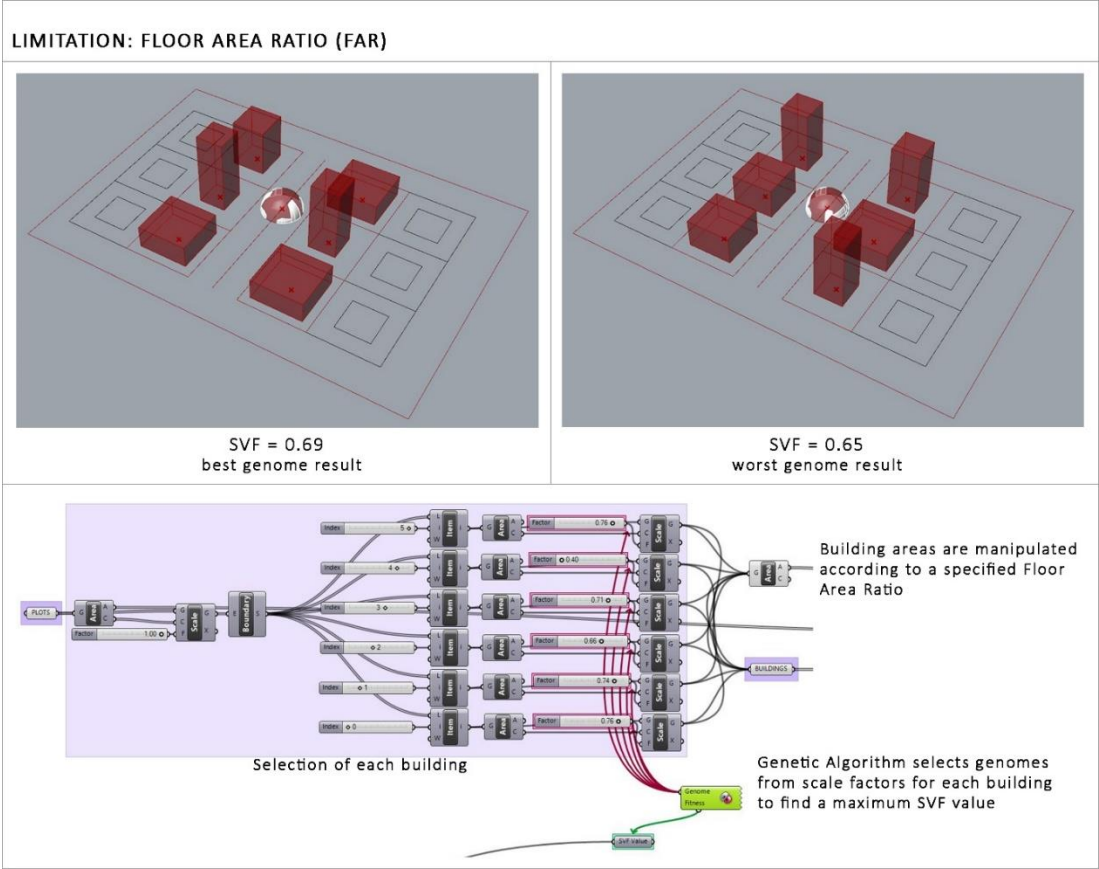


Figure 3.19: The SVF simulation based on the Floor Area Ratio (for each building)

Additionally, different form configurations, which are obtained from the same simulation, are given in Figure 3. During the fitness process, Galapagos calculated SVF values by testing different height and size values for each building while maintaining the building volume. As seen in Figure 3.20, the tool of Genetic Algorithm establishes different design alternatives, which cannot be predicted or achieved by the calculation of SVF values by designers and planners. Therefore, this tool provides better solutions for the mitigation of UHI by maximizing the SVF value with many form alternatives.

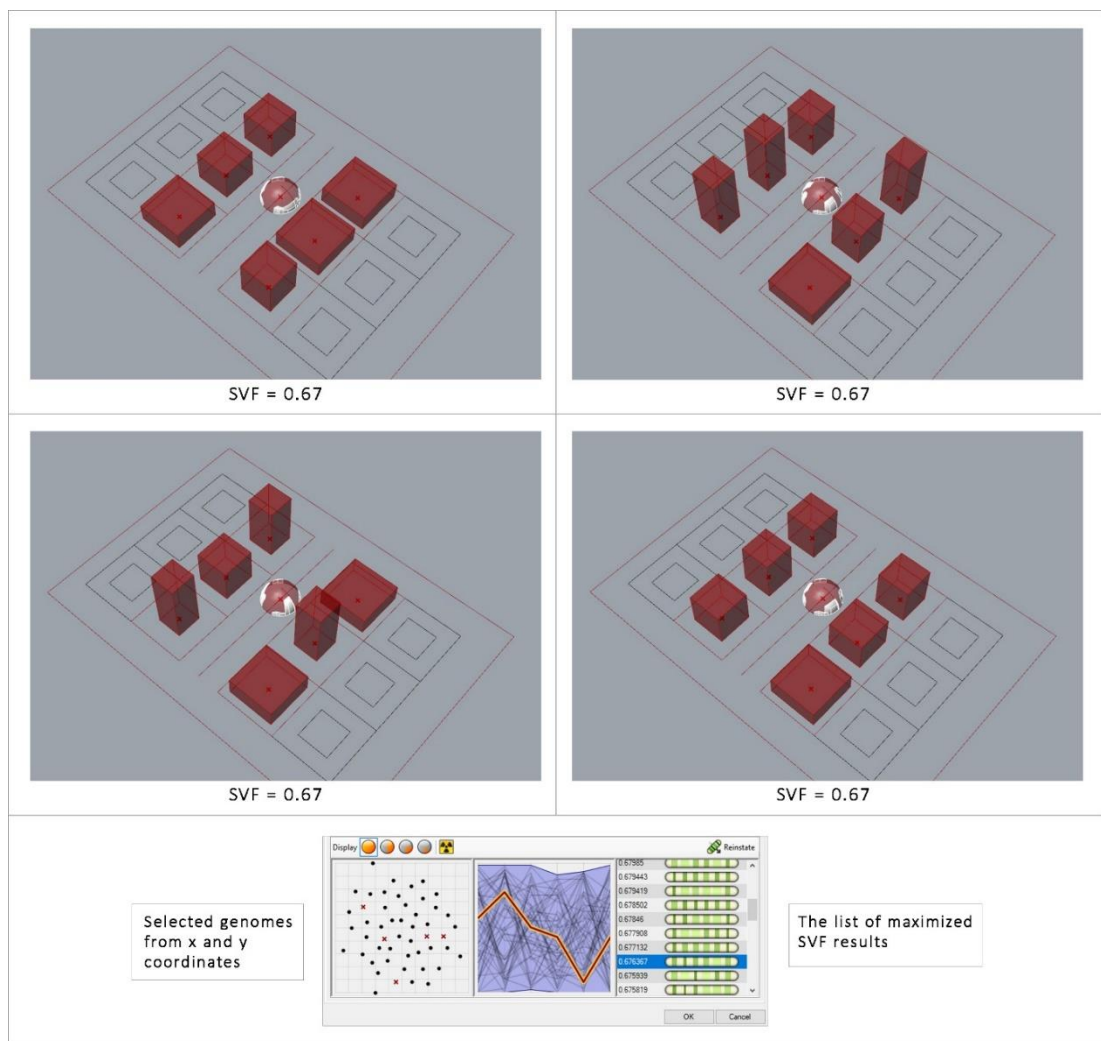


Figure 3.20: Different form configurations for the same ‘FAR simulation’ result

CHAPTER 4

APPLICATION OF THE MODEL IN ACTUAL URBAN CONTEXT: PERFORMANCE ASSESSMENT OF AN URBAN TRANSFORMATION

As a main aim of this study, a parametric model has been developed to mitigate Urban Heat Island (UHI) effect that is based on urban geometry components. By using three-dimensional building data of urban areas, SVF values can be calculated to estimate heat island intensity. In this context, the proposed model is utilized for analyzing geometrical features of selected urban areas, calculating SVF values and heat island intensity of that areas, and generating form compositions to achieve the minimized effect of UHI development. For the demonstration of the applicability of the proposed parametric model, and for the integration of parametric modelling with urban design and urban planning practices, this model should be applied and experienced in an actual urban context.

Therefore, new housing development areas, which are transformed through urban regeneration projects, can be considered for the selection of the case study area. By applying this proposal to the urban regeneration area, a comparison can be made between demolished informal fabric, renewed (existing) urban fabric and design alternatives to be generated by the model in regard to their contribution to the UHI effect.

Another aspect of the case area selection criteria is that while the scope of urban regeneration projects generally aims to provide livable housing and complementary infrastructure facilities, and thus transformation practices only give priority to the

improvement of the indoor environment quality by neglecting thermal comfort of the outdoor environment. Despite numerous studies have been conducted to emphasize emerging problems from increased UHI effect in urban areas, mitigation strategies couldn't gain a place in urban design and planning practices in Turkey. In this respect, the application of the proposed parametric model on the renewed urban area can give an idea that the site may be designed differently, by generating many design alternatives that mitigate the heat island intensity.

In addition, the implementation of this proposal over an actual urban area also provides designers and planners to be able to use the parametric modelling tool at an early stage of design and planning processes. Aim of this study is to provide an integration between parametric modelling and the development planning system on the basis of the climate-responsive urban design approach, and thus the model will promote parametric thinking, and open up new discussions in this regard.

For the case study area selection from one of the neighborhood areas in the city of Ankara, remarkable changes in land use of Eskişehir road and its surroundings, which is defined as a developmental center line by upper scale decisions, have been taken into consideration. Many investments, such as public institutions, shopping malls, colleges and business centers, that have been increasingly located in that place cause to accelerate the transformation of informal housing areas. Therefore, Mustafa Kemal neighborhood is determined as the study area where the most intensive and rapid development in the region is experienced.

4.1. Case Study Area: Mustafa Kemal Neighborhood

Mustafa Kemal Neighborhood is a developed part of the city where public institutions, business centers and residential-office mixed project areas haven been mainly taken place in recent years, and thus this neighborhood area can be considered as a transit zone between these new developments due to it maintains its residential building area characteristics. Because of the southwestern corridor of Ankara has a tendency to

develop and transform rapidly, the land use of this neighborhood has been changed by investments, upper scale plans, and implementation plans decisions.

When the land use maps for the years of 1970, 1997 and 2005, which are prepared by the Ankara Metropolitan Municipality, are examined, in 1970, it is seen that Mustafa Kemal neighborhood consisted of a few public institutions and housing areas, which were mainly dominated by informal dwellings. At the beginning of the 1980s, as a result of the implemented development plans, there were predominantly 1-2 storey buildings in the area. In 1988, the building density of this area was increased for the first time by suggesting 2-3 storey buildings through reclamation development plans. Following this development, in the 1990s, due to the increase in the development of the central business area where the public institutions increasingly located on the Eskişehir road, it was decided to increase each building height by one floor (not exceeding 4 floor) by changing previous plan decisions with revision plans (Eceral et al., 2010). Thus, as seen in Figure 4.2, the land use of this area has changed considerably from 1970 to 1997.



Figure 4.1: Land use situation of Mustafa Kemal Neighborhood in 1970 (Source: Eceral et al., 2010)

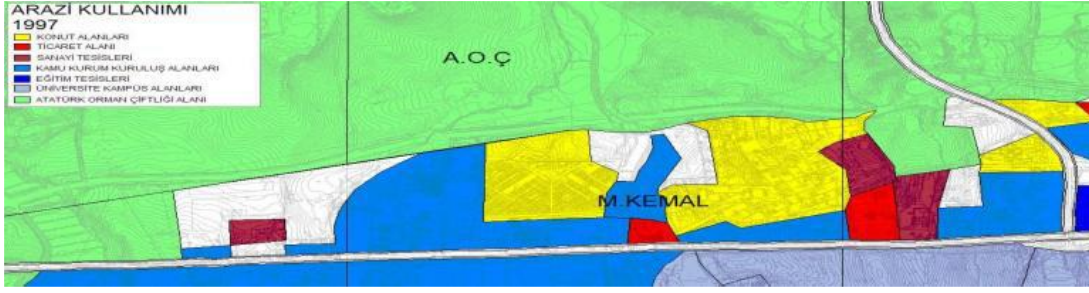


Figure 4.2: Land use situation of Mustafa Kemal Neighborhood in 1997 (Source: Eceral et al., 2010)



Figure 4.3: Land use situation of Mustafa Kemal Neighborhood in 2005 (Source: Eceral et al., 2010)



Figure 4.4: Satellite image of Mustafa Kemal Neighborhood in 2018 (Source: Google Earth)

By 2000s, it is observed that in Figure 4.3, the land use was varied with an increasing number of public institutions, residential areas, industrial areas and also urban service areas. At that period, the Ankara Metropolitan Municipality established a new master plan, which is named as 2023 Capital Ankara Master Plan. According to the master plan report, the total population of Mustafa Kemal neighborhood was 5349, and the size of that area was 369 hectares in 2000. This report indicated that the size of

developed areas was 54 hectares while the informal housing areas covered an area of 6 hectares. Additionally, it was reported that there were 168 people living in the squatter houses, but the population at that settlement was increased to 528 people with reclamation development plans.

Moreover, this master plan provided an intervention by declaring urban transformation and regeneration project areas at two sites in this neighborhood. As given in Figure 4.5, the urban regeneration areas contain unplanned housing developments, which are surrounded by central business areas. In these areas, it was envisaged to make urban transformation projects that based on renewal strategies by providing transfer of development rights, and to build a healthy urban environment by improving housing durability. From 2000s to present, the urban fabric has remarkably changed that is related to upper scale plan decisions. Accordingly, a sub-part of the transformed housing area is selected as a case study area.

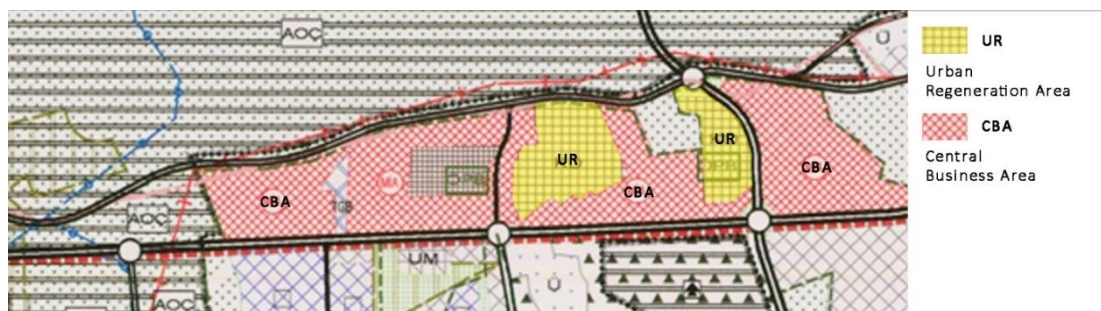


Figure 4.5: 2023 Master Plan decisions for central-west area of Ankara (Source: Ankara Metropolitan Municipality, 2006)



Figure 4.6: Case study area selection from Mustafa Kemal neighborhood

Figure 4.7 illustrates the transformation of the informal housing area into a regular planned area in the sub-part of Mustafa Kemal neighborhood between the years of 2005 and 2018. The case study area is a typical exemplification of the intervention on the shanty settlement (a) by superimposing an ordinary plan layout. Even though this settlement does not carry all morphological characteristics of a typical informal urban fabric (a higher density, a more tight tissue, etc.), this area still represents that typology in general terms. Moreover, because the transformed housing area (b) has a different morphological characteristics (density, layout, etc.) from mass housing areas, which are produced through urban regeneration projects, and also has a homogeneous layout, this area can be considered as a representation of a typical residential area in the context of urban planning practices in Turkey. Therefore, selection of this area may provide an appropriate base for the investigation of UHI effect.



Figure 4.7: Satellite images of the case study area for 2005 (a) and 2018 (b) years



Figure 4.8: Comparison of the figure-ground map of the informal housing area (a) and the transformed housing area (b)



Figure 4.9: Comparison of the street network of the informal housing area (a) and the transformed housing area (b)

4.2. Case Study Analysis: SVF Calculation

As a first stage of the application of the proposed model is that analysis of the case study area to calculate SVF values. By introducing this area to the customized algorithmic setting, the model automatically responds to the requirements. After defining morphological components (block, plot and building) of the area and creating spines between the blocks, the algorithm can be intervened while running to determine measuring points according to the morphological characteristics of that field, such as street width, building size and distances between buildings. For example, the radius of the hemisphere is set as 6 meters for that area where the actual width of the street is 10-15 meters. In other words, the radius is determined as half of the street width to ensure that the base of the hemisphere fits on the street.

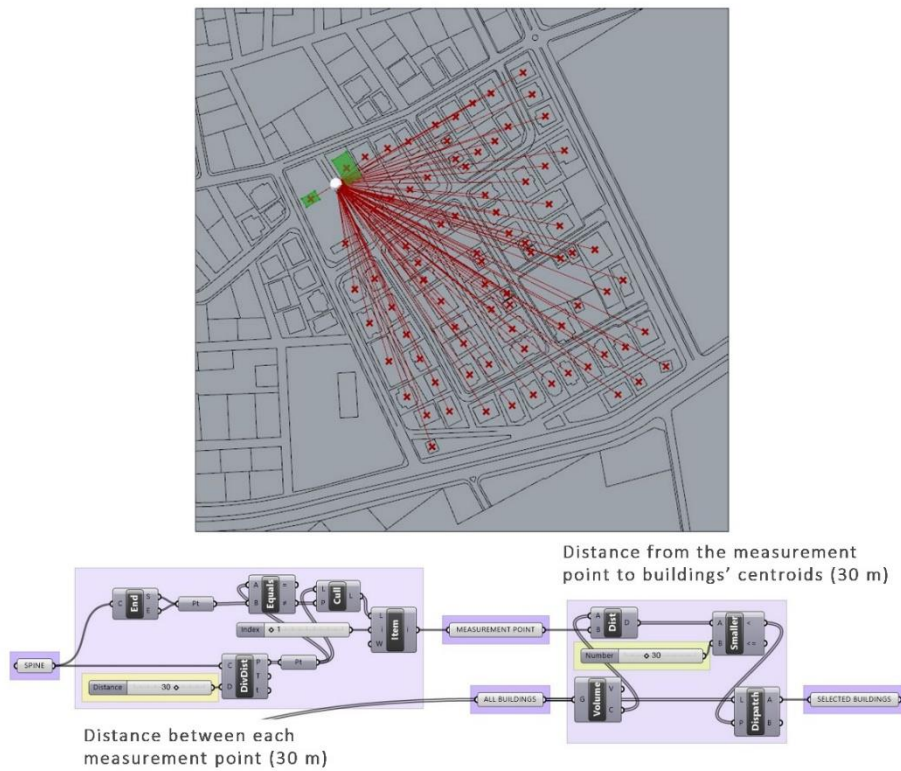


Figure 4.10: Algorithmic setting of the building selection for each measurement point

Also, as seen in Figure 4.10, in order to ensure a homogenous measuring point distribution, the distance between each measurement point is specified as 30 meters. Then, for the selection of the buildings to be projected on the hemisphere, the distance between measurement point and buildings' centroids is defined as 30 meters to limit the building selection. The reason behind the determination of the distance between measurement points and buildings is that the SVF calculation for an urban area should include all buildings in that area. Therefore, the specified distance for this study ensures that at least 2 buildings can be projected on the hemisphere. Also, the distance (30 meters) prevents the selection of more than 6 buildings to avoid the iteration of building projection.

By multiplying this sub-algorithm, selection of all buildings to be used for SVF calculation is provided. Figure 4.11 illustrates application of the algorithms to all components, which are represented with different colors, such as selected buildings are light-red, hemispheres are dark-red and surface area of projected buildings are white colored.



Figure 4.11: Application of the algorithmic set of analysis on the area

Additionally, Figure 4.12 shows the setting of algorithms that is used for SVF calculation. The set of algorithm for building data provides an information to the next step, which is based on the building selection and SVF calculation of each measurement point by using selection results. As seen at the right-bottom of the same figure, all SVF values from measurement points are aggregated in one single algorithm that calculates average SVF value to use as an input data for the UHI intensity equation. Briefly, by applying this analysis, SVF values for each point, the mean SVF value of the whole area, and UHI intensity of that area can be calculated.

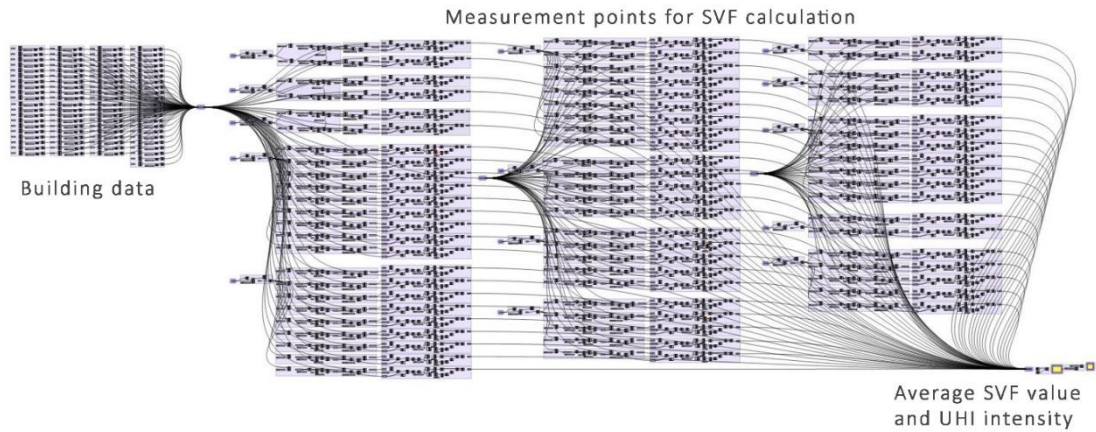


Figure 4.12: Algorithmic setting of the analysis phase of the proposed model

In the case study area, SVF calculation results can be differentiated from one measurement point to another one due to these points are well-distributed on the area to ensure the selection of all buildings. Each SVF value represents one of the morphological characteristics of the study area, and thus the mean SVF value can give an idea about the whole area. Accordingly, Figure 4.3 shows two different measurement points with different SVF values because of their surroundings. One of them is surrounded by 4-5 storey buildings while the other one is not obstructed by any building, so their sky view factors are calculated as 0.66 and 1.0, respectively.

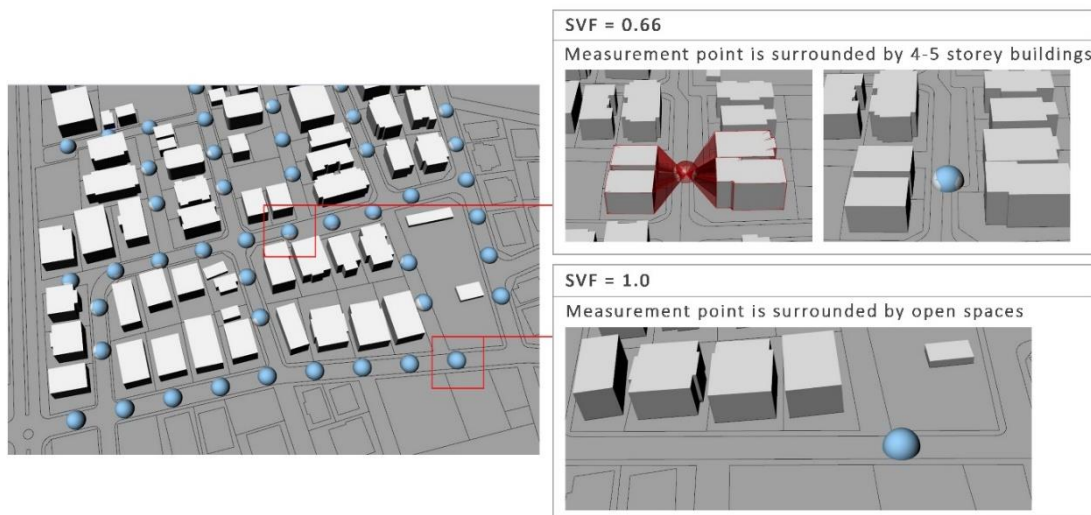


Figure 4.13: Detail sections from the SVF calculations

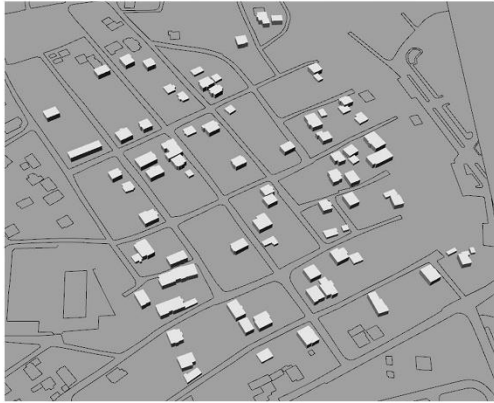

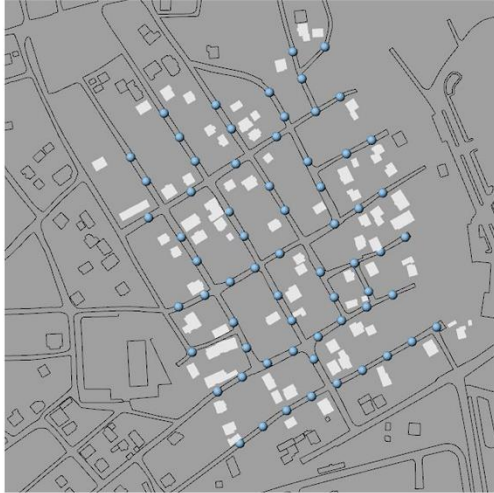

	Informal Housing Area	Actual Urban Transformation
BUILDING HEIGHT	 <p>1-2 storey buildings</p>	 <p>4-5 storey buildings</p>
MEASUREMENT	 <p>Average SVF value= 0.91</p> <p>UHI intensity = 2.48°C</p>	 <p>Average SVF value= 0.75</p> <p>UHI intensity = 4.75°C</p>

Figure 4.14: Comparison of measurement results (SVF and UHI intensity) of informal and actual urban transformation areas

In the context of the SVF calculation, to compare the current state of the case study area with its informal fabric before the implementation of urban transformation, the analysis phase of the proposed model is applied on both of them. As stated in the algorithmic setting of analysis section in the previous chapter, the proposed model applies both the SVF measurement algorithm and Oke's (1987) formulation to calculate UHI intensity, which is based on the SVF result. Therefore, by applying this algorithm both former and current states of the area can be analyzed. As a result of the

application it was found that the informal housing area with 1-2 storey buildings have a higher mean SVF value (0.91) than the formal one (SVF=0.75). Thus, heat island intensity was calculated in lower degree (2.48°C) at there. By increasing building density with plan decisions, the contribution of the newly developed housing area to the magnitude of UHI effect is also increased. As a result of this analysis, comparison of the alteration in land-use at the same area shows the importance of morphological indicators of urban geometry on the UHI development.

4.3. Simulation Application for the Mitigation of UHI Effect

As a second stage of the proposed model, a simulation is applied on the case study area to search form variations that mitigate heat island intensity compared to the current state of the area. In this context, a specified Floor Area Ratio (FAR), which is given by the Implementation Development Plan of this area as 1.3 ratio, is used as a limitation during the all simulation processes. Implementation of this ratio ensures the building volume to remain constant in each simulation for different scenarios. Also, the usage of the same limitation provides adherence of generated form compositions and design alternatives to plan decisions to be able to compare all simulation results with informal and formal fabric of this area where the transformation is occurred according to this plan decisions. To generate various form variations to discuss changes in the typological formation of the area, a few scenarios are determined in regard to the UHI effect. By defining different type of scenarios, this research aims to test well-known urban forms in the urban design practices. In addition, simulation results provide a discussion of the effect of changes in the height-to-width ratio on the heat island intensity for each formation. By modifying size and distance parameters during the simulations to test changes in the building and street setbacks, different building forms have been obtained that apart from the specified form generations by scenarios. Thus, the comparison of SVF values and H/W ratios for the changes in the building forms and open spaces between buildings provide a better understanding of the effect of urban geometry on the UHI development.

4.3.1. Generation of Form Variations

By applying simulation on the case study area, four main types of urban forms have been obtained in regard to the scenarios. The first scenario is formed on the basis of a typical formation, which is called as point block formation. Point blocks present a placement of the block as model for compact urban form by current urban demands. The point block's typology consists of low-rise buildings (6 storey or less), mid-rise buildings (within a range of 7 to 12 storey), and high-rise buildings (13 storey and above). It can also be described as a block, which is isolated from other buildings, and is located on its own plot without sharing any walls with the next building. Therefore, this type of formation contains front and back yards, also has side yard setbacks to avoid an intersection with other buildings. The second scenarios is determined to represent row-housing development. Unlike the point block formation, the row-house model usually tends to have lower building height, which is typically between 2 and 5 storey. In other words, the row-house models are formed by a group of low-rise residential buildings, and are arranged in a sequence of rows. This type of long and narrow strip series of houses that shares both sides of their walls to provide a parallel orientation to the street. Thus, this arrangement allows each building to have a deep rear yard by omitting front and side yards to create continuous isolated private spaces.

As opposed to the arrangement of row-housing development, the third scenario is based on the shortening of the long rows by placing buildings perpendicular to the street line. This type of formation, which can be called as converted row-housing development, consists of 3 or 4 storey buildings, and presents narrow house typology because it has usually no more than 10-13 meters depth. The converted row-house model shares one-side of wall with the next building, and thus only side yards become private spaces by neglecting front and rear yards. Lastly, the fourth scenario is formed as a particular type of perimeter blocks. The perimeter block formation demonstrates a direct relationship between street and buildings, and forms isolated common spaces between the buildings. The type of perimeter block provides public facing edge where buildings are arranged parallel to the street line, and locates private spaces within the block. This formation also presents multiple dwellings with 2 or 3 storey. In brief,

during the simulations, four different architectural forms (the point block, the row-house, the converted row-house and the perimeter block) have the same Floor Area Ratio (FAR) to provide same density, but they present divergent microclimatic conditions in terms of heat island intensity.

For the first scenario, the simulation algorithm is specified to test point block typology. Due to the same Floor Area Ratio (1.3) is determined for all plots in the case study area, the floor area of the buildings decreases as building height increases. In addition, the same building height for each plot has been provided intentionally to get homogeneous urban tissues. Thus, simulation results can be classified as low-rise buildings and mid-rise buildings. As given in Figure 4.15, for the same building density, changes in the building heights directly affect the mean SVF values, and thus contribute to the magnitude of heat island intensity. Also, Table 4.1 illustrates changes in the building height, the average footprint area and the Building Coverage Ratio (BCR) in regard to the fixed Floor Area Ratio (FAR).

Table 4.1: Simulation results of the first scenario

	FAR	BCR	Building Height (m)	Average Footprint Area (m ²)	Average SVF Value
1	1.3	0.42	9	379	0.7553
2	1.3	0.30	12	271	0.7506
3	1.3	0.25	15	224	0.7492
4	1.3	0.20	18	181	0.7473
5	1.3	0.16	24	143	0.7511
6	1.3	0.12	30	110	0.7617

For example, the 3-storey point block formation, with the average footprint of buildings as 379 m², causes 4.78°C heat island intensity. When the building height increases from 3-storey to 6-storey, the UHI intensity has reached up to 4.89°C. Hence, simulation results show that increased building sizes on the vertical plane have greater effect on the rise in the air temperature than the horizontal one. In other words, the UHI effect increases as the building height increases.

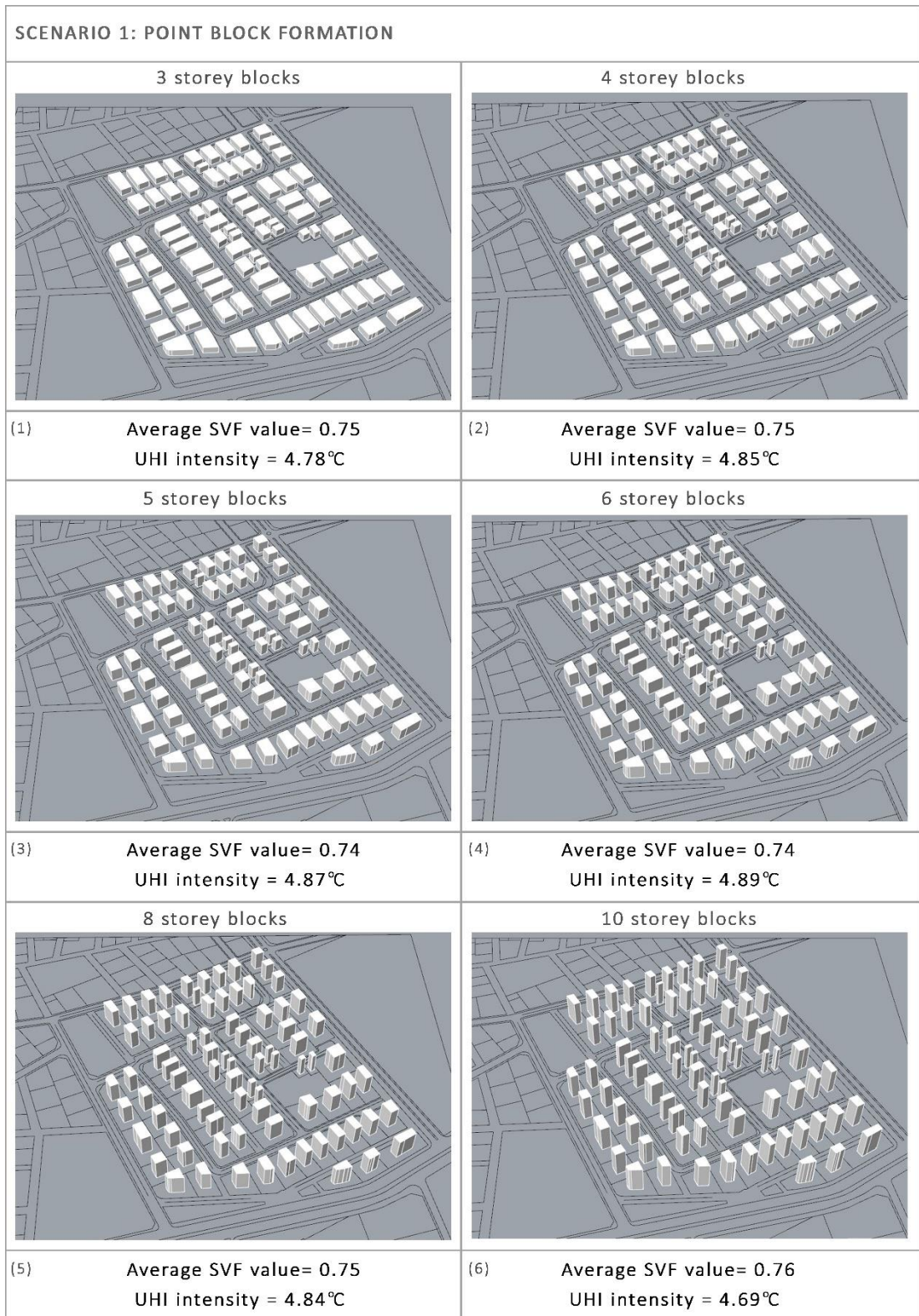


Figure 4.15: Comparison of simulation results for the first scenario

However, even if it seems that low-rise buildings have an advantage in heat loss up to a certain height (up to 8-storey), increased porosity level, which is caused by increasing building height (over 8-storey) with decreasing footprint size, conduces to a decrease in heat island intensity (0.20°C). Increased open spaces between buildings that provide high level of visibility of sky help to reduce ambient air temperature by increasing the emittance of long-wave radiation. Therefore, compact urban tissues may become disadvantaged for the mitigation of UHI effect. As a result of these simulations, the increase in the building height can be interpreted as an influential factor, but at that point, open spaces between buildings (setbacks, street width) may gain priority than the building height in terms of the magnitude of heat island intensity.

In the case of first scenario, the point block formation, further simulations are generated to test mixed building heights, and to achieve better results for the mitigation of UHI intensity. Therefore, simulation algorithm is set up to ensure that each building will provide the specified Floor Area Ratio (1.3) within its own plot, regardless of other building heights. In other words, for this simulation, Genetic Algorithm tests all possibilities for each building by changing their heights. To provide the test of many possibilities, the necessity of establishing buildings at the same height in the same block has been neglected.

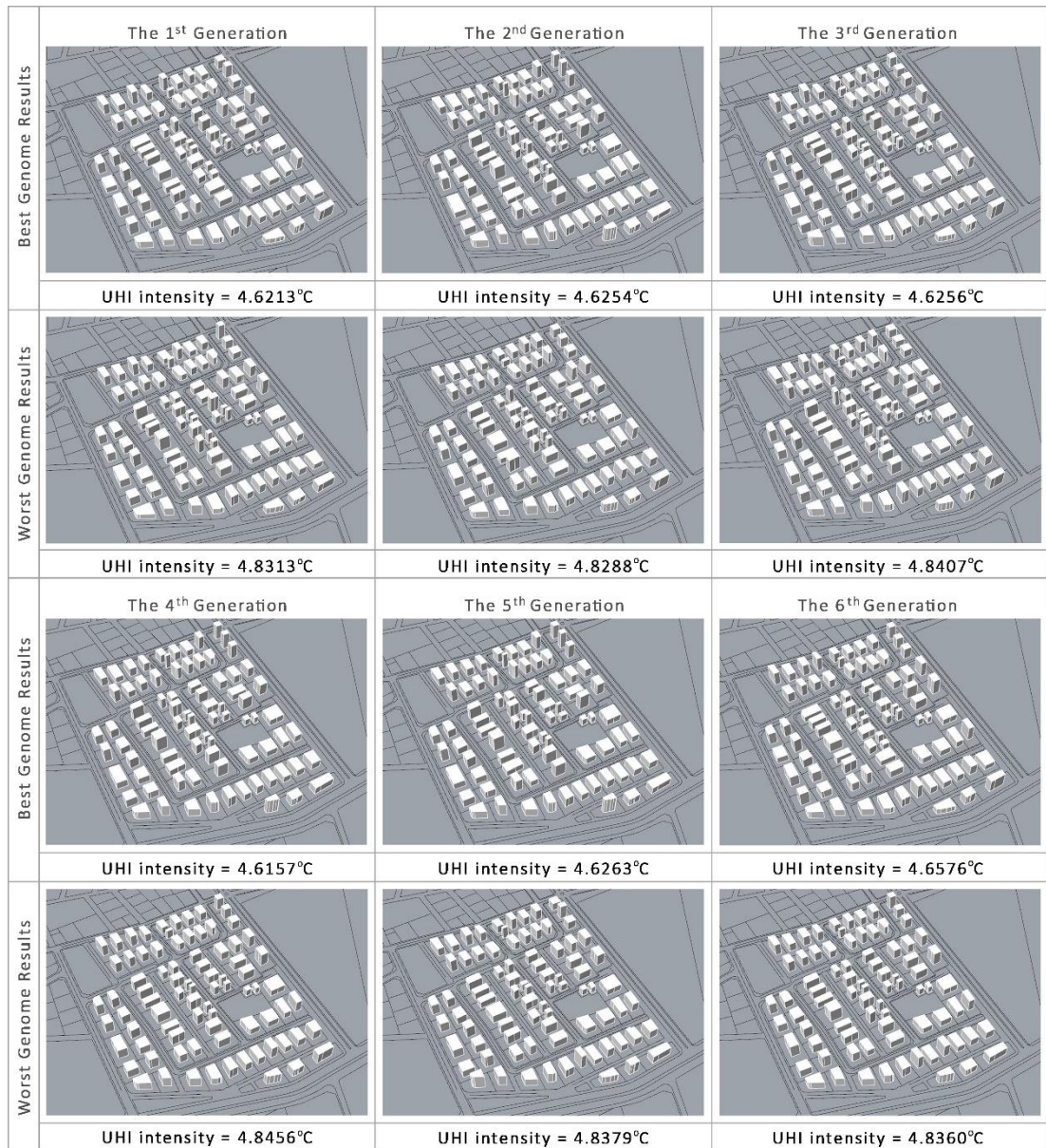


Figure 4.16: Design variations for the first scenario (from 1st to 6th generation)



Figure 4.17: Design variations for the first scenario (from 7th to 15th generation)

As seen in Figure 4.16 and Figure 4.17, the task of the simulation is to generate point block forms with the optimum values (the maximum SVF value with the minimum UHI intensity) for the specified building area. The minimum values of UHI intensity, which are represented as best genome results for each generation, outline the dimension of form-based heat island mitigation. To ensure the high level of various possibilities, and to achieve fittest results, this simulation tests 15 generations with 50 genomes (form samples) in each generation that makes totally around 750 (15x50) form samples. Even though the simulation results have some similar form variations, the different best and worst results are presented. The comparison of produced a series of form variation results show that the minimum heat island intensity (4.52°C) with 0.77 mean SVF value has been obtained at the 15th generation. The building typology of this formation consists of 4 to 8 storey buildings that averagely has 18 meters height (average 6-storey blocks). The simulation results also show that the imperceptible changes in the building heights can provide a decrease in the air temperature.

For the second scenario, building size and distance parameters are mainly modified to generate row-housing development via simulation algorithm. Figure 4.18 illustrates the comparison of the mean SVF values and UHI intensity results for each generation. Additionally, Table 4.2 gives an information about the changes in the building heights, sizes and ratios. As opposed to the first scenario, the effect of increased setbacks on the UHI development is tested for the same building typology in the second scenario.

Table 4.2: Simulation results of the second scenario

	FAR	Average BCR	Building Height (m)	Average Footprint Area (m ²)	Average SVF Value
1	1.3	0.55	6	571	0.7229
2	1.3	0.27	15	276	0.6629
3	1.3	0.40	9-12	417	0.6974
4	1.3	0.40	9-12	417	0.7997

Simulation results show that an increase in the building height causes an increase in the air temperature. To illustrate, the highest UHI intensity (6.06°C) with the lowest mean SVF value (0.66) is calculated for the highest building typology. (5-storey

buildings). Due to the row-housing development consists of narrow canyons with long façade facing streets, building height become one of the most important factor for this formation. However, simulation results also show that the UHI effect can be reduced by modifying setbacks to increase the open spaces between buildings, and to promote heat loss within that spaces. For example, when the front yard setbacks are modified by the simulation, heat island intensity decreases from 5.58°C to 4.16°C for 3 or 4 storey blocks. As a result of that, because the street-lined building rows cause narrow urban canyons, the UHI effect can be mitigated by providing wider distances between buildings.

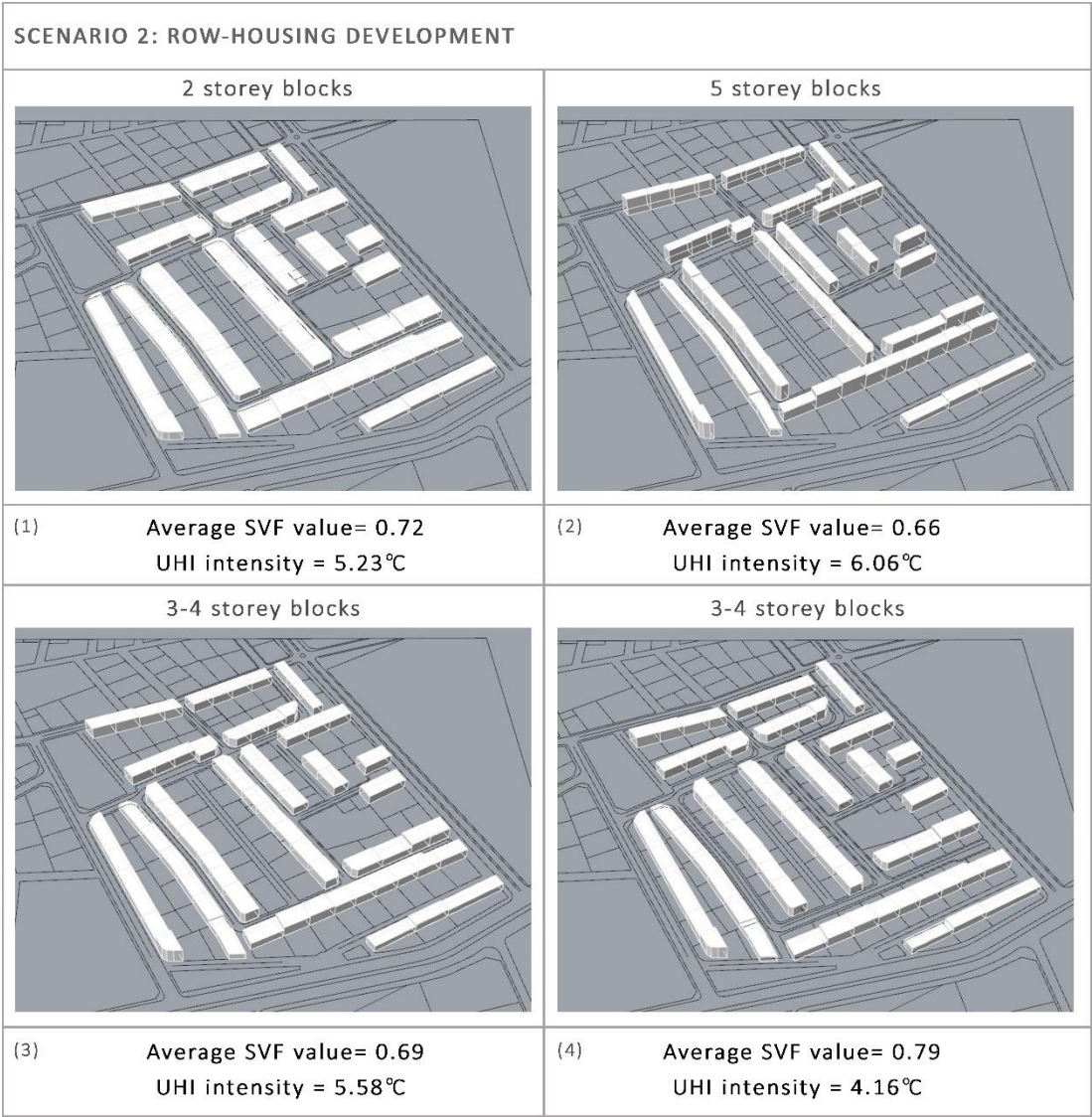


Figure 4.18: Comparison of simulation results for the second scenario

The third scenario is also formed on the basis of the row-housing development with a main difference from the former scenario. To avoid the formation of long narrow urban canyons, which is one of the greatest contributors to the UHI development, and to promote permeable street patterns by minimizing street-facing facades, converted row-housing development is specified as the third scenario. Unlike the parallel orientation to the street line, in this simulation, building rows are arranged perpendicular to the street axis. As given in Figure 4.19, converted row housing typology consists of 3-4 storey buildings. Also, Table 4.3 illustrates the changes in the Building Coverage Ratio and average footprint areas for different building heights.

Table 4.3: Simulation results of the third scenario

	FAR	Average BCR	Building Height (m)	Average Footprint Area (m ²)	Average SVF Value
1	1.3	0.50	6-9	507	0.7501
2	1.3	0.38	9-12	391	0.7489
3	1.3	0.38	9-12	391	0.7464
4	1.3	0.38	9-12	391	0.7369

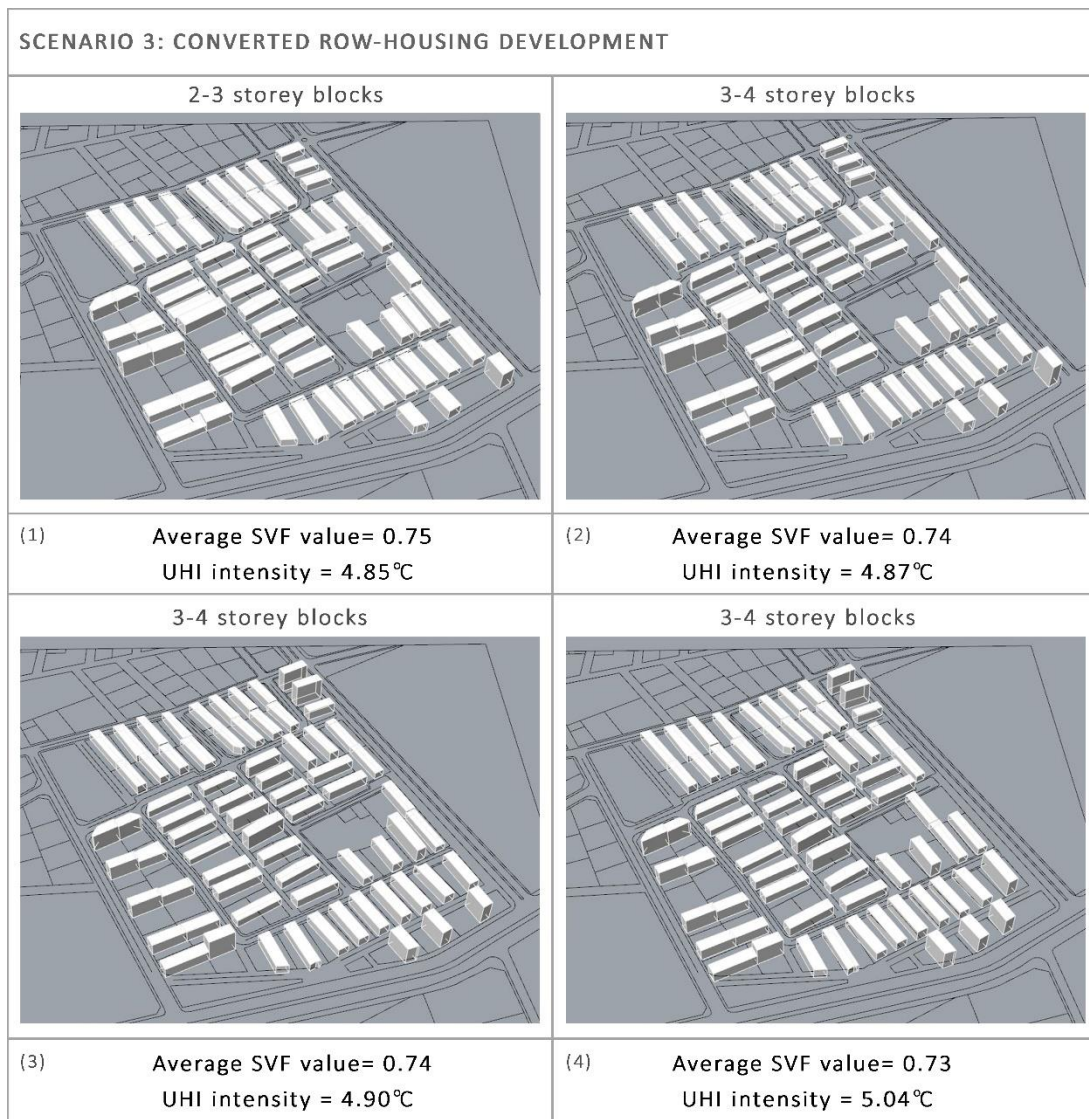


Figure 4.19: Comparison of simulation results for the third scenario

Through the comparison of the first (2-3 storey blocks) and second (3-4 storey blocks) simulation results, the effect of building height on the magnitude of heat island intensity is determined. When the height of each building is increased by 3 meters (1-storey), the mean SVF value decreases by 0.1 that leads to an increase of 0.2 degrees in the air temperature. Additionally, by comparing the results of third and fourth simulations, the influence of the side yard setbacks of buildings with the same height on the UHI effect is examined. The changes in the side yard setbacks result in wider or narrower distances between buildings, which are located in the same block. Since the SVF measurement was made on the street axis to examine the formation of UHI

effect for urban canyons, the correlation between heat island intensity and distances between buildings within the blocks could not be defined exactly. Nevertheless, as a result of that simulations, a decrease in the mean SVF value (from 0.74 to 0.73) with an increase in the UHI intensity (from 4.90 to 5.04) was observed.

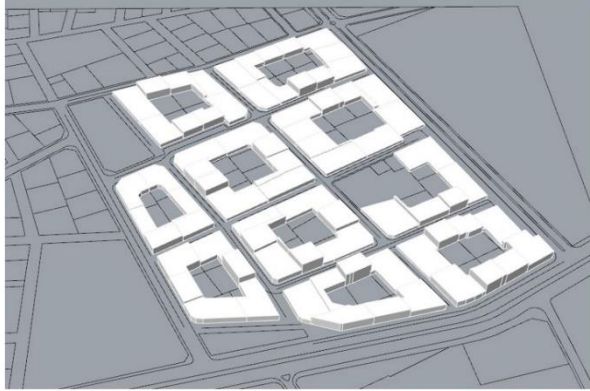
The last simulation, which is specified as perimeter block formation, is based on the increment of the size of courtyards. Since this simulation provides the same Floor Area Ratio (FAR) for each block, the changes in the open spaces between buildings directly affect the building height. This typology creates narrow street canyons due to the configuration of the perimeter block model, and thus flanked streets by buildings causes the development of UHI effect. As given in Table 4.4, the lowest building typology (1-2 storey buildings) has the highest SVF value (0.7408), which decreases as the building height increases.

Table 4.4: Simulation results of the fourth scenario

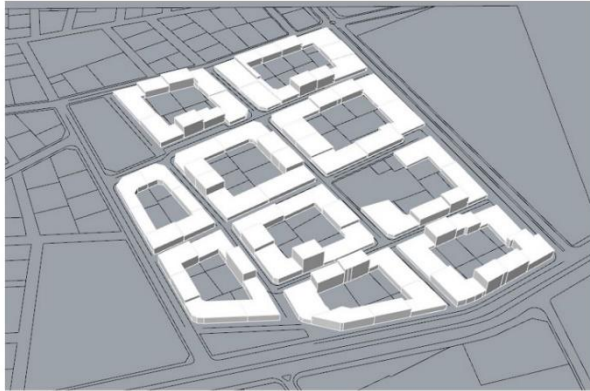
	FAR	Average BCR	Average Building Height (m)	Average Footprint Area (m ²)	Average SVF Value
1	1.3	0.79	3-6	770	0.7408
2	1.3	0.68	6	657	0.7116
3	1.3	0.54	9	524	0.6941

As a result of that formation, the minimum heat island intensity (4.98°C) was demonstrated. On the contrary, the highest UHI intensity (5.63°C) with the lowest SVF value (0.6941) was observed at the third simulation result that generates 3-storey narrow buildings. Nevertheless, as seen in Figure 4.20, as the building height decreases, the floor area of buildings expands, so the internal space of the blocks gets narrower that might cause a rise in the air temperature in that areas.

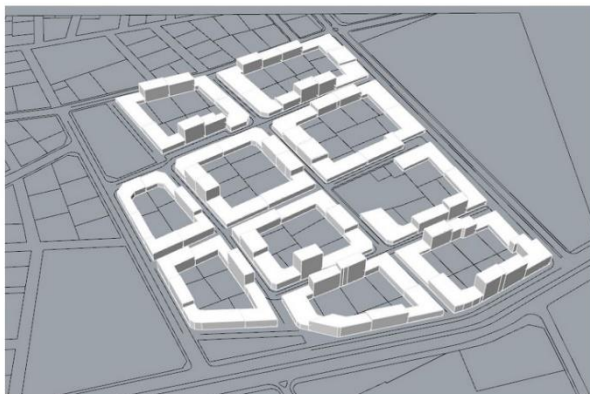
SCENARIO 4: PERIMETER BLOCK FORMATION



(1) Average SVF value= 0.74
UHI intensity = 4.98°C



(2) Average SVF value= 0.71
UHI intensity = 5.39°C



(3) Average SVF value= 0.69
UHI intensity = 5.63°C

Figure 4.20: Comparison of simulation results for the fourth scenario

4.3.2. Overview of the Findings

Simulation results are examined by comparing form configurations generated by the simulation algorithm with the actual case study area. Among generated form variations, those with the minimum heat island intensity are selected for the comparison. As seen in Figure 4.21, the former typology of the urban area (informal housing area) has the lowest UHI intensity (2.48°C) due to it has a very loose tissue with 1-2 storey buildings. The transformation of the area to a more compact tissue with 4-5 storey buildings results in an increase in the heat island intensity.

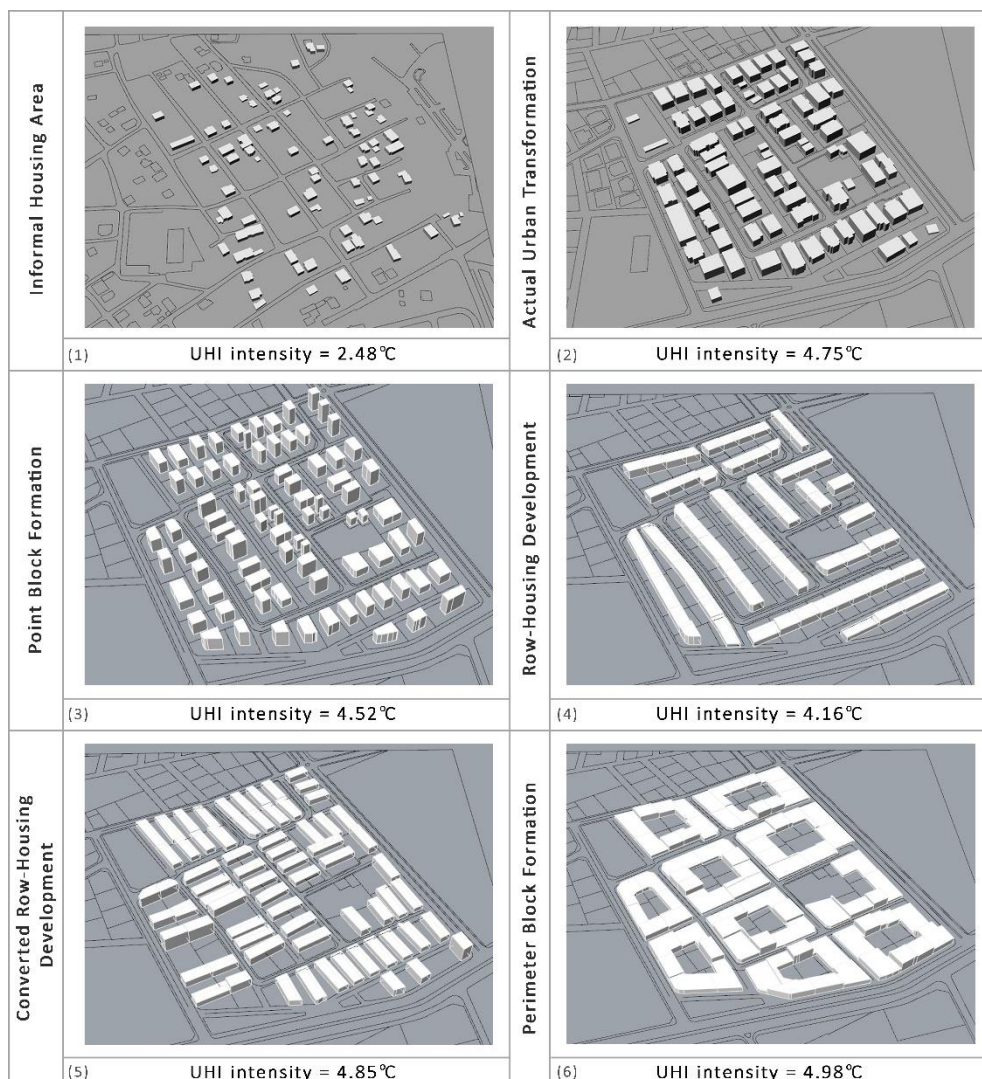


Figure 4.21: Comparison of the actual morphology of the area before and after transformation (top row) with the alternative form variations generated by the simulation (bottom row)

Comparison of alternative form variations shows that the formation of narrow urban canyons causes an increase in heat island intensity. For example, the perimeter block formation has the highest UHI intensity (4.98°C) due to the building arrangement of this typology that promotes the formation of narrow canyons. Even though the row-housing development consists of long canyons that are aligned with attached buildings, increased front yard setbacks provide a wider canyon effect. Therefore, the lowest heat island intensity (4.16°C) has been obtained.

Based on that findings, the variety of form compositions shows that compact urban tissues have disadvantages on the thermal balance of urban canyons. The compactness level affects the rate of heat loss that might be perceived as a rise in the ambient air temperature. As the permeability of urban tissues increases with changes in the building size, the visibility of sky increases that promotes the stored heat release. Therefore, loose urban tissues seem to have a lower heat island intensity. Briefly, based on that evaluations, it is seen that the building height, the street setbacks, the continuity of street-facing facades and the porosity level of the urban tissue are the key variables to mitigate heat island intensity.

Within the context of this study, the proposed model gives ideas about the effect of variables on the UHI development by comparing generated form variations. The generative design approach has been carried out to overcome the issue of UHI effect in urban areas by integrating analysis and simulation processes. Therefore, the application of the model enriches the possibility of design solutions that might be guidance to the need for the mitigation of UHI intensity.

CHAPTER 5

CONCLUSION

The aim of this research is to investigate the potentials of parametric modelling for analyzing morphological components of urban areas, and generating form variations to mitigate the Urban Heat Island (UHI) effect. This chapter presents a comprehensive summary of the research to identify the relationship between urban geometry and the development of heat island intensity, and to emphasize the need for an integrative model of analysis and design processes to mitigate UHI effect in urban areas. Most importantly, this research proposes a parametric model as a methodology to bring an analytical and generative perspective to urban design and planning practices with regard to the problematic issue of UHI development. Therefore, based upon the extensive discussions on the initial discussions on the objectives, methodology and outcomes of the application of the model in an actual urban context, the final chapter seeks to improve a better understanding of the use of parametric modelling tools for further heat island studies.

5.1. The Main Problematic Issues to Revisit

The phenomenon of Urban Heat Island (UHI) has been one of the major issues regarding the perceived thermal comfort and spatial quality of the urban environment. The attention to this issue has been increased in recent years due to changes in the thermal balance of the environment, as an outcome of the urbanization, brought several problems that directly affect the urban livability. Emerging problems from increased heat island effect require new methodological approaches to mitigate that effect by

specifying and modifying the influential factors on the development of heat island intensity. Based on that arguments, this research identified the formation of UHI effect with basic physical principles of energy balance, and the main contributors, such as urban population, urban geometry, surface materials, lack of vegetation areas and anthropogenic heat release, to heat island effect in the literature review chapter.

Detailed definitions and explanations showed that the increase in the ambient air temperature is mainly caused by changes in the energy fluxes. To make it more clear, higher air temperature in urban areas can be explained by increased energy storage capacity through absorption and storage of solar radiation in higher amount. Moreover, inadequate reflection of incoming radiation and reduced heat loss cause a more intensive UHI effect. Controlling all these energy fluxes (heat gain, heat loss and heat storage) to mitigate UHI intensity requires taking into account all influential factors in the urban environment. However, the aim of this study was formed on the basis of improvement of the generative urban design practices in regard to the mitigation of UHI effect, so the effect of thermal properties of surface materials, anthropogenic heat sources, evaporative surfaces (vegetation areas and water bodies), climatic conditions and geographic features of urban areas on the UHI development are not within the scope of this study. Considering the dimension of the relation between heat island intensity and differentiation in the urban morphology, this research was designed to demonstrate the effect of geometrical features of urban areas while characterizing the calculation of UHI in regard to the urban geometry.

In the literature review chapter, it has been emphasized that, urban geometry has a certain effect on the UHI intensity by generating deep and narrow urban canyons, which limit the visibility of sky. In other words, the form of the urban fabric can restrict the emittance of long-wave radiation that results in the reduction of the heat loss. That is why, the methodological approach of this study was formed on the calculation of UHI intensity by using Oke's (1987) formulation, which is based on the measurement of Sky View Factor (SVF). Determination of the visibility of sky between buildings by measuring SVF value varies depending on the components of the urban form. Within the context of this study, these components were specified to

the findings of the previous heat island studies.

At the end of the literature review part, the outcomes of the existing methods on the heat island investigations show that simulation-based studies have the lack of searching form variations to achieve better design proposals in regard to the mitigation of UHI intensity. Previous studies in the field of urban morphology and heat island relation have presented limited number of tested form configurations, and restricted knowledge on the generative design solutions in the context of urban tissue formation. Based on that evaluation, it has been seen that the gap in this field necessitates the development of new tools to promote urban design and planning practices into the generative perspective. That is why this study put forward a new methodological framework for the concept of the mitigation of UHI effect. Within the context of this study, a new model has been proposed by introducing parametric modelling tools.

In the third chapter, methodical approach and algorithmic settings of the proposed model have been introduced. Based on the proposed parametric model, this research enriches decision making mechanism in the design process by implementing Genetic Algorithm into the urban form and pattern generation operations. The application of the model, which integrates analysis and simulation processes, provides designers to specify parameters in regard to their design issues, and to produce alternative design solutions according to analysis results by presenting a flexible and performative design tool. Even though there is a number of experienced limitations throughout the research process, the application of this parametric model on an actual urban context provides many contributions.

In the fourth chapter, specifically to examine the outcomes of the application, the model proposal was applied on the selected residential area in the Mustafa Kemal neighborhood. For the application of the model, algorithmic set of analysis was customized to use of 3D building data, which provides information about the building height, building size, and distances between buildings, of the area in order to calculate SVF values and UHI intensities. It should be noted that other parameters, such as material information of buildings, type of ground coverages, vegetation areas, traffic

related heat release and weather conditions, of the case study area were neglected, and thus only geometrical features of this area have taken into consideration throughout the research. Therefore, calculated heat island intensities only represents the heat increase based on the urban form.

Additionally, in the simulation process, form compositions and configurations were generated to mitigate UHI intensity with regards to the basic building codes within the development planning system in Turkey. These codes, in turn, have been utilized as the parametric indicators of the algorithmic model. That is why, the Floor Area Ratio (FAR) was determined as the independent variable of the model to maintain the same building density of the case study area while modifying other morphological parameters such as setback distance, height and floor coverage. Thus, changes in the input parameters were kept within a certain range by using limitations that provides to generate comparable form compositions within the same layout. From those implications it has been seen that form variations generated by the proposed model presented divergent heat island intensities. Therefore, application of the model and evaluation of the simulation results provided many contributions to the generative design approach in regard to the heat island studies.

5.2. Main Findings and Contributions of the Research

Application of the proposed model on the actual urban context provided analysis and simulation results with generated form compositions for that area. Main findings of this research are derived from the simulation results that indicate UHI intensity varies in accordance with the morphological formation. Comparison of the generated four types of urban forms (point block, row-housing, ‘converted row-housing’ and perimeter block) do apparently demonstrate divergent results.

Simulation result of the point block formation show that permeability level of the urban tissue is the key to mitigate UHI intensity. The wider open spaces between buildings, which are provided by increasing building heights, promote heat loss with a higher ratio of the visibility of sky. As building height decreases, the compactness level of the

urban tissue increases that leads to a rise in the ambient air temperature. Based on that findings, it has been seen that loose urban tissue with mid-rise buildings has a lowest UHI intensity among the other point block formations. Nevertheless, it should be noted that loose urban tissues should not be generalized as a better design solution without considering the shading effect of the buildings. As Bakarman and Chang (2015) stated, shallow urban canyons are exposed the more incoming solar radiation due to the insufficient shading effect that results in higher air temperatures in that areas.

Apart from the comparison of compactness level of urban tissues, another type of urban form, which is row-housing development, opened a discussion on the effect of street setbacks on the UHI effect. Simulation results show that increased front yard setbacks can reduce the heat island intensity, even if the buildings are arranged to form long urban canyons. Additionally, the perimeter block formation was responsible for the increase in UHI intensity by creating narrow urban canyons. From those findings it was obvious that narrow street formations with the continuity of street-facing facades cause a rise in the ambient air temperature.

To sum up, in this research, the proposed model was applied on the selected case study area (Mustafa Kemal neighborhood in Ankara) to generate various form variations in regard to the UHI development. Throughout the study, it has been emphasized that the aim of the research is to improve a generative design approach while investigating form compositions to mitigate UHI intensity. Within this context, the neighborhood area, where the UHI effect was increased due to the transformation process, opened up opportunities to test the model proposal, and to compare possible from alternatives that could be implemented instead of the current one. Therefore, application of the model aimed to evaluate simulation results to achieve some design recommendations that can be used to mitigate UHI intensity in the urban design and planning practices.

Even though evaluations on the form variations are limited to generalize design solutions, this research has contributed to the field of urban design by providing a generative approach that triggers the formation of urban morphology in regard to UHI effect. This research has also provided a contribution to the improvement of an

operational design platform that brings up evidence-based design to the agenda.

Evidence-based design pursued by the use of computational methods in spatial analysis to reveal the intrinsic design problems emphasizes the importance of performative design approach. Also, it produces design principles based on the research findings, to achieve better design solutions (Karimi and Vaughan, 2014). Similarly, the framework of this research promotes the integration of analysis and simulation processes to generate possible design solutions rather than searching for an ideal form in certain optimality on many aspects of spatial planning and design. Therefore, the model application proposed by the research should be considered a kind of design support system informing the complex process of urban design from the specific perspective of UHI effect.

5.3. Main Limitations of the Research

It is important to recognize that there were several limitations related to the proposed model and the research process. The most significant limitation of the model is, in fact, about the parametric modelling process itself. Since parametric modelling tools are specified to the field of architectural design, the use of parametric models in urban design and planning practices is quite a new methodological approach yet to be developed within a systemic (morphological) framework. Additionally, in the field of heat island investigations, parametric modelling has almost never been used except in a few studies resulted with limited evaluations. Therefore, more design research is necessitate to improve the use of parametric modelling tools and techniques among urban designers.

Another practical limitation of the model is that modelling process takes long time, because it requires to set a lot of simultaneous operations for analysis and simulation applications. As the algorithmic setting of these operations becomes a complicated task, it turns to a more time-consuming process. Moreover, the implication of the Genetic Algorithm for the form generation process, performs a long-running operation without interaction with the designer. In other words, this tool requires a lot of waiting

to test each form samples to achieve better design solutions. (In the case of our research, each form generation trial according to the specified scenarios took up to 40 hours, in total. As the complexity level increased, the waiting period increased to even more than two days.)

On the other hand, in the current context of the research, simulation algorithm was set up for the specified building typology without articulation on the building façade. Since variation in the building setback has a significant importance on the measurement of SVF value, it would be preferable to investigate that effect on the heat island intensity within the scope of another study.

Furthermore, as stated in the summary of the research section, many other influential factors, such as surface materials, ground covers and weather conditions, on the heat island intensity were excluded from the methodological framework of the research, the evaluations of generated form variations were limited to produce design codes, and to generalize them. It may be misleading to recommend a certain urban form to mitigate UHI effect where many parameters have not been tested yet. Therefore, simulation results should be considered as an alternative typologies for the case study area instead of a specialized set of design recommendations. From those outcomes, it is obvious that the current research should be expanded to investigate more form variations by including new variables to the simulation process.

Last but not the least, it should be emphasized that the simulated alternative form-typologies do not imply a kind of ‘good urban form’ models to be addressed for the general theory of urban design. In other words, the specific form typologies generated as the ‘best performed models’ should not be regarded as the optimum urban typologies to be applied in every context. More concretely, the least compact model of urban fabrics which have been simulated as the best-performed form-typology, in this respect, are the best alternatives only with regards to the issue of UHI effect specifically discussed in the research. That means any parametric research in search for generating ‘good urban form(s)’ has to take other fundamental aspects of urban design (i.e. legibility, integration, coherence etc.) in order to come up with an

integrated and inclusive morphological approach in urbanism..

5.4. Recommendations for Future Studies

Proposing a parametric model is quite motivation for opening up a methodological discussion on the basis of generative approach to the problematic issue of UHI effect. Increase in the utilization of the parametric modelling tools and techniques will provide designers and planners to have a robust perspective on evidence-based urban design in regard to the thermal balance of the environment. Based on the findings and limitations of this research, some preliminary recommendations have emerged to enhance the utility of the proposed model. By following these recommendations, researchers will have much better opportunities to improve decision-making mechanism while searching for better design solutions to mitigate UHI effect.

Considering the extent of the model proposal for the analysis of urban areas to calculate the SVF value and UHI intensity, it can be suggested that researchers should consider the reevaluation of this measurement tool to achieve better estimation results. The SVF calculation on the street axis is an important tool for the estimation of UHI intensity, but it should not be the only consideration. Generated form compositions to mitigate UHI intensity within urban canyons may create uncomfortable climatic conditions in the internal spaces between buildings. Therefore, future studies may respond to the need for a more comprehensive measurement tool for urban areas by improving the algorithmic setting of analysis.

Regarding the form generation in this study, morphological components of the urban form, which are specified as building height, building size and distance between buildings, are the only variables that are used to mitigate heat island intensity. Hence, the current research should be enhanced to assess the effect of building orientation on the UHI development by applying airflow and solar radiation simulations. Generation of form compositions by manipulating building orientation to enhance the cooling effect of air flow may become an object of a further investigation. In addition to the building orientation, the impact of building setbacks on the heat island intensity should

be investigated by researchers. Briefly, considering the necessity for further improvement of the parametric approach in urban heat island studies with different applications, this research can be taken as the initial step to guide the forthcoming studies in future.

REFERENCES

- Akay, A. (1996). *Kentsel mekanlarda oluşan ısı adası etkisinin azaltılmasında sürdürülebilir peyzajın öneminin Ankara kenti örneğinde araştırılması*. Unpublished master thesis, Graduate School of Natural and Applied Sciences, Ankara University, Ankara.
- Akbari, H., Berdahl, P., Levinson, R., Wiel, S., Miller, B., & Desjarlais, A. (2006). *Cool color roofing materials*. California Energy Commission PIER Program, Lawrence Berkeley National Laboratory (LBNL), and Oak Ridge National Laboratory (ORNL).
- Akbari, H., Davis, S., Huang, J., Dorsano, S., & Winett, S. (1992). *Cooling our communities: A guidebook on tree planting and light colored surfacing*. US Environmental Protection Agency (EPA). Washington DC.
- Alavipanah, S., Wegmann, M., Qureshi, S., Weng, Q., & Koellner, T. (2015). The role of vegetation in mitigating urban land surface temperatures: a case study of Munich, Germany during the warm season. *Sustainability*, 7, 4689-4706.
- Arkon C. A. & Özkol, Ü. (2013). Effect of urban geometry on pedestrian-level wind velocity. *Architectural Science Review*, 57, 4-19.
- Arnab, I. Z., Ali, T., Shidujaman, M., & Hossain M. M. (2013). Consideration of environmental effect of power generation: Bangladesh perspective. *Energy and Power Engineering*, 5, 1521-1525.
- Asaeda, T., Ca, V. T., & Wake, A. (1996). Heat storage of pavement and its effect on the lower atmosphere. *Atmospheric Environment*, 30, 413-427.
- Ashrafizadeh, S. A., & Tan, Z. (2018). *Mass and energy balances: Basic principles for calculation, design, and optimization of macro/nano systems*. Springer: Cham.
- Bakarman M. & Chang, J. D. (2015). The Influence of height/width ratio on urban heat island in hot-arid climates. *Procedia Engineering*, 118, 101-108.

Banihashemi, M. (1995). *The effect of albedo modification on residential roof and indoor temperatures*. Unpublished master thesis, College of Social Sciences, San Jose State University, San Jose.

Bejan, A. (2013). *Convection heat transfer, 4th edition*. John Wiley & Sons: New Jersey.

Bergman, T. L., Lavine, A. S., Incropera, F. P., & Dewitt, D. P. (2011). *Introduction to heat transfer, 6th edition*. John Wiley & Sons: New York.

Bilgili, B. C. (2009). *Ankara kenti yeşil alanlarının kent ekosistemine olan etkilerinin bazı ekolojik göstergeler çerçevesinde değerlendirilmesi üzerine bir araştırma*. Unpublished doctoral dissertation, Graduate School of Natural and Applied Sciences, Ankara University, Ankara.

Bohnenstengel, S. I., Hamilton, I., Davies, M., & Belcher, S. E. (2014). Impact of anthropogenic heat emissions on London's temperatures. *Quarterly Journal of the Royal Meteorological Society*, 140, 687-698.

Brunt, D. (1952). *Physical and dynamical meteorology*. Cambridge University Press, New York.

Canan, F. (2017). Kent geometrisine bağlı olarak kentsel ısı adası etkisinin belirlenmesi: Konya örneği. *Çukurova Üniversitesi Mühendislik Mimarlık Fakültesi Dergisi*, 32, 69-80.

Cao, Z., Wu, Z., & Ma, W. (2018). Effect of anthropogenic heat release on temperature in different types of built-up land in Guangzhou, China. *Progress in Geography*, 37, 515-524.

Chen, L., Ng, E., An, X., Ren, C., Lee, M., Wang, U., et al. (2012). Sky view factor analysis of street canyons and its implications for daytime intra-urban air temperature differentials in high-rise, high-density urban areas of Hong Kong: A GIS-based simulation approach. *International Journal of Climatology*, 32, 121-136.

Cheung, H. K. W., Coles, D., & Levermore, G. J. (2016). Urban heat island analysis of Greater Manchester, UK using sky view factor analysis. *Building Services Engineering Research and Technology*, 37, 5-17.

Chokachian, A., Perini, K., Giulini, S., & Auer, T. (2017). *Mathematical generative*

approach on performance based urban form design. International Conference on Urban Comfort and Environmental Quality, Genova.

Chrysoulakis, N. & Grimmond, C. S. B. (2016). Understanding and reducing the anthropogenic heat emission. In M. Santamouris & D. Kolokotsa (Eds.), *Urban climate mitigation techniques* (pp. 27-40). Routledge: New York.

Clarke, J. F., Ching, J. K. S., & Godowitch, J. M. (1982). *An experimental study of turbulence in an urban environment*. US Environmental Protection Agency, United States.

Cleugh, H. A., & Oke, T. R. (1986). Suburban-rural energy balance comparisons in summer for Vancouver, B.C. *Boundary Layer Meteorology*, 36, 351-369.

Damm, A., Köberl, J., Prettenthaler, F., Rogler, N., & Töglhofer, C. (2017). Impacts of + 2°C global warming on electricity demand in Europe. *Climate Services*, 7, 12-30.

Dousset, B. M. (1992). *Remote sensing of urban microclimates and their relationship to land use: A case study of the Los Angeles basin*. Unpublished doctoral dissertation, University of California, Los Angeles.

Duckworth, E. & Sandberg, J. (1954). The effect of cities upon horizontal and vertical temperature gradients. *Bulletin of American Meteorological Society*, 35, 198-207.

Eceral, T., Varol, Ç., & Alkan, L. (2010). *Kentsel Arazi Değer Artış Süreci: Ankara Mustafa Kemal Mahallesi Örneği*, Toprak Mülkiyeti Sempozyum Bildirileri, 307-25.

Erell, E., Pearlmutter, D., & Williamson, T. (2011). *Urban microclimate: Designing the spaces between buildings*. Earthscan: London.

Fouillet, A., Rey, G., Laurent, F., Pavillon, G., Bellec, S., Guihenneuc-Jouyaux, C., et al. (2006). Excess mortality related to the August 2003 heat wave in France. *International Archives of Occupational and Environmental Health*, 80, 16-24.

Givoni, B. (1989). *Urban design in different climates*. WCAP-10, World Meteorological Organization, Geneva.

Goh, K. C. & Chang, C. H. (1999). The relationship between height to width ratios and the heat island intensity at 22:00 h for Singapore. *International Journal of Climatology*, 19, 1011-1023.

Grimmond, C. S. B., & Oke, T. R. (2002). Turbulent heat fluxes in urban areas:

Observations and a local-scale urban meteorological parametrization scheme (LUMPS). *Journal of Applied Meteorology*, 41, 792-810.

Gülten, A. (2014). *Kentsel yüzeylerde ısı adası etkisinin simülasyon yöntemi ile araştırılması*. Unpublished doctoral dissertation, Graduate School of Natural and Applied Sciences, Fırat University, Elazığ.

Hamdi, R. & Schayes, G. (2008). Sensitivity study of the urban heat island intensity to urban characteristics. *International Journal of Climatology*, 28, 973-982.

Hammerle, M., Gal, T., Unger, J., & Matzarakis, A. (2011a). Introducing a script for calculating the sky view factor used for urban climate investigations. *Acta Climatologica et Chorologica*, 44-45, 83-92.

Hammerle, M., Gal, T., Unger, J., & Matzarakis, A. (2011b). Comparison of models calculating the sky view factor used for urban climate investigations. *Theoretical and Applied Climatology*, 105, 521-527.

Heiple, S. C. (2007). *Using building energy simulation and geospatial modeling techniques to determine high resolution building sector energy consumption profiles*. Unpublished master thesis, College of Engineering and Computer Science, Portland State University, Oregon.

Honjo, T. & Takakura, T. (1991). Simulation of thermal effects of urban green areas on their surrounding areas. *Energy and Buildings*, 15, 443-446.

Hosler, C. L. & Landsberg, H. E. (1977). The effect of localized man-made heat and moisture sources in mesoscale weather modification. *Energy and Climate*, National Academy of Sciences, Washington, DC.

Hu, Y., White, M., & Ding, W. (2016). An urban form experiment on urban heat island effect in high density area. *Procedia Engineering*, 169, 166-174.

Huang, Y. J., Akbari, H., & Taha, H. (1990). The wind shielding and shading effects of trees on residential heating and cooling requirements. *American Society of Heating, Refrigerating and Air-Conditioning Engineers*, 96, 1403-1411.

Jauregui, E. (1990). Influence of a large urban park on temperature and convective precipitation in a tropical city. *Energy and Buildings*, 15-16, 457-463.

Kakon, A. N. & Nobuo, M. (2009). *The sky view factor effect on the microclimate of*

a city environment: A case study of Dhaka city. 7th International Conference on Urban Climate, Yokohama.

Kalma, J. D. (1974). An advective boundary-layer model applied to Sydney, Australia. *Boundary Layer Meteorology*, 6, 351-361.

Karaosman, S. K. (2006). Yeşil çatılar ve sürdürülebilir bina değerlendirme sistemleri. 3. Çatı ve Cephe Kaplamaları Sempozyumu, İstanbul.

Karimi, K. & Vaughan, L. (2014). *An evidence-based approach to designing new cities: the English New Towns revisited*, Chapter 22 in *explorations in urban design: An urban design research primer*, 261-276.

Katili, A. R., Boukhanouf, R., & Wilson, R. (2015). *Space cooling in buildings in hot and humid climates: A review of the effect of humidity on the applicability of existing cooling techniques*. Conference: SET, Nottingham.

Landsberg, H. E. (1981). *The urban climate*. Academic Press: London.

Lau, K. K. L., Thorsson, S., Lindberg, F., & Holmer, B. (2015). *Street geometry design and its effect on mean radiant temperature: A parametric study based on numerical modelling*. 9th International Conference on Urban Climate jointly with 12th Symposium on the Urban Environment, Toulouse.

Lee, S. H., Song, C. K., Baik, J. J., & Park, S. U. (2008). Estimation of anthropogenic heat emission in the Gyeong-In region of Korea. *Theoretical and Applied Climatology*, 96, 291-303.

Liao, J. W. L. & Cavaleri, M. M. (2014). *The study of sky view factor in urban morphologies: Computational tools and methods of analysis*. 30th International Plea Conference, Ahmedabad.

Lopez, C. S. P., Sala, M., Tagliabue, L. C., Frontini, F., & Bouziri, S. (2016). Solar radiation and daylighting assessment using the Sky-View Factor (SVF) analysis as method to evaluate urban planning densification policies impacts. *Energy Procedia*, 91, 989-996.

Marther, P. M., & Koch, P. (2011). *Computer processing of remotely-sensed images: An introduction, 4th edition*. Wiley-Blackwell: Chichester.

Matuschek, O. & Matzarakis, A. (2010). *Estimation of sky view factor in complex*

environment as a tool for applied climatological studies. 7th Conference on Biometeorology, Freiburg.

Millennium Ecosystem Assessment (MEA). (2005). *Ecosystems and human well-being: Synthesis*. Island Press, Washington, DC.

Money, D. (2000). *Weather and climate*. Nelson: Cheltenham.

Montavez, J. P., Gonzalez-Rouco, J. F., & Valero, F. (2008). A simple model for estimating the maximum intensity of nocturnal urban heat island. *International Journal of Climatology*, 28, 235-242.

Nakata, C. M. & Souza L. C. L. (2013). Verification of the influence of urban geometry on the nocturnal heat island intensity. *Journal of Urban and Environmental Engineering*, 7, 286-292.

Nakata-Osaki, C. M., Souza, L. C. L., & Rodrigues, D. S. (2015). *A GIS extension model to calculate urban heat island intensity based on urban geometry*. 14th International Conference on Computers in Urban Planning and Urban Management, Cambridge.

Naughton, M. P., Henderson, A., Mirabelli, M. C., Kaiser, R., Wilhelm, J. L., Kieszak, S. M., et al. (2002). Heat-related mortality during a 1999 heat wave in Chicago. *American Journal of Preventive Medicine*, 22, 221-227.

Nunez, M. & Oke, T. R. (1977). The energy balance of an urban canyon. *Journal of Applied Meteorology*, 16, 11-19.

Oke, T. R. & East, C. (1971). The urban boundary layer in Montreal. *Boundary Layer Meteorology*, 1, 411-437.

Oke, T. R. (1973). City size and the urban heat island. *Atmospheric Environment*, 7, 769-779.

Oke, T. R. (1976). The distinction between canopy and boundary-layer urban heat islands. *Atmosphere*, 14, 268-277.

Oke, T. R. (1982). The energetic basis of the urban heat island. *Quarterly Journal of the Royal Meteorological Society*, 108, 1-24.

Oke, T. R. (1987). *Boundary layer climates*, 2nd edition. Routledge: London.

- Oke, T. R. (1988a). The urban energy balance. *Progress in Physical Geography*, 12, 471-508.
- Oke, T. R. (1988b). Street design and urban canopy layer climate. *Energy and Buildings*, 11, 103-113.
- Oke, T. R., Johnson, G. T., Steyn, D. G., & Watson, I. D. (1991). Simulation of surface urban heat islands under ideal conditions at night: Diagnosis and causation. *Boundary Layer Meteorology*, 56, 339-358.
- Oke, T. R., Spronken-Smith, R. A., Jauregui, E., & Grimmond, C. S. B. (1999). The energy balance of central Mexico City during the dry season. *Atmospheric Environment*, 33, 3919-3930.
- Oke, T.R. (1981). Canyon geometry and the nocturnal urban heat island: Comparison of scale model and field observations. *Journal of Climatology*, 1, 237-254.
- Parker, D. S. & Barkaszi, S. F. (1997). Roof solar reflectance and cooling energy use: Field research results from Florida. *Energy and Buildings*, 25, 105-115.
- Pearlmutter, D., Krüger, E. L., & Berliner, P. (2009). The role of evaporation in the energy balance of an open-air scaled urban surface. *International Journal of Climatology*, 29, 911-920.
- Priyadarsini R. & Wong, N. H. (2006). Parametric studies on urban geometry, air flow and temperature. *International Journal on Architectural Science*, 6, 114-132.
- Quah, A. K. L. & Roth, M. (2012). Diurnal and weekly variation of anthropogenic heat emissions in a tropical city, Singapore. *Atmospheric Environment*, 46, 92-103.
- Sailor D. J. & Lu, L. (2004). A top-down methodology for developing diurnal and seasonal anthropogenic heating profiles for urban areas. *Atmospheric Environment*, 38, 2737-2748.
- Sailor, D. J. (1994). Sensitivity of coastal meteorology and air quality to urban surface characteristics. *American Meteorological Society*, 8, 286-293.
- Sani, S. (1973). Observations on the effect of a city form and functions on temperature patterns. *Journal of Tropical Geography*, 36, 60-65.

Santamouris, M., Adnot, J., Alvarez, S., Klitsikas, N., Orphelin, M., Lopes, C., et al. (2004). *Cooling the cities: Rafraichir les villes*. Paris: Les Presses.

Santamouris, M., Asimakopoulos, D. N., Assimakopoulos, V. D., Chrisomallidou, N., Klitsikas, N., Mangold, D., et al. (2001). *Energy and climate in the urban built environment*. James & James: London.

Scherba, A. J. (2011). *Modeling the impact of roof reflectivity, integrated photovoltaic panels and green roof systems on the summertime heat island*. Unpublished master thesis, College of Engineering and Computer Science, Portland State University, Oregon.

Shahidan M. F. (2011). *The potential optimum cooling effect of vegetation with ground surface physical properties modification in mitigating the urban heat island effect in Malaysia*. Unpublished doctoral dissertation, Cardiff University, Cardiff.

Shahmohamadi, P., Che-Ani, A. I., Ramly, A., Maulud, K. N. A., & Mohd-Nor, M. F. I. (2010). Reducing urban heat island effects: A systematic review to achieve energy consumption balance. *International Journal of Physical Sciences*, 5, 626-636.

Shaker, R. & Drezner, T. D. (2010). A new technique for predicting the sky-view factor for urban heat island assessment. *Geographical Bulletin - Gamma Theta Upsilon*, 51, 85-96.

Shishegar, N. (2013). Street design and urban microclimate: Analyzing the effects of street geometry and orientation on airflow and solar access in urban canyons. *Journal of Clean Energy Technologies*, 1, 52-56.

Şimşek, Ç. K. (2013). *İstanbul'da kentsel iklim üzerine antropojenik etkiler: Kent ısı adalarının incelenmesi*. Unpublished doctoral dissertation, Graduate School of Natural and Applied Sciences, Yıldız Teknik University, İstanbul.

Stafoggia, M., Forastiere, F., Agostini, D., Biggeri, A., Bisanti, L., Cadum, E., et al. (2006). Vulnerability to heat-related mortality: A multicity, population-based, case-crossover analysis. *Epidemiology*, 17, 315-323.

Stewart, I. D. (2011). *Redefining the urban heat island*. Unpublished doctoral dissertation, The University of British Columbia, Vancouver.

Suomi, J. (2014). *Characteristics of urban heat island (UHI) in a high-latitude coastal city: A case study of Turku, SW Finland*. Unpublished doctoral dissertation, Graduate

- School of Mathematics and Natural Sciences, University of Turku, Turku.
- Svensson, M. (2004). Sky view factor analysis - implications for urban air temperature differences. *Meteorology Applications*, 11, 201–211.
- Taha, H. (1997). Urban climates and heat islands: Albedo, evapotranspiration, and anthropogenic heat. *Energy and Buildings*, 25, 99-103.
- Taha, H., Akbari, H., & Rosenfield, A. (1991). Heat island and oasis effects of vegetative canopies: Micro-meteorological field-measurements. *Theoretical and Applied Climatology*, 44, 123-138.
- Taha, H., Sailor, D., & Akbari, H. (1992). *High-albedo materials for reducing building cooling energy use*. Energy & Environment Division, Lawrence Berkeley Laboratory, University of California, Berkeley.
- Takebayashi, H. (2017). Influence of urban green area on air temperature of surrounding built-up area. *Climate*, 5, 60.
- Takkanon, P. (2016). *A study of height to width ratios and urban heat island intensity of Bangkok*. 4th International Conference on Countermeasures to Urban Heat Island, Singapore.
- Tham, K. W. (1993). Conserving energy without sacrificing thermal comfort. *Building and Environment*, 28, 287-299.
- Tymkow, P., Tassou, S., Kolokotroni, M., & Jouhara, H. (2013). *Building services design for energy efficient buildings*. Routledge: New York.
- U.S. Environmental Protection Agency (EPA). (2008). Urban heat island basics. In *Reducing urban heat islands: Compendium of strategies*. Draft. <https://www.epa.gov/heat-islands/heat-island-compendium>.
- U.S. Environmental Protection Agency (EPA). (2012). Cool pavements. In *Reducing urban heat islands: Compendium of strategies*. Draft. <https://www.epa.gov/heat-islands/heat-island-compendium>.
- UNCHS (Habitat). (2001). *Implementing the habitat agenda: The 1996-2001 experience*, Report on the Istanbul+5 Thematic Committee, 25th Special Session of the United Nations General Assembly, New York.
- Unger, J. (2009). Connection between urban heat island and sky view factor

approximated by a software tool on a 3D urban database. *International Journal of Environment and Pollution*, 363, 1-3.

United Nations Department of Economic and Social Affairs (UNDESA). (2011). *World economic and social survey 2011: The great green technological transformation*.

United Nations, Department of Economic and Social Affairs, Population Division. (2017). *World population prospects: The 2017 revision, Volume II: Demographic profiles* (ST/ESA/SER.A/400).

United Nations, Department of Economic and Social Affairs, Population Division. (2016). *The world's cities in 2016: Data booklet* (ST/ESA/SER.A/392).

Voogt, J. A. (2004). Urban heat islands: Hotter cities. *American Institute of Biological Sciences*.

Voogt, J. A., & Oke, T. R. (2003). Thermal remote sensing of urban climates. *Remote Sensing of Environment*, 86, 370-384.

Wong N. H. & Chen, Y. (2009). *Tropical urban heat islands: Climate, buildings and greenery*. Taylor & Francis: New York.

Yılmaz, E. (2013). *Ankara şehrinde ısı adası oluşumu*. Unpublished doctoral dissertation, Graduate School of Social Sciences, Ankara University, Ankara.

Yuan, C. & Chen, L. (2011). Mitigating urban heat island effects in high density cities based on sky view factor and urban morphological understanding: A study of Hong Kong. *Architectural Science Review*, 54, 305-315.

Yüksel, Ü. D. (2005). *Ankara kentinde kentsel ısı adası etkisinin yaz aylarında uzaktan algılama ve meteorolojik gözlemlere dayalı olarak saptanması ve değerlendirilmesi üzerinde bir araştırma*. Unpublished doctoral dissertation, Graduate School of Natural and Applied Sciences, Ankara University, Ankara.

Zareiyan, B. (2011). *Performance of roof materials high SRI, low SRI, and green roof in California climate zone 8 Los Angeles, California*. Unpublished master thesis, School of Architecture, University of Southern California, Los Angeles.